NAVAL POSTGRADUATE SCHOOL

MONTEREY, CALIFORNIA

THESIS

STARTUP CONTROL OF THE TOPAZ-II SPACE NUCLEAR REACTOR

by

Cal D. Astrin

September, 1996

Thesis Advisor: Oscar Biblarz

Approved for public release; distribution is unlimited.

REPORT DOCUMENTATION PAGE

Form Approved OMB No. 0704-0188

1. AGENCY USE ONLY *(Leave blank)*	2. REPORT DATE September, 1996	3. REPORT TYPE AND DATES COVERED Master's Thesis

4. TITLE AND SUBTITLE
STARTUP CONTROL OF THE TOPAZ-II SPACE NUCLEAR REACTOR

5. FUNDING NUMBERS

6. AUTHOR(S)
Astrin, Cal D.

7. PERFORMING ORGANIZATION NAME(S) AND ADDRESS(ES)
Naval Postgraduate School
Monterey CA 93943-5000

8. PERFORMING ORGANIZATION REPORT NUMBER

9. SPONSORING/MONITORING AGENCY NAME(S) AND ADDRESS(ES)

10. SPONSORING/MONITORING AGENCY REPORT NUMBER

11. SUPPLEMENTARY NOTES
The views expressed in this thesis are those of the author and do not reflect the official policy or position of the Department of Defense or the U.S. Government.

12a. DISTRIBUTION/AVAILABILITY STATEMENT
Approved for public release; distribution is unlimited.

12b. DISTRIBUTION CODE

13. ABSTRACT *(maximum 200 words)*

The Russian designed and manufactured TOPAZ-II Thermionic Nuclear Space Reactor has been supplied to the Ballistic Missile Defense Organization for study as part of the TOPAZ International Program. A Preliminary Nuclear Safety Assessment investigated the readiness to use the TOPAZ-II in support of a Nuclear Electric Propulsion Space Test Mission (NEPSTP). Among the anticipated system modifications required for launching the TOPAZ-II system within safety goals is for a U.S. designed Automatic Control System. The requirements and desired features of such a control system are developed based upon U.S. safety standards. System theory and design are presented in order to establish the basis for development of a hybrid control model from available simulations. The model is verified and then used in exploration of various control schemes and casualty analysis, providing groundwork for future Automatic Control System design.

14. SUBJECT TERMS
Thermionics, TOPAZ-II, Startup, Control

15. NUMBER OF PAGES 160

16. PRICE CODE

17. SECURITY CLASSIFICATION OF REPORT	18. SECURITY CLASSIFICATION OF THIS PAGE	19. SECURITY CLASSIFICATION OF ABSTRACT	20. LIMITATION OF ABSTRACT
Unclassified	Unclassified	Unclassified	UL

NSN 7540-01-280-5500

Standard Form 298 (Rev. 2-89)
Prescribed by ANSI Std. 239-18 298-102

Approved for public release; distribution is unlimited

STARTUP CONTROL OF THE TOPAZ-II SPACE NUCLEAR REACTOR

Cal D. Astrin
Lieutenant, United States Navy
B.S., University of New Mexico, 1989

Submitted in partial fulfillment
of the requirements for the degree of

MASTER OF SCIENCE IN ASTRONAUTICAL ENGINEERING

from the

NAVAL POSTGRADUATE SCHOOL
September 1996

ABSTRACT

The Russian designed and manufactured TOPAZ-II Thermionic Nuclear Space Reactor has been supplied to the Ballistic Missile Defense Organization for study as part of the TOPAZ International Program. A Preliminary Nuclear Safety Assessment investigated the readiness to use the TOPAZ-II in support of a Nuclear Electric Propulsion Space Test Mission (NEPSTP). Among the anticipated system modifications required for launching the TOPAZ-II system within safety goals is for a U.S. designed Automatic Control System. The requirements and desired features of such a control system are developed based upon U.S. safety standards. System theory and design are presented in order to establish the basis for development of a hybrid control model from available simulations. The model is verified and then used in exploration of various control schemes and casualty analysis, providing groundwork for future Automatic Control System design.

TABLE OF CONTENTS

I. INTRODUCTION 1

II. BACKGROUND 3

A. SPACE NUCLEAR POWER APPLICABILITY 4

B. SPACE NUCLEAR POWER PROGRAMS 5
1. United States Space Nuclear Power Programs 5
2. Former Soviet Union Nuclear Power Programs 7

C. TOPAZ INTERNATIONAL PROGRAM 9

III. BASIC THEORY 13

A. THERMIONIC ENERGY CONVERSION 13
1. General Characteristics 13
2. Principles of Operation 13
3. Thermionic Efficiency 13
4. Thermionic Emission 14
5. Gas-filled Converters 16
6. Thermionic Modes of Operation 17

B. FISSION REACTOR THEORY 17
1. Fission 17
2. Neutron Energy 17
3. Criticality 18
4. Neutron Life Cycle 18
5. Reactor Control 19
6. Delayed Neutrons 19
7. Reactivity 20
8. Reactor Kinetics Equations 21

IV. TOPAZ II DESCRIPTION 23

A. OVERVIEW 23
1. Mission Requirements 23
2. System Description 24

B. REACTOR SUBSYSTEM 26
1. Overview 26
2. Moderator 27
3. Thermionic Fuel Elements 28
4. Radial Reflector and Control Drums 30

C. HEAT REJECTION SYSTEM 30
1. Overview 30
2. Electromagnetic Pump 32

D. SECONDARY SYSTEMS 32
1. Radiation Shielding 32
2. Cesium Supply System 32
E. INSTRUMENTATION AND CONTROL 34
1. Instrumentation 34
2. Control System 37
3. Protection System 38
V. SYSTEM STARTUP 43
A. MISSION PHASES 43
1. Pre-Launch 43
2. Launch 43
3. On-orbit 44
4. Startup Phase 44
B. STARTUP SEQUENCE 44
1. Startup Limits 45
2. Startup Sequence 46
C. SYSTEMS TESTING 48
1. Loss of Coolant Accident 48
2. Cesium Oscillations 49
VI. STARTUP CONTROL 55
A. AUTOMATIC REGULATION SYSTEM 55
B. SYSTEM MODELING 56
1. Current Models 56
2. Reactor Kinetics 58
3. Reactivities 59
4. Thermal Model 68
5. Thermionic Emission Model 73
6. Control Drum Model 75
7. Hybrid Control Model 75
C. CONTROL SYSTEM DESIGN 83
D. DESIGN EVALUATION 85
E. SCENARIO ANALYSIS 86
1. Reactivity Addition Casualty 86
2. Loss of Coolant Accident 88
3. Cesium Pressure Oscillations 90
VII. CONCLUSIONS 93
VIII. RECOMMENDATIONS 95
APPENDIX. SIMULINK® PROGRAM CODE 97

LIST OF REFERENCES 145

INITIAL DISTRIBUTION LIST 147

ACKNOWLEDGEMENTS

I wish to thank Professor Oscar Biblarz for his encouragement, support, and guidance throughout my research. I also wish to thank Dr. Mohamed S. El-Genk and Dmitry Paramonov of the University of New Mexico for their generous assistance in modifying their simulator code. I would also like to extend my appreciation to all the TIP researchers and technicians who rendered invaluable aid in developing a thorough understanding of the TOPAZ-II system. I would especially like to give thanks to Frank Wyant and Oleg Izhvanov.

I. INTRODUCTION

A key element among the long term technological requirements for advanced space missions is the required development of a suitable high power electrical generation system. A joint National Aeronautics and Space Administration (NASA)/Department of Defense (DoD) review committee determined that Space Nuclear Power (SNP) is the best option for meeting demands for certain high power and long life applications. The Strategic Defense Initiative Organization (SDIO), now the Ballistic Missile Defense Organization (BMDO), led the effort to acquire Soviet technology in order to advance SNP science within the United States. Within this process, the Russian TOPAZ-II space nuclear power system has been part of a joint testing program since December 1991. (Malloy et al., 1994)

The TOPAZ-II system provides power using thermionic energy conversion. This process is a form of direct conversion in which heat is converted into electricity without intermediate energy transformation stages. Unlike conventional heat-power systems, thermionic conversion requires no moving mechanical parts. This eliminates the need for frequent maintenance, making it particularly suited for use as an electrical-power source for deep-space probes and various other space vehicles. Thermionic systems have low system weight and the ability to withstand acceleration higher than 30 times the force of gravity. The heat for thermionic devices may come from any convenient source. The TOPAZ-II design uses nuclear fission heat generation, which allows a high power level over long system life, independent of location in the solar system.

The SDIO initially intended use of the TOPAZ-II reactor for a Nuclear Electric Propulsion Space Test Program (NEPSTP) Mission but launch of the TOPAZ-II requires determination that the mission could be performed safely and with reasonable costs. A Preliminary Nuclear Safety Assessment performed by a team organized by SDIO determined that modifications would be required to meet U.S. safety requirements. Among these changes is the requirement to design and build an Automatic Control System (ACS) to U.S. standards. The Russian ACS is a relatively massive analog system that cannot be flight qualified and does not incorporate certain desired features. (Flight Safety Team, 1992)

Additionally, the TOPAZ-II system could be made more robust through minor alteration of system design. Certain mission profiles for space nuclear power applications include operation for long periods at reduced power levels. Recent research (Benke, Venable, 1995) demonstrated work on the road to feasibility of the TOPAZ-II system for use in such missions.

The goal of this work is the initial design of a start-up control system that meets all safety requirements and is robust enough to enable the expanded mission possibilities of the TOPAZ-II reactor.

II. BACKGROUND

The successful exploitation and exploration of space will require ever increasing amounts of electrical power. Future missions that will demand large power sources include high-bandwidth communications and remote sensing satellites, deep space exploration, extraterrestrial manufacturing, manned missions to Mars, and colonization of the Moon. Many of these tasks will take place in harsh environments where solar power is limited, intermittent, or unavailable. Nuclear power and thermionic conversion can serve as a compact, durable energy source that is capable of long-term operation in radiation belts, deep-space vacuum, and hostile atmospheres.

Direct energy conversion is a process by which heat is changed into electrical energy without the use of intermediate stages or moving mechanical parts as required in such conventional systems as the Rankine cycle. The two main methods of direct conversion incorporated with a nuclear heat source are thermoelectric and thermionic. In a thermoelectric power generator, a temperature differential between the upper and lower semiconductor material being generates power.

The thermionic method uses two electrodes. The emitter is heated to a sufficiently high temperature to emit electrons. The collector, which receives the emitted electrons, functions at a much lower temperature. Thermionic converters can operate at significantly higher radiator temperatures than the thermoelectric process; resulting in smaller radiator size and mass. This higher temperature range potentially leads to much higher overall efficiency. Thermionic conversion systems also restrict the high-temperature region to the fuel and the emitter. This permits the use of lighter and cheaper low temperature structural materials. (Paramonov and El-Genk, 1994)

Both the United States and the former Soviet Union have conducted advanced research on direct energy conversion systems. In 1965, the U.S. launched its only experimental thermoelectric nuclear reactor space system ever flight-tested, the SNAP-10A. The Soviet Union had an extensive space nuclear power program that included 35 nuclear

reactors; incorporating both thermoelectric and thermionic methods. TOPAZ-II is the most technologically advanced single-cell thermionic system ever built. By March 1994, all TOPAZ-II space power reactors in the Russian inventory have been brought into the United States for use in the TOPAZ International Program (TIP). Researchers from Russia, France, the United Kingdom, and the United States conduct nonnuclear testing at the New Mexico Engineering Research Institute (NMERI) in Albuquerque, New Mexico.

A. SPACE NUCLEAR POWER APPLICABILITY

The dominant factors that determine the choice of electrical power source are the electric power level required and planned use duration. Nuclear power is particularly suitable for applications that demand high power levels over a long period of time. Typical examples of such missions are for operation of large space platforms, lunar bases, high power communication and remote sensing satellites, specialized deep-space probes, and a Mars landing. Thermionic systems with nuclear reactor heat sources are optimal for electrical requirements in the range of 10 kW to 1000 kW (Larson and Wertz, 1992).

Nuclear power has several advantages over conventional power. These systems typically have a compact size with a low to moderate mass. Nuclear power may be provided over a long mission lifetime in hostile environments, independent of the sun. A nuclear reactor system exhibits very high hardness with respect to natural nuclear radiation, nuclear or laser threats, and meteorite or pellet impingement. These systems exhibit high stability and maneuverability. However, there are many concerns with respect to the use of these systems. Chief among these considerations is the potential environmental impact, which imposes the requirement for a strict safety analysis reporting program (Larson and Wertz, 1992). Additionally, space reactor and direct energy conversion technology is less developed than either chemical or solar power. Past nuclear missions have included several important space programs including Apollo and all major interplanetary probes (Benke, 1995). In sum, space nuclear power is a vital niche technology whose importance will grow with our future exploitation of the solar system.

B. SPACE NUCLEAR POWER PROGRAMS

Space nuclear power has been under development since the birth of space exploration. The majority these programs have been conducted in the United States and the former Soviet Union.

1. United States Space Nuclear Power Programs

A favorable political environment and high public support for nuclear power technologies fostered its development from the mid-1950's to the early 1970's. The first major space use of nuclear power was in the Transit 4A navigational satellite, launched in June of 1961, which employed the Systems for Nuclear Auxiliary Power (SNAP) version 3B source. This power system relied upon a Radioisotope Thermoelectric Generator (RTG), a method that uses radioactive decay processes as a heat source. RTG's are highly reliable as proved in the performance record of 24 U.S. missions, including Pioneer, Viking, and Voyager (Benke, 1995)

The 1955 Project Rover program at Los Alamos National began research of space nuclear technology. This program was the start of 18 years of nuclear rocket research and development that advanced the search for a suitable high temperature reactor. The Nuclear Engine for Rocket Vehicle Application (NERVA) program demonstrated the high thrust and specific impulse capabilities of a high power density nuclear rocket (Angelo and Buden, 1985).

U.S. development of nuclear reactors for space electric power applications began in 1957 with the production of the SNAP-2 reactor. This system combined a thermal uranium zirconium-hydride reactor as a heat source with a liquid mercury Rankine cycle for the thermal to electric power conversion. Following the SNAP-2 system was parallel development of SNAP-8 and SNAP-10 programs. The SNAP-8 system was essentially a scaled-up version of the SNAP-2 system, providing a higher power level. The SNAP-10A system used the thermoelectric conversion method in place of the Rankine cycle.

In April 1965, as part of the SNAPSHOT mission, SNAP-10A was the first reactor ever launched and orbited, and the last such system flown by the U.S. The

SNAP-10A system generated approximately 600 watts of electrical power in an orbital altitude of about 1300 km. This reactor operated at power for 43 days before the on-board Reactor Control Unit (RCU) safety system initiated an automatic shutdown. An apparently false detection of spacecraft voltage regulation failure caused this event. The downlinked spacecraft data indicated that system operation was normal prior to this event. (Malloy, 1994). This incident highlights the importance of RCU design to overall system reliability and safety.

After major advances in solar power, space nuclear reactor technology languished in the 1970's. Thermionic research had developed to the point that it had supplanted thermoelectric development by 1969. American researchers tested several thermionic devices; however, no complete reactor system using thermionics has ever been built in the United States. The U.S. space program continued to use nuclear power sources, mainly plutonium fueled RTG's.

During the 1980's, the inauguration of the Strategic Defense Initiative (SDI) revitalized space nuclear research. The SDI program spurred the development of the Space Power Advance Reactor (SPAR), later renamed SP-100, to meet projected 100 kW electric needs. The Department of Energy (DoE), NASA, the Defense Advance Research Projects Agency (DARPA) established a combined program. These organizations conducted trade-off studies comparing thermoelectric, thermionic, Rankine, Brayton, and Stirling energy conversion methods. The lack of reliability and performance data for thermionic systems within the U.S. resulted in the choice of a thermoelectric design for the SP-100 system. In order to exploit the superior power to mass ratio of in-core thermionic power conversion, DoD and SDIO began the Thermionic Fuel Element Verification Program (TFEVP) in 1985. Development of the SP-100 system has essentially been discontinued with the change in the political situation following the end of the Cold War. (Malloy et al., 1994). Figure 1, below, shows a drawing of the SP-100 mission concept.

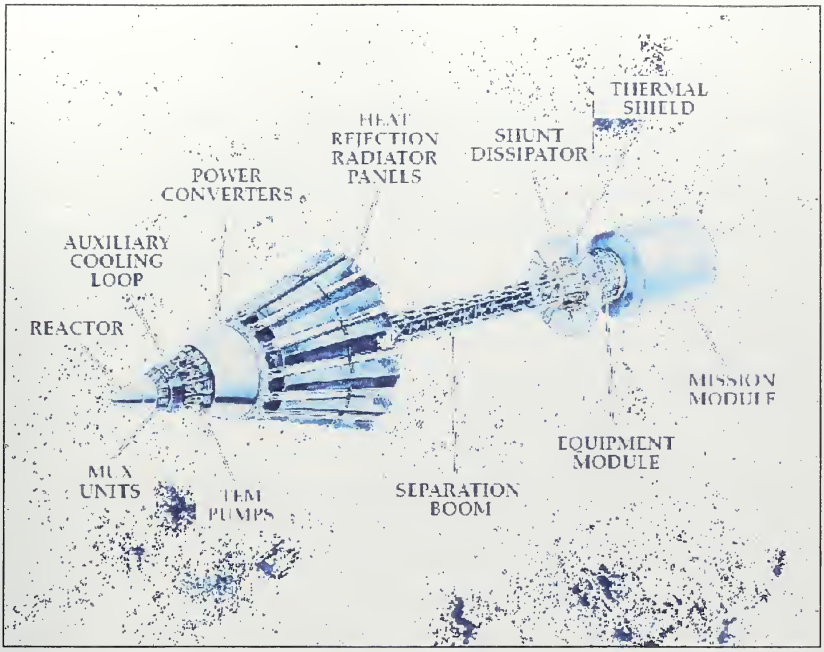

Figure 1. SP-100 U.S. Space Reactor.

2. Former Soviet Union Nuclear Power Programs

Soviet space nuclear power design began in the 1960's, with several systems that were largely derivative of early U.S. efforts (Malloy et al., 1994). The Soviet space nuclear power development benefited from a more constant level of effort, resulting in a total of 38 reactors launched over the history of its space program (Benke 1995).

The first Soviet space nuclear power system, the BOUK reactor, was launched in 1967. This reactor configuration utilized thermoelectric conversion in a configuration similar to the U.S. SNAP-10A system. This 1-2 kWe reactor design was extensively used in the Radar Ocean Reconnaissance Satellite (RORSAT) program, which launched an estimated 33 satellites. Nuclear power was the preferable source since a solar powered RORSAT would have limited to an orbital lifetime of a few days due to the effects

of atmospheric drag on the large solar panels. The orbital life of the RORSAT system was approximately 100 days. (Malloy et al., 1994).

The inadvertent reentry of COSMOS-954, a RORSAT system, caused the most well known space nuclear power incident. In 1977, this satellite dispersed reactor material over a 600 km path in northern Canada (Angelo and Buden, 1985). The end-of-life orbital boost system did not activate due to a telemetry fault (Malloy, 1994). Following this mishap, the United Nations adopted international nuclear space reactor design and operating principles. In order to achieve a "nuclear safe" orbit, improved RORSAT design automatically separated the reactor core from the satellite and placed it in a higher altitude of approximately 950 km at the end of mission life. (Further discussion of nuclear safety considerations is found in Chapter V, Safety and Functional Requirements.)

The Soviet drive for higher altitude surveillance lead to the development of the COSMOS systems. The two reactors, COSMOS-1818 and COSMOS-1867, were launched in flight tests conducted in February and July of 1987. These satellites were test platforms for an advanced reactor design utilizing multi-cell thermionic conversion techniques. Both tests were extremely successful, lasting for 142 days and 342 days respectively (Paramonov and El-Genk, 1994).

A multi-cell thermionic fuel element (TFE) uses a stacked series of short thermionic cells, rather than the long unitary fuel element of the single-cell design. The TOPAZ Space Nuclear Power System (SNPS) (translated from the Russian designation: ТОПАЗ Космическая Ядерная Энергетическая Установка — КЯЗУ) developed multi-cell technology. The ENISY program produced a single-cell design. American researchers incorrectly designated the ENISY program as TOPAZ-II (Voss, 1994). TOPAZ itself subsequently became known as TOPAZ-I in the U.S. No single-cell TFE system was ever flight tested, although 26 ENISY reactor systems were built. Testing of 19 of these systems took place between 1970 and 1989 (Schmidt et al., 1994).

C. TOPAZ INTERNATIONAL PROGRAM

The TOPAZ International Program (TIP) was an outgrowth of the reduced tensions at the end of Cold War. Both the U.S. and Russia faced large funding reductions and program cancellation in all space related nuclear research. With the inefficiencies in the former Soviet Union, the problem severity was much worse in Russia. Many research institutes faced extinction unless they could learn to compete in the new environment.

Mr. John Kiser of International Scientific Products in San Jose, California, a consultant for the SDIO program, toured the former Soviet Union in 1988 to develop technology transfers to the U.S. During this trip, he contacted the Kurchatov Institute, a developer of the TOPAZ-II system. (Malloy et al., 1994).This led to Russian participation in the Sixth Symposium on Space Nuclear Power Systems, held in Albuquerque, NM, in January 1989. At this symposium, the Russian delegation indicated their willingness to sell TOPAZ-type space power systems to the U.S. In a remarkable example of cooperation in the face of much institutional reluctance and bureaucratic inertia, the U.S. Government purchased two non-fueled TOPAZ-II systems and associated test and support hardware in 1992. The SDIO funded investigation of the TOPAZ-II reactor system in support of the Nuclear Electric Propulsion Space Test Program (NEPSTP). This mission was intended to provided an early flight test with the inclusion of electric thrusters. SDIO was reconstituted as the Ballistic Missile Defense Organization (BMDO), resulting in NEPSTP program cancellation in 1994. The project continued as the Topaz International Program (TIP). (Wyant, 1994). Below is an image of a TOPAZ-II system at the NMERI facility (Figure 2).

Figure 2. TOPAZ-II System at NMERI (From Malloy, 1994).

The TIP is truly an international program. Scientists, engineers, and technicians from Russia, the United Kingdom, and France have conducted research at the Thermionic System Evaluation Test (TSET) facility in the NMERI complex in Albuquerque, NM (Fairchild et al. 1992). The New Mexico Alliance for Thermionics, which includes the University of New Mexico, Sandia National Laboratory, and Los Alamos National Laboratory, provides research support (Benke 1995). The BMDO Program provides funding through the, administration of the U.S. Air Force Phillips Laboratory. (The program may be shifted to the Defense Nuclear Agency.)

The TIP involves the testing and evaluation of TOPAZ-II system units, where nuclear fuel is replaced by tungsten heaters (Paramonov and El-Genk, 1994). The primary goal of this program is to gain understanding of the capabilities and limitations of thermionic space nuclear power technology. Much of the basic thermionics research has

focused upon correlating insulator degradation to TFE lifetimes (Malloy et al., 1994). A stand alone TFE Test Rig allows TFE characteristic measurement. The test, monitoring, and control equipment of a Baikal Test Stand permitted performance evaluation of the TOPAZ-II power system. The TSET team has measured system parameters and characteristics in addition to various shock and vibration testing performed with reference to the MIL-STD-1540B flight qualification requirements.

III. BASIC THEORY

The TOPAZ-II system uses thermionic direct energy conversion with a nuclear fission reactor heat source. Direct energy (or static) conversion devices mainly use electrons as a working fluid rather than a vapor or gas characteristic of more conventional heat energy systems. This class of devices includes fuel cells, batteries, solar cells, thermoelectric and thermionic conversion mechanisms. A nuclear fission reactor is a device for producing heat from a controlled fission chain reaction. Fission is the process of splitting a heavy nucleus into smaller fragments and is accompanied by large energy release.

A. THERMIONIC ENERGY CONVERSION

1. General Characteristics

A thermionic conversion system consists of two electrodes separated by a gap. The analogy of a heat engine with electrons a working fluid serves as a description of its characteristics. A "hot plate" or emitter is heated to a sufficiently high temperature that electrons are "boiled" off. These electrons travel to the significantly cooler collector where they "condense." The gap between these electrodes is typically filled with an extremely low pressure gas or vapor. (Benke, 1995)

2. Principles of Operation

Electron emission from the emitter is similar to steam generation in heat engines. A thermionic converter may also be considered as a thermoelectric converter that uses plasma or vacuum as a conductor. The thermionic mechanism produces a potential difference between the two electrodes. When an external load is connected, this potential drives a current flow. By this process, part of the thermal energy that liberated the electrons is converted directly into electrical power. (Huang, 1988)

3. Thermionic Efficiency

The heat engine comparison is useful in understanding the factors which effect thermionic efficiency. The Carnot efficiency, which is based upon the temperature

differences between source and sink, determines the maximum efficiency attainable. The main inefficiencies of the thermionic cycle are:

a. Radiative Heat Transfer

Heat transferred by radiation from the emitter to the collector is unavailable for energy conversion and is a loss. Heat rejection from the radiators is a loss inherent to the system.

b. Thermal Losses

Heat leakage through insulators and other undesirable paths reduces the efficiency of the cycle.

c. Back Emission

Because the collector also has heat energy, some fraction of the collector electrons will have enough energy to deliver a current density to the emitter. This current reduces the overall forward electron flow. While the collector is at a lower temperature than the emitter, its lower work function results in the back emission losses described above.

d. Space Charge Effect

The emission of negatively charged electrons into the gap creates an overall space charge. A charge region creates an electrostatic field that inhibits the flow of additional electrons towards the collector. This effect limits the maximum current density.

4. Thermionic Emission

In metals and semiconductor materials under certain conditions, a layer of electrons is loosely bound in a region known as the Fermi cloud. The force binding an electron in this layer is given in Equation (1), below:

$$F = \frac{e^2}{16\pi\varepsilon_0 x^2} \qquad (1)$$

where F = force (Newtons)
e = electronic charge (Coulombs)
ε_0 = permittivity of free space
x = distance from surface (m)

The work function, φ, describes the energy required to liberate the electron by overcoming the work function. The value of φ is unique to each material and has little temperature dependence in the normal range of thermionic conversion operation. Much thermionic material research concentrated on the development of desirable materials with good work functions and other acceptable properties in the high temperature environment within a converter's enclosure. Current density from the emitter is a function of the rate at which electrons escape. The Richardson-Dushman equation, Equation (2), describes the relationship among the variables affecting emission current.

$$J_0 = RT^2 exp\left(-\frac{e\varphi}{kT}\right) \qquad (2)$$

where J_0 = current density (amps / m^2)
R = material constant
T = absolute temperature (K)
e = electronic charge (coulombs)
φ = work function (Volts)
k = Boltzmann's constant

This equation is useful in demonstrating the desirability of a high emitter temperature and the importance of carefully selecting materials (Angrist 1987). However, higher emitter temperatures also contribute to an increase of the radiation heat transfer as shown in the following equation, Equation (3):

$$Q = A\varepsilon\sigma\left(T_{emitter}^4 - T_{collector}^4\right) \quad (3)$$

where Q = radiative heat transfer (W)

A = area (m^2)

ε = effective emittance

σ = Stefan - Boltzmann constant

T = absolute temperature (K)

This formula also stresses the importance of collector temperature. A lower collector temperature will increase radiation heat transfer from the emitter and reduces the amount of back emission. Higher collector temperatures are important in reducing the system radiator size, which also has a T^4 efficiency dependence at a cost however, of higher back emission losses. Optimum collector operating temperature requires a design trade-off study. (Angelo and Buden, 1985)

5. Gas-filled Converters

The strong impact of space charge build-up upon thermionic efficiency has direct consequences for converter design. Two methods of limiting this effect are minimizing gap size and introducing a plasma. The desired gap distance in a vacuum converter for useful current production is on the order of the Debye length. Debye length is the average distance traveled by an electron during the period of plasma isolation, and is on the order of 1 μm (Rasor 1991). Because this represents a severely restrictive tolerance, vacuum converters have few practicable applications.

A gas-filled (or plasma diode) thermionic converter uses space charge neutralization in order to increase gap width significantly (up to at most 0.5 mm) (Rasor, 1991). This device continuously generates positive ions that neutralize the electrostatic field near the emitter by canceling the negative charge of the electrons.

Cesium is the most commonly used gas used in plasma diodes because it has the lowest ionization potential of any element (Angelo and Buden, 1985). Cesium also promotes a low work function, φ, which provides additional benefits. Cesium adsorbs to

both the emitter and collector. Adsorption is the adhesion of a single layer of molecules to the surfaces of solid bodies or liquids with which they are in contact. This effect lowers the work functions of both electrodes, increasing overall converter efficiency. A liquid reservoir provides cesium through evaporation. Its production rate is dependent upon gas pressure and reservoir temperature. Efficient ion production requires emitter temperature approximately 3.6 times reservoir temperature (Angrist, 1987).

6. Thermionic Modes of Operation

The mode of operation in a thermionic converter is characterized by the mechanism of the neutralizing ion generation. In the unignited mode, surface ionization is the dominant production source. In the ignited or arc mode, inelastic collisions with electrons in the gap produce the majority of ions. The volume ionization in the ignited mode can generate a net positive space charge if the device is operated beyond the transition point. Collisions in the gap region cause ionization losses, creating a voltage deficiency V_d. Experimental data and theoretical investigation shows that minimum V_d and maximum efficiency is achieved with small value of the product of cesium pressure (P_{Cs}) and electrode gap width (w) (Angrist, 1987). Operationally, this performance sensitivity requires careful adjustment for converter optimization.

B. FISSION REACTOR THEORY

1. Fission

Nuclear fission is the process in which the nucleus of an atom splits into two smaller nuclei. Fission is a spontaneous or induced event that usually requires massive atoms to occur. In a reactor, induced fission is primarily a result of the excitation of a nucleus with a neutron. Fission results in a large energy and radiation release, nuclear fission fragment formation, and the emission of more neutrons. A chain reaction occurs if these neutrons go on to induce additional fissions. (Leachman, 1965).

2. Neutron Energy

The atomic absorption of an incident neutron forms a compound nucleus. Fissionable radioisotopes vary in the critical compound nucleus energy levels required to

induce fission. For example, ^{235}U is fissionable by slow neutrons whereas ^{238}U requires fast neutrons. The average energy of the neurons that maintain the chain reaction forms a basis for fission reactor classification. A thermal reactor operates with neutrons having a velocity distribution similar to that of materials at ambient temperatures. Intermediate or quasi-thermal reactors use higher neutrons energies. A fast reactor propagates the fission chain reaction with the high energy (~1 Mev) neutrons that are released from a fission event.

Since a fission neutron is born with such high kinetic energy, it must be slowed to maintain a chain reaction a thermal or quasi-thermal reactor. A moderator material produces this slowing down by enabling scattering reactions. Fast reactors do not require moderation.

3. Criticality

Criticality is essentially a measure of the probability that neutrons produced in one generation will cause fissions in the next. A reactor is **critical** if, on the average, one neutron from a fission event induces a subsequent fission. In a critical reactor, both the fission rate and power are constant. The multiplication factor, k, describes the overall chain reaction condition. This factor is defined mathematically as the ratio of fissions produced in one generation to the number of fissions in the previous one (see Equation (4)).

$$k = \frac{\text{number of fissions in generation n + 1}}{\text{number of fissions in generation n}} \qquad (4)$$

In a critical reactor, $k = 1$. If $k < 1$, a chain reaction will not be maintained and the reactor is said to be subcritical. If $k > 1$, the reactor is supercritical; power and fission rate increase.

4. Neutron Life Cycle

To maintain criticality, the chain reaction must produce one neutron for every neutron lost. Within each generation, a series of events defines the neutron life cycle. Although some fast fissions occur in all reactors, the majority of the fissions in a thermal or quasi-thermal reactor require that a neutron be slowed without escaping. These neutrons are

absorbed within the reactor. An absorption into a non-fissionable material (a nuclear poison), removes a neutron from the fission process. Additionally, only a certain percentage of the absorptions into fissionable material actually induce fission. These fissions provide the additional neutrons to renew the cycle into the next generation.

Specific reactor components are designed in order to change the probabilities that the average neutron will complete any step within the fission life cycle. A moderator increases the likelihood of neutron slowing down. Neutron absorptive control devices (control drums or control rods) directly remove neutrons from this cycle. Additionally, many reactors are equipped with a reflector that minimizes leakage by deflecting neutrons back into the core where they may take place in the fission process.

5. Reactor Control

Reactor control is achieved through the manipulation of neutron absorbing devices within the reactor. These mechanisms use materials that have extremely high cross-sections for neutron absorptions. The most common control method govern criticality by changing the geometry of these absorbers with respect to neutron producing regions with the core. Since any factor that changes fission probabilities within the neutron Life Cycle will affect the chain reaction, other controlling mechanisms are possible. Routine regulation is required to start up and change reactor power and to overcome the effects of gradual fuel depletion and the build-up of poisonous fission product daughters. A reactor control system must also provide a means of emergency shutdown in order to ensure reactor safety.

6. Delayed Neutrons

Not all the neutrons produced during the fission process are born immediately after fission. Some of the fission fragment daughters undergo further nuclear reactions that result in delayed neutron release. The half-life of delayed neutron production varies from about 1 sec to 1 minute. Since prompt neutrons are produced in about 10^{-14} seconds after neutron absorption, the effect of the delayed neutrons is to reduce the generation lifetime. This makes the process controllable by bringing the time scale into a range controllable by the reactor control system.

The fraction neutrons that are born delayed is the delayed neutron fraction, β. Since delayed neutrons are produced by decay processes, they are born at a lower energy lever than prompt neutrons. The relatively slower delayed neutrons are less likely to leak out, and therefore more likely to be thermalized and cause fission. The effective delayed neutron fraction, $\overline{\beta}$, accounts for this effect within reactor kinetics equations.

7. Reactivity

Reactivity, ρ, is the primary parameter used in reactor control theory. Reactivity is a measure of the departure from criticality. Reactivity is positive in a supercritical reactor, zero in a critical reactor, and negative when a reactor is subcritical. Any parameter change that increases criticality is said to add positive reactivity. Conversely, any event that tends to shut down the reactor adds negative reactivity. The primary reactivity control variables are control mechanism position and temperature feedback. Reactivity is mathematically defined with respect to criticality, as shown in Equation (5).

$$\rho = \frac{k-1}{k} \qquad (5)$$

where: ρ = reactivity
k = criticality

Note: Reactivity is often reported in units of 10^{-2}, and is expressed with a '$' symbol.

a. Control Drum Worth

The TOPAZ-II reactor uses a control drum design in which sections of neutron absorbing material may be rotated. Turning the control drum moves this neutron absorber away from the center of the core. This decreases the probability that a neutron will reach the control drum, increasing the chance that fission will occur, adding positive reactivity. The reactivity of the control drums is with respect to position is the control drum worth.

b. Temperature Coefficient of Reactivity

The temperature effect is especially important since it provides direct, immediate feedback to power changes. The parameter relating change in temperature to reactivity addition is the temperature coefficient of reactivity, α_T. A temperature change may add positive or negative reactivity, usually depending on the material involved. For the TOPAZ-II reactor, two effects are particularly important: Doppler broadening and Einstein oscillation.

An increase in temperature is initially accompanied by an negative value of α_T due to resonance absorption in ^{238}U. Resonance absorption is the process by which discrete neutron certain energy levels are preferentially captured as the neutrons slow down. These neutron captures do not result in fission, removing neutrons from the cycle. As the core temperature increases, a larger spectrum of energy levels are absorbed. This effect is known as Doppler broadening or spreading and adds negative reactivity.

The Einstein oscillation effect is important in the Topaz-II moderator, which contains interstitial hydrogen. A higher moderator temperature increases the frequency of collisions and thermal interactions, which excites the hydrogen into higher energy levels. These higher energy levels have lower cross sections for capture and scattering, which results in more neutrons being available for the fission process. Therefore, the temperature increase results in the addition of positive reactivity, which contributes to a positive value of α_T.

8. Reactor Kinetics Equations

The reactor kinetic equations relate power changes to the effects of delayed neutrons and reactivity changes. In this equation, the delayed neutrons are lumped in to N groups, based upon the decay constants of the precursors. These equations are valid for a small reactor with a uniform neutron flux distribution. (Paramonov and El-Genk, 1994)

$$\frac{dP(t)}{dt} = \frac{\rho(t) - \bar{\beta}(t)}{\ell^*} P(t) - \sum_{i=1}^{N} \lambda_i C_i(t) + Q(t) \qquad (6)$$

$$\frac{dC_i(t)}{dt} = \frac{\beta_i}{\ell^*} T(t) - \lambda_i C_i(t) \quad (i = 1, N) \qquad (7)$$

where: P = reactor power (W)

$\bar{\beta}$ = effective delayed neutron fraction

ρ(t) = reactivity

λ_i = delayed neutron fraction of ith group

β_i = decay constant of the delayed neuttron precursor

ℓ^* = prompt neutron lifetime

C_i = equivalent delayed neutron precursor concentration

$Q(t)$ = fission equivalent source power

The initial conditions for Equations (6) and (7) are given below:

$$P(t_0) = P_0$$
$$C_i(t_0) = \frac{\beta_i Q_0}{\ell^* \lambda_i} \qquad (8)$$

The reactivity input is calculated with Equation (9):

$$\rho(t) = \underset{\text{external}}{\rho_{ex}(t)} + \underset{\text{doppler}}{\rho_f^D(t)} + \underset{\text{temperature feedback}}{\sum_i \rho_i^E(t)} \qquad (9)$$

IV. TOPAZ II DESCRIPTION

A. OVERVIEW

1. Mission Requirements

The TOPAZ-II space power system is a 6 kWe unit that was designed for geosynchonous missions with up to three year duration (Malloy et al., 1994). Figure 3 shows an artist's conception of a TOPAZ-II spacecraft in a mission configuration.

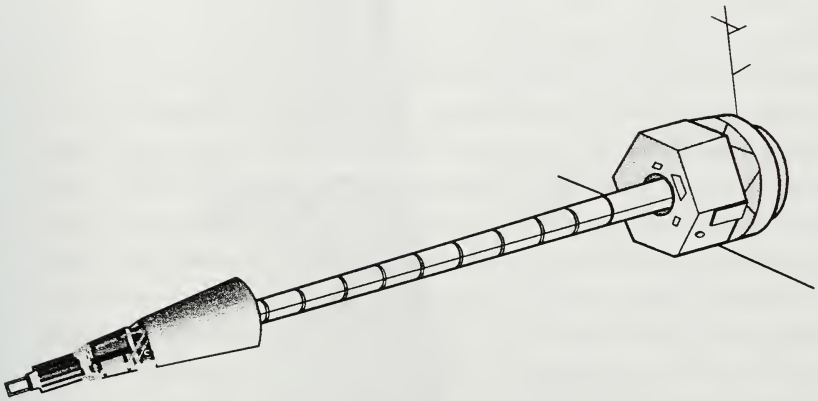

Figure 3. TOPAZ-II Mission Configuration. (From Schmidt et al., 1994).

The general requirements for the TOPAZ-II design were: (Flight Safety Team, 1992)

1. System mass less than 1061 kg, excluding controller and power supply system.
2. Electrical power 6 kWe, 27 volts, 3 year life span, 95% reliability.
3. Shelf life of 10 years after manufacture.
4. Reactor shall remain subcritical before reaching orbit.
5. Reactor coolant must not freeze.

Among these requirements, the last two have directly influence the start-up control design. The interdiction against inadvertent criticality prior achieving mission

altitude is a nuclear safety concern. The prevention of coolant freezing limits the time available for the system to become self-sustaining.

2. System Description

The major TOPAZ-II subsystems are: the Reactor and combined thermionic converters, the Coolant System, Secondary systems, such as radiation shielding and cesium supply, the Power System, the Instrumentation and Control (I & C) System.

The TOPAZ-II reactor provides electrical power with the generation of waste heat and radiation. Highly enriched uranium fuel heats the thermionic emitter, enabling electron flow. The liquid metal coolant system transfers waste heat to the radiator, limiting collector temperature. An electromagnetic (EM) pump provides the motive force for coolant flow. A radiation shield attached to the lower part of the reactor limits the neutron and gamma dose rate to the rest of the spacecraft. The cesium system supplies cesium (Cs) to the interelectrode gap, improving converter efficiency. A power supply system provides energy before the system is producing any usable electricity and regulates power production when the reactor is self-sustaining. The Instrumentation and Control (I & C) system monitors conditions, accomplishing start-up, operational control, and emergency shut down functions. I & C neutron and thermal detectors measure reactor power. The automatic control system (ACS) uses these signals to command control drive units which position control drums within the reactor subsystem. Figure 4 shows the locations of these subsystems.

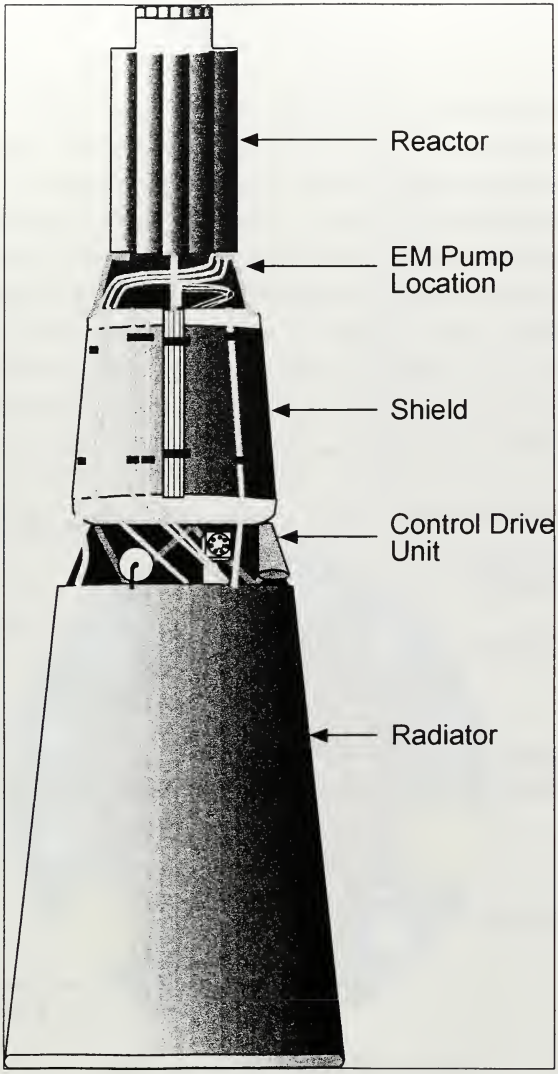

Figure 4 TOPAZ-II System. (From Flight Safety Team, 1992).

B. REACTOR SUBSYSTEM

1. Overview

The TOPAZ-II reactor is a small, zirconium hydride ($ZrH_{1.85}$) moderated, epi-thermal design with a highly enriched ^{235}U fuel. The Reactor Subsystem contains 37 single-cell TFE's that combine the fission heat source with the thermionic converters. The reactor subsystem also consists of a zirconium hydride ($ZrH_{1.85}$) moderator, a beryllium reflector, 12 control drive mechanisms, and connections with the Cooling and Secondary Subsystems. Figure 5 shows a reactor top view, Figure 6 provides a side view. The TFE's are cylindrical and fit into vertical slots within the moderator. Three of the TFE's directly power the EM pump, the remaining 34 provide electricity to other TOPAZ-II and spacecraft loads. The TOPAZ-II design allows for fueling from the top of the reactor at the launch site, minimizing transportation safety concerns. (Schmidt et al., 1994)

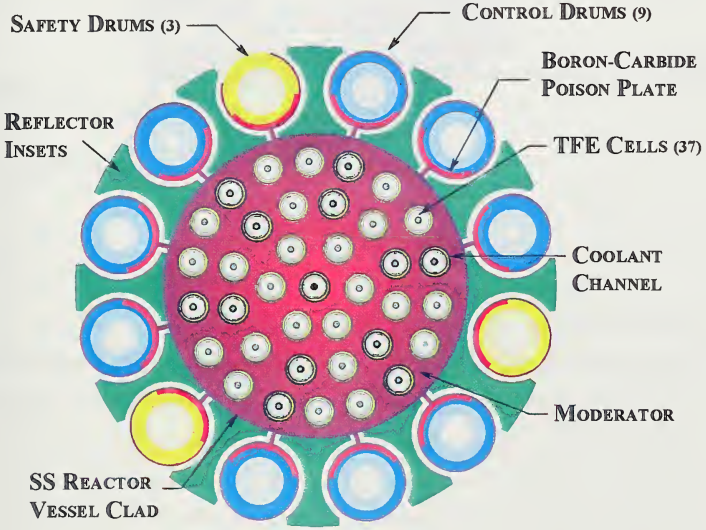

Figure 5. Reactor Top View. (From Malloy et al., 1994).

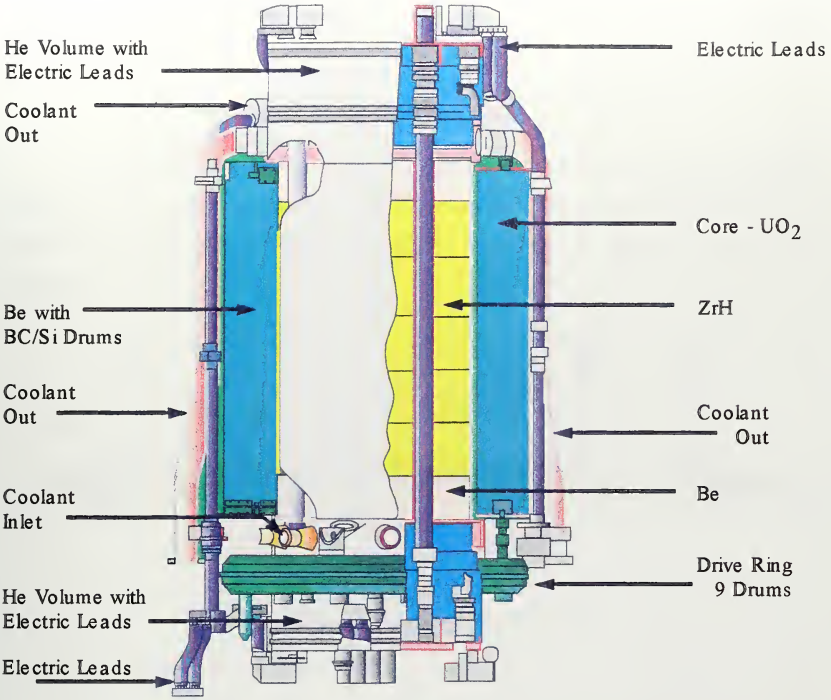

Figure 6. Reactor Side View.

2. Moderator

The moderator material is $ZrH_{1.85}$ formed into block and enclosed in a pressurized stainless steel housing that also contains the working sections of the TFE's, axial Be reflectors, and the connections to other systems. The axial reflectors are locate on the top and bottom of the moderator section. Interstitial hydrogen provides the high cross section for scattering required for fast neutron moderation. Therefore, maintenance of hydrogen pressure is essential for criticality. A pressurized mixture composed of 50% hydrogen and 50% carbon dioxide (CO_2) within the moderator inhibits hydrogen release and improves heat transfer. The reactor housekeeping telemetry reports this moderator gas

pressure. Reactor materials and coatings are specifically designed to minimize hydrogen diffusion. (Voss, 1994)

3. Thermionic Fuel Elements

Each TFE has an inner fuel section enclosed by the emitter, gap and collector of the thermionic converter. An insulating layer separates the collector from a stainless steel outer jacket. Figure 7 shows the TFE with its associated spacers and insulators.

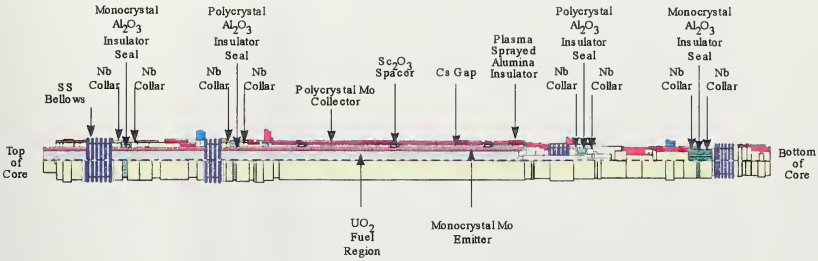

Figure 7. Thermionic Fuel Element (After Voss, 1994).

a. Fuel Section

The fuel is composed of 96% ^{235}U enriched uranium oxide (UO_2) formed into cylindrical fuel pellets with a hollow center. This center section is the release path for radioactive fission products. Beryllium (Be) and Beryllium oxide (BeO) reflector pellets are positioned on top and bottom of the fuel stack. A heater assembly replaces the fuel section for non-nuclear testing. Nominal fuel temperature is between ~1500 C to 1650 C. (Schmidt et al., 1994).

b. Thermionic Section

The emitter is a monocrystal of molybdenum with 3% niobium added for strength. A layer of tungsten formed by chemical vapor deposition establishes the desired emitter work function. This tungsten layer is in the form of the ^{184}W isotope, minimizing parasitic neutron capture. Helium (He) fills the 0.5 mm width interelectrode gap prior to start-up, providing superior heat transfer characteristics. Cesium replaces He after

the Cs supply system is placed in operation. The collector is formed from polycrystalline molybdenum with a plasma sprayed alumina (Al_2O_3) insulator outer coating. The thermionic section transforms approximately twenty percent of the heat energy from the emitter into electron flow. The collector temperature is approximately 627 C (900 K) during operation. A helium gap, located between the collector insulator and the inner coolant tube, which improves heat transfer while maintaining electrical insulation. Figure 8 provides a cross section of a TFE working section. (Voss, 1994)

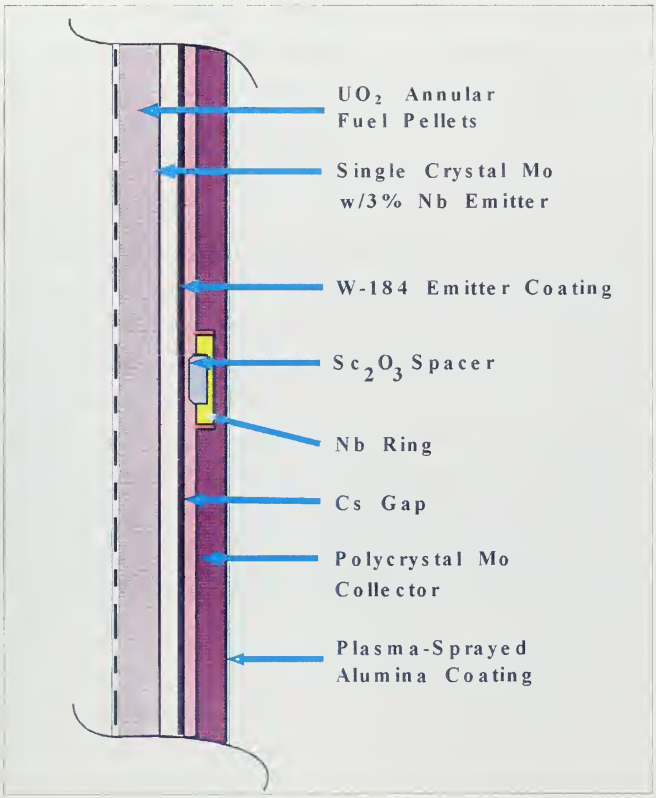

Figure 8. TFE Working Section. (After Flight Safety Team, 1992).

4. Radial Reflector and Control Drums

A beryllium (Be) reflector encloses the moderator section. The Be material is divided between static Be inserts and the twelve rotating drum assemblies (See Figure 5). Two stainless steel bands hold the radial reflectors in place against spring pressure. An electrical signal from the automatic control system can initiate reflector release, providing emergency shut-down ability. High temperatures or mechanical shock equivalent to a 50 m fall will also split the bands. The Be control drums have a section of boron carbide (B_4C) that spans 120 degrees. Boron has a very high cross section for neutron absorption. A control drive system positions nine control drums nearly simultaneously. An independent mechanism positions three of the control drums, the safety drums, during start-up.

C. HEAT REJECTION SYSTEM

1. Overview

The sodium potassium (NaK) coolant system removes waste heat from the reactor. The schematic diagram provided below (Figure 9), shows the connections between coolant system components: the direct current powered EM pump, a volume accumulator, a radiator, electrical heaters, piping, pressure and temperature monitoring equipment. The EM pump provides the motive force for coolant flow. The volume accumulator allows for thermal expansion and contraction. The electric heaters are used during the pre-launch preparation phase to prevent NaK freezing. Waste energy from the thermionic process heats coolant from 743 K to 843 K during its single pass through the core to the upper plenum. Coolant then flows to the radiator, where heat is rejected to space. The EM pump returns the coolant to the lower inlet plenum, where the cycle repeats. (Paramonov and El-Genk, 1994)

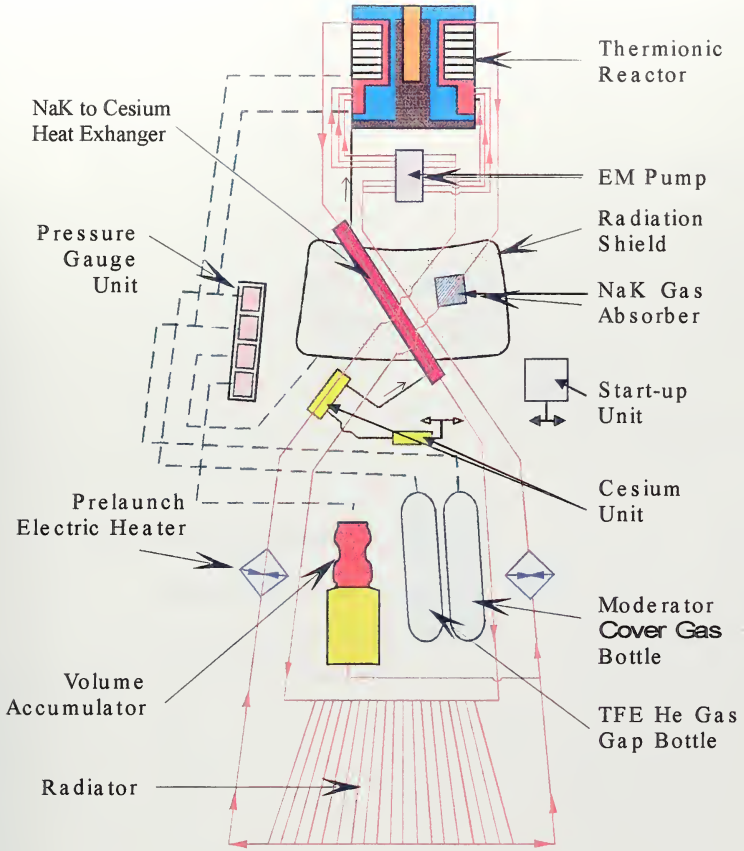

Figure 9. Primary Coolant System.

The design requirement that coolant freezing be prevented is critical to system startup operation. Since NaK freezes at -11 C, the design minimum temperature is -5 C. Prior to launch, electric heaters maintain coolant temperature. Prior to startup, intermittent the operation of the EM circulates coolant, equalizing NaK temperatures using residual heat. A thermal blanket covers the radiator in order to limit heat losses. This blanket is ejected shortly after the reactor reaches the point of adding heat. The cover was a requirement for the geosynchonous orbit of the Soviet flight test. A U.S. mission with a

lower operational orbit may not need a blanket due to the reduced time from launch to reactor startup. (Flight Safety Team, 1992)

2. Electromagnetic Pump

The EM pump is a DC powered unit that operates on the Faraday principle. Since the NaK coolant is a liquid metal, it is a good electrical conductor. An electromotive force is generated perpendicular to an electric current and a magnetic field. During normal operating conditions, three TFE's connected in parallel provide EM pump power. Startup batteries power the EM pump intermittently prior to reactor startup. During startup, battery current limits the flow rate to 25% (~0.4 kg/s). When coolant temperature in the lower collector reaches 235 C, the battery current switches to maximum. Flow rate increases from 50% (~0.8 kg/s) to 100% (~1.3 kg/s) as reactor power increases and the TFE's provide useful voltage. (Kwok, 1993)

D. SECONDARY SYSTEMS

1. Radiation Shielding

A lithium hydride, stainless steel encased, radiation shield attenuates neutron and gamma radiation. The shield is located behind the reactor in order to minimize dose rate to the payload and other TOPAZ-II components. Penetrations in this shield are angled, which reduces radiation streaming. Since radiation levels outside the reactor are significantly above background, an eight meter boom will separate the TOPAZ-II SNPS from the payload and spacecraft bus, as previously shown in Figure 3 (Flight Safety Team, 1992). At this distance, radiation spreading sufficiently minimizes the effect upon the payload.

2. Cesium Supply System

The Cesium Supply System (CSS) provides Cs to the interelectrode gap in order to increase thermionic efficiency. Figure 10 shows the overall system diagram. Cs condenses on a small radiator within the Cs regulator (see Figure 11). A "wick" formed of wound stainless steel wires transports Cs from the radiator. Cs vaporizes as it moves along the wick, establishing a relatively constant supply during normal operating conditions. A throttle valve establishes a nominal Cs pressure of 2 Torr to the reactor. A release line

provides a bleed-off path through which ~0.5 g/day of Cs and impurities vent into space. This process maintains the required Cs purity of 99.999% (Flight Safety Team, 1992). Since only ~1 kg of Cs is supplied, the loss of Cs is a limiting factor for mission duration (Schmidt et al., 1994).

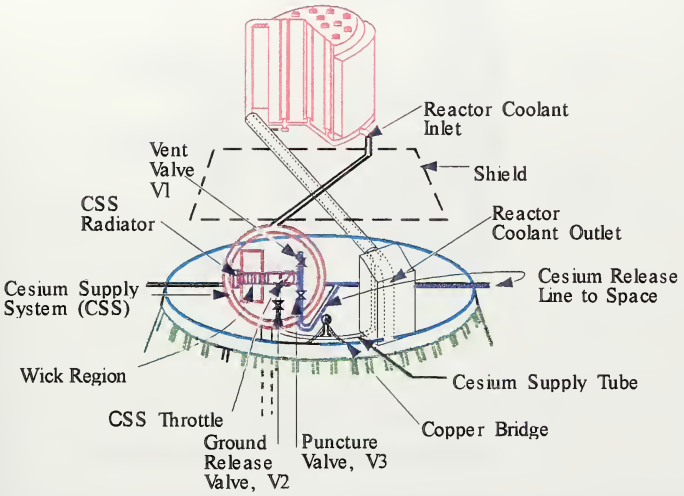

Figure 10. Cesium Supply System.

Helium (He) gas fills the interelectrode gap prior to startup. He is used because of its non-reactivity and excellent thermal conductivity. As the CSS heats up, Cs mixes with He. During the startup sequence, a puncture valve (V3), opens the release path into space. Cs then replaces He, which is preferentially vented due to its high diffusion rate.

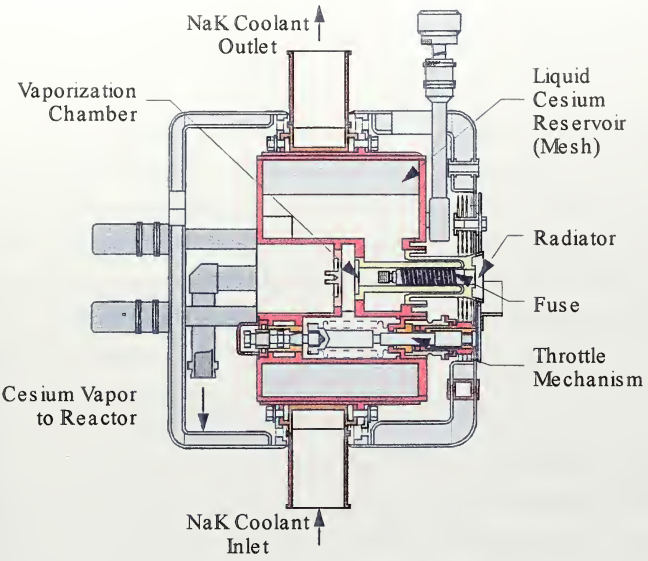

Figure 11. Cesium Regulator and Reservoir (After Morris et al., 1994).

E. INSTRUMENTATION AND CONTROL

The Instrumentation and Control (I & C) system provides for the remote monitoring, control, and reporting of system status. The I & C subcomponents include the measuring instruments and the Automatic Control System (ACS).

1. Instrumentation

TOPAZ-II measuring instruments include devices for monitoring neutron power, temperatures, pressures, and control drum positions.

a. Neutron Flux Measurement

A measurement of neutron flux provides indication of reactor power. Two ionization chambers (IC's) containing uranium coated plates are located adjacent to the reactor. Nuclear reactions of the neutrons with the uranium produce

ionization, which enables current flow. When neutron flux is at a level corresponding to 100% power, the IC output is approximately 1 ma.

The ACS uses the highest of the two IC currents as its control input for reactor power level. Since the Russian designed IC's are insensitive to power levels below ~6% power, the U.S. design will include two to four hafnium or gadolinium Self-Powered Neutron Detectors (SPND's). Not only do SPND's provide accurate indications of low neutron power, they can be used as a reliable alternate indication at higher power levels. The SPND signal would be suitable for use as a safety monitoring system input. (Flight Safety Team, 1992)

b. Temperature Measurement

The I & C system uses two types of temperature monitoring: Chromel-Alumel thermocouples (T/C's) and platinum resistance temperature detectors. Paired T/C's measure reactor coolant inlet and outlet temperatures inside the pipe wall. These T/C's have a six second response time, which may limit their utility as an input to a reactor control scheme. The RTD's measure coolant temperatures at the radiator, control EM pump operation during startup, and allow for system monitoring prior to launch.

c. Pressure Measurement

Figure 12 presents a diagram for the pressure sensors in the I & C system. Pressure sensors monitor the following parameters:

1. Moderator gas pressure.
2. TFE gap gas pressure.
3. Shield gap gas pressure.
4. NaK volume accumulator gas pressure.
5. Startup battery electrolytic pressure.
6. Control drum assembly pressure.

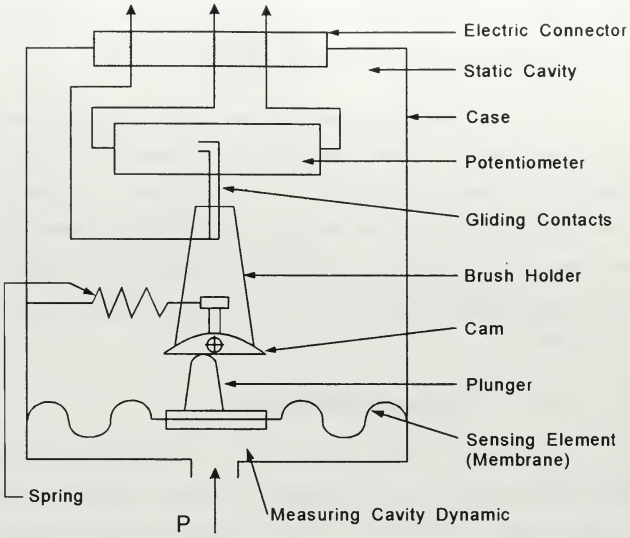

Figure 12. Pressure Sensor. (Flight Safety Team, 1992).

The pressure signals are used for telemetry purposes only, they do not provide any control function inputs. Since the volume accumulator pressure would provide indication of a coolant leak, it may be useful as a safety system input.

d. Control Drum Position Determination

There are three means of control drum position monitoring. The primary method uses the control drum position sensor. The sensor provides an analog measurement of position indication. A roller assembly within the control drum unit positions a rotor element. This rotor varies the coupling of a 1 kHz signal in a transducer, causing an amplitude change in signal coil output. The backup method counts control system signal pulses to the drive motor, which provides a more accurate measure of drum position as long as the control drum motor is operating normally. Additionally, limit switches indicate drum travel has reached the upper (154°) or lower (0°) bound of travel.

2. Control System

a. Overview

The ACS components are the Telemetry and Command System (TCS), the Automatic Regulation System (ARS), and the Electric Power Supply System (PSS). The TCS processes commands, relays telemetry, and sequences startup actions. The ARS receives inputs from the instrumentation and generates a control signal to position the control drum assembly. It also conducts shutdown and protective control actions. ARS design requirements specify a thermal control range of 0 to 150% power with an accuracy of ±700 W. The PSS regulates power supplied to the spacecraft bus, maintaining bus voltage at 27±0.8 volts. John Hopkins Applied Physics Laboratory (APL) has designed a modified PSS with a lower weight and without the gas pressurized coolant requirements of the Russian system.

b. Control Drum Drive System

Each control drum contains a B_4C neutron absorbing poison plate. The positioning of each poison plate with respect to the main core controls reactor criticality. The control drum drive system rotates the nine control drums. The maximum angle range is from 0° to 180° at speeds of 1.4°/s. The drive assembly is sealed in an argon gas pressurized enclosure since the mechanism is not designed to operate in a vacuum. The assembly consists of a stepper motor, drive train, main drum, position indication devices, temperature sensors, and pressure sensors.

A signal from the ARS powers the stepper motor. A gas tight bellows transfers torque from the reduction gear to the drive train. The drive shaft backlash is 1° to the main drum. This drum has slots through which cams connected to the bottom of the control drums are linked. (Flight Safety Team, 1992)

The control drum cam and main drum slot design enables a very fine control of thermal power. Each control drum will only rotate once the slot edge comes in contact with the cam. On a drum reversal, only one drum will move initially, followed by

other drums as more slot edges make contact. This feature establishes a planned hysteresis of 9° in moving the control drums. (Voss, 1994)

3. Protection System

The protection subsystems within the TOPAZ-II design are the Safety Drum Drive System and the Reflector Ejection system.

a. Safety Drum System

Three drums with a combined reactivity worth of -$2.0 are held in the "IN" position prior to reactor startup. This provides sufficient shutdown margin to prevent an inadvertent criticality accident in most probable accident scenarios not involving water flooding or immersion. The *NEP Space Test Program Preliminary Nuclear Safety Assessment* recommends addition safeguards in order to meet U.S. design criteria for these additional possibilities. Each safety drum is connected to a direct current drive motor that is controlled by the TCS. After the TCS initiates safety drum rotation during startup, the drums rotate until a limit switch cuts off power at ~180°. (Flight Safety Team, 1992)

b. Reflector Ejection System

The reflector system provides a quick means of initiating emergency reactor shutdown. The reflector segments and drums are held against spring pressure by a stainless steel band with fusible links. A high current signal from the TCS will melt the links in ~0.25 seconds, releasing the bands, which causes reflector disassembly. The loss of the reflector reactivity will leave the reactor subcritical.

The Russian safety system design included three pairs of events that would initiate reflector ejection:

1. Receipt of 2 ejection commands from the ground, in series.
2. Receipt of 2 emergency rocket shut off signals.
3. Two launch vehicle emergency signals.

The Russian design did not include any provision for reflector ejection once the system was operating in orbit. U.S. design philosophy would require this protection, especially in view of the much lower altitude mission profiles envisioned for a TOPAZ-II flight test.

V. SAFETY AND FUNCTIONAL REQUIREMENTS

A. NEPSTEP MISSION

1. Overview

The Nuclear Electric Propulsion Space Test Program (NEPSTP) mission was an outgrowth of *America's Space Exploration Initiative*, developed during the Bush administration (Synthesis Group, 1991). Since current policy precludes any U.S. reactor launches, NEPSTP development remains suspended, and exact mission details are undetermined. The original flight evaluation mission plan called for a launch into 1000 km to 2000 km transfer orbit, where the TOPAZ-II reactor system startup would begin. Due to concerns for the system's impact on the space environment, this transit orbit altitude was raised to 5250 km, minimizing interference with the Cosmic Ray Observer mission. After a series of tests, electrical thrusters using xenon propellant will increase the altitude until the spacecraft attains a 36000 km circular high Earth orbit (HEO).

2. Purpose

The primary mission goal is to evaluate the use of nuclear electric propulsion for orbital transfer applications, with particular emphasis placed upon measuring the self-induced environment produced by the system when operating. The secondary goal is to test diverse electric thrusters and evaluate the performance of the TOPAZ-II system.

3. Mission Details

The mission is divided into three main phases: pre-operational, operational, and post-operational. Figure 13 shows a diagram of these phases. The pre-operational phase includes launch and checkout. During the operational phase, nuclear electric propulsion raises the spacecraft to HEO. Reactor shutdown and system venting occurs in the post-operational phase.

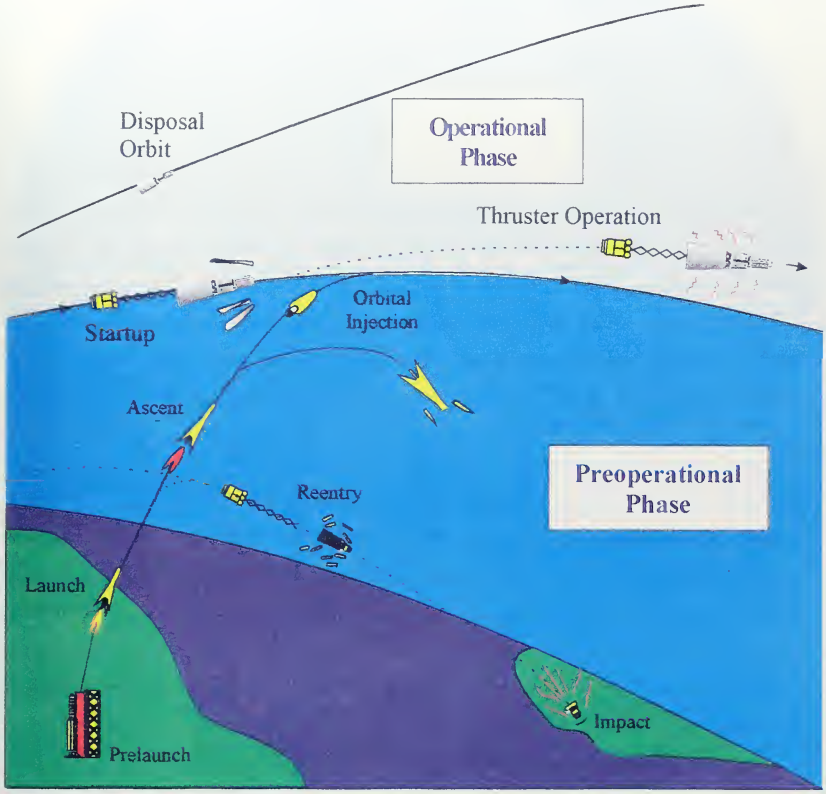

Figure 13. NEP Mission Phases & Scenarios. (From Marshal, 1994).

a. Pre-operational Phase

The planned NEPSTP mission launch site is the Cape Canaveral Air Force Station, in Cape Canaveral, Florida.. The spacecraft mass will be approximately 3500 kg, which will require a medium sized launch vehicle to reach transfer orbit. This initial circular orbit will have an inclination angle of 28.5° at a minimum altitude of 5250 km. Both ground and launch vehicle signals will be capable of initiating emergency reflector disassembly in order to minimize the probability of inadvertent criticality upon vehicle

reentry. Prior to launch, final assembly, nuclear fueling, and systems checkout will verify readiness.

b. Operational

Once the spacecraft has been placed into transfer orbit, the payload boom will extend from the TOPAZ-II reactor system. Since the NaK coolant is kept from freezing by residual heat, reactor startup must be initiated within about eight hours of launch. Within one hour from extension, the reactor should be self-sustaining, with the TFE system powering all loads and performing battery charging. Following a series of tests, the nuclear electric propulsion system will be activated. The thrust will be directed along the vehicle's velocity vector, increasing altitude while maintaining an essentially circular orbit. The TOPAZ-II system will take an estimated 500 days to reach about 3600 km altitude. (Flight Safety Team, 1992)

For most of the operational period, the spacecraft will be unable to communicate with the mission control center. This has important implications for control system design since the spacecraft must be capable of autonomous control. This requires the addition of supervisory control and a means for an emergency shutdown, features not found in the Russian design. Additionally, provisions must be made for automatic shutdown if contact with the ground station is lost for an extended period of time.

c. Post-operational

In accordance with requirements to minimize radiological consequences of the NEPSTP, safe disposal requirements are an essential part of mission planning. Once the mission is complete, the reactor must be shut down with systems vented. Disposal requires that the system be in a "sufficiently high" orbital altitude. A sufficiently high orbit is one in which the expected orbit lifetime is long enough to ensure that the curie content of the core decays to the intrinsic actinide levels of the fuel prior to burn-up.

B. SAFETY

1. Philosophy

U.S. and Russian design philosophies differ. The Russian design was tailored for a specific mission involving initial criticality at geosynchonous orbit. The U.S. Topaz-II Flight Safety Team performed additional preliminary safety analysis since the U.S. mission scenario includes possible accidents not viable within the Russian flight profile. Figure 14 shows profiles of some pre-operational accidents. Russian design emphasized operational reliability over the risk of premature shutdown. No provisions were made for automatic shutdown at the end of the mission. The reactor would eventually shutdown due to the loss of reactivity caused by hydrogen leakage and other expected phenomena. Furthermore, reflector ejection, the primary rapid means of reactor shutdown, is inoperable in the Russian design after the spacecraft is released from the launch vehicle. The only operational safeguard is the temperature regulator, which limits coolant temperature to less than 600 C. (Flight Safety Team, 1992)

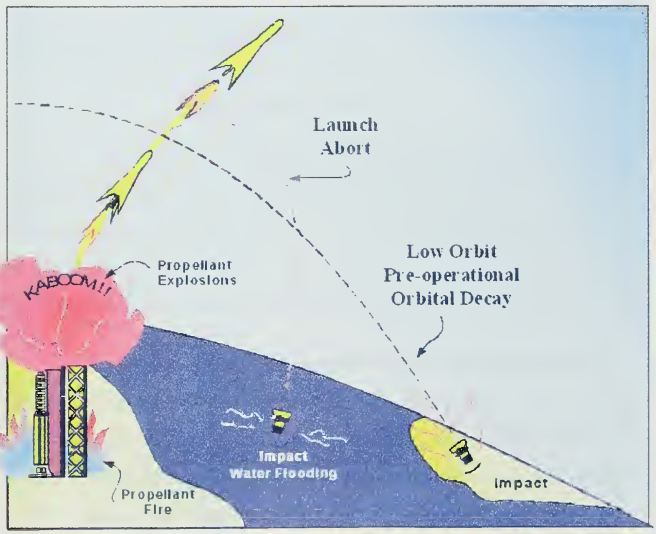

Figure 14. Pre-operational Accident Scenarios. (From Marshal, 1994).

2. Safety Requirements

The primary goal of the Topaz-II safety policy is to reduce risks to as low as reasonably achievable. This policy has two main concerns; safety and environmental protection. Safety requirements are a fundamental consideration for any nuclear program. Many safety provisions are legislated in U.S. and international law. Since a reactor accident involves the potential release of radioactive materials, a space nuclear power mission must comply with U.S. environmental law and obligations under Article IX of the Outer-Space Treaty, which provides for international protection of the outer-space environment (Larson et al, 1992). Implementation of these requirements has provisions that fall into the following categories:

a. Reactor Startup

The reactor shall not be operated at significant power levels until the spacecraft reaches a sufficiently high orbit. The basis for this provision that the curie content of the core is based upon the time-history profile of the activation processes of the fission reaction. Pre-orbital operation of the reactor could expose the ground crew and any emergency impact site to undue risk.

b. Inadvertent Criticality

A reactor relies upon a specific geometry and placement of materials to maintain a sustainable chain reaction. All plausible accident scenarios must be analyzed to ensure that inadvertent criticality does not result. Impact induced criticality would be uncontrollable since control and monitoring systems would also fail. A subcritical reactor will not increase its radioactive inventory and emits far less gamma and neutron radiation.

Initial results of Monte-Carlo-based neutronic analysis show that the reactor would be supercritical following water flooding and immersion with intact radial reflectors. A wet sand scenario produced the worst-case configuration. Therefore, in order to prevent inadvertent criticality, the U.S. implementation of the design requires modifications. The current proposal plans for keeping four fuel elements external to the

core until the initiation of reactor startup. This change will ensure that an accidental critical configuration would not be attained.

3. Radiological Release

The release of radioactive material during operations and following any probable accident scenarios must be minimized. This provision reduces any impact upon the Earth environment and decreases the potential interference with other space missions. Consideration of the Cosmic Ray Observer mission led to an increase in the operational orbit altitude.

4. Disposal

The TOPAZ-II design and mission requirements stipulates provisions for safe disposal. System operation shall be limited to a sufficiently high altitude for on-orbit disposal. Unlike the initial Russian design, the control system will assure reactor shutdown at the end of mission life. (Flight Safety Team, 1992)

5. Re-entry

Prior to initial high power operation, the TOPAZ-II system does not present a significant radiological hazard. Safe re-entry considerations rely upon following requirement for reactor startup and the prevention of inadvertent criticality. The system mechanical design provides for minimal debris dispersal upon impact.

VI. SYSTEM STARTUP

A. MISSION PHASES

The following sequence is based on the NEPSTP mission profile with the incorporation of proposed U.S. design changes.

1. Pre-Launch

Spacecraft assembly includes reactor fueling and low power testing. Prior to launch, an umbilical monitors system operation, charges the startup battery, and provides power for NaK coolant heating. A T_{min} regulator maintains the liquid metal coolant at about 100 C. The minimum temperature for launch is 40 C, which is based upon maintaining enough heat to provide an eight hour margin to prevent NaK freezing. The Automatic Control System (ACS) is also energized.

2. Launch

Immediately after launch, the reflector ejector system is enabled. A series of two signals (an "allow" signal and an "eject" signal) sent from the launch vehicle or ground control can start the reflector ejection sequence. The reflector ejection initiation signal is a 0.1 amp pulse of 0.1 second duration that closes an eject contact. Closure of this contact sends high current from the startup battery through the ejection band locks, which melt within 0.25 seconds, allowing spring force to cause reflector ejection. (Flight Safety Team, 1992)

During the orbital transfer phase, NaK coolant temperature is maintained by periodic cycling of the electromagnetic (EM) pump. The pump circulates the residual heat energy, leveling NaK temperatures. Estimated battery capacity allows for approximately eleven cycles of 90 second pump operation prior to TFE power production. Figure 15 gives a graphical representation of the results of a simulation of temperature regulation action. This analysis agrees with the estimate of eleven cycles. Note that most of the pump

operation occurs during the final hours of this phase. Shortening the orbital transfer time may significantly reduce the required startup battery capacity.

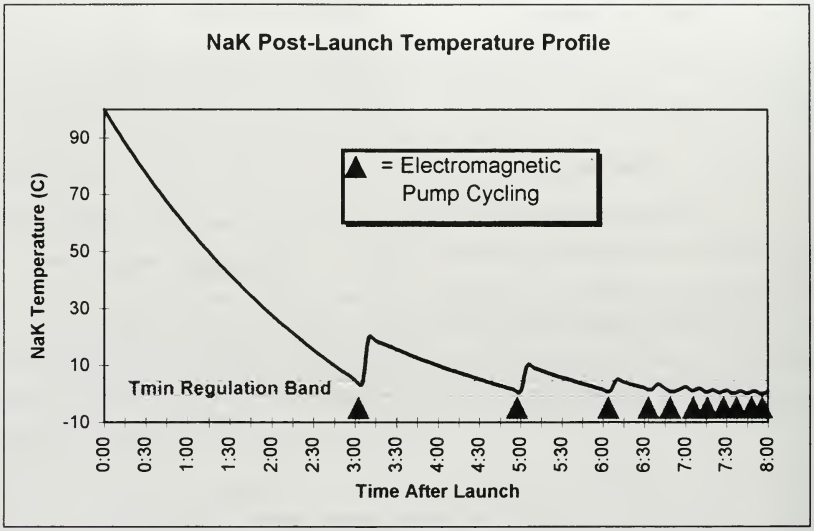

Figure 15. Post Launch Tmin Regulation.

3. On-orbit

After the spacecraft has been placed in a stable minimum altitude orbit, the boom deploys, separating the TOPAZ-II from the payload and control system. A series of tests will ensure that the system is ready for startup.

4. Startup Phase

The Russian design would perform an automatic reactor start following boom deployment, with a ground command signal as a backup. John Hopkins Applied Physics Laboratory (APL) recommends enabling startup with ground command only. This modification brings the system into closer compliance with U.S. safety. The two startup signals are "Unlock Startup" and "Startup."

B. STARTUP SEQUENCE

1. Startup Limits

Thermal limits form the basis for the operational limits during startup. The peak core temperature (T_{CL}) is limited to a maximum of 2000 C. The temperature limits for the reactor moderator and vessel are 800 C. Table 1 presents the resulting operational restrictions. Operation outside these limits will result in undesired changes in material properties and place excessive mechanical stress upon the system.

Operating Power Range (kW)	Limit	
	Power Rate	Tcoolant
5-35	600 W/s	600 C
35-115	80 W/s	600 C
115	Steady State Operation	600 C

Table 1. Reactor Power Startup Limits.

Figure 16 shows the time history of the control band formed by this piece-wise linear control law. The design criterion for the controller are to maintain thermal power between 0 to 150% of maximum nominal thermal power of 115 kW.

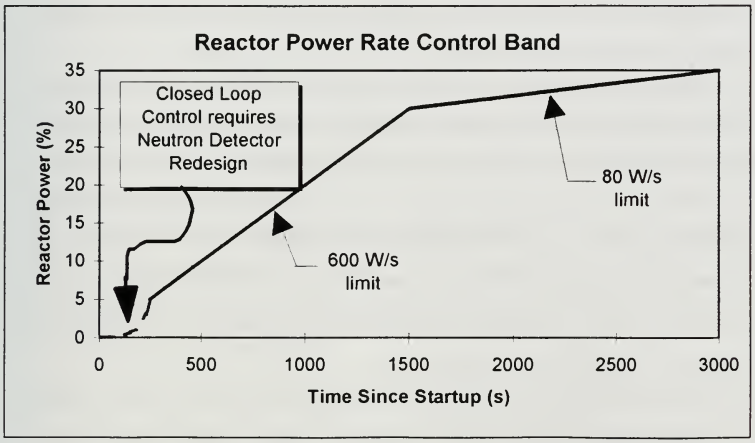

Figure 16. Reactor Power Startup Control Band

2. Startup Sequence

1. Receipt of the "Unlock Startup" signal turns on the Automatic Regulating System (ARS). This enables the neutron power and coolant temperature limit regulation control of the control drum system in accordance with the startup limits. Thermal cover ejection is also enabled.
2. The four withdrawn fuel elements are inserted. Since the mechanism that would restrain and insert these elements is not yet designed, the time required for this step is uncertain. However, it is probably on the order of ten seconds.
3. The three Safety drums are rotated outwards, providing +$2.0 δk worth of reactivity from the shutdown value of -$6.0 δk (Paramonov and El-Genk, 1994). This step requires approximately 8.5 seconds. The current safety drum drive motor is not wired for reverse rotation, which would provide a redundant backup safety feature. Since these motors are not designed to withstand the harsh radiation environment of an operating reactor, rotation inward could only be possible prior to operation at power.. Therefore, the usefulness of wiring the motor for reverse operation requires analysis of probable startup casualties. The capacity for reverse safety drum operation after full reactor startup requires complete redesign of the motor.
4. Control drums positioned to 154° and back to 145° in accordance with preset limits. Although this step uses open loop control, the ARS regulation is operational and would initiate control drum inward rotation if a set-point is reached. At this stage, ARS action could only occur following some casualty. This regulation is the primary reactor safety response for analysis purposes. The initial control drum movement will provide excess reactivity $0.30 δk at 0 C to $0.70 δk at 70 C. The reactor is now supercritical, with power increasing with period of 20 to 4 seconds, respectively.
5. At Five percent (5%) reactor power, the Minimal Control Level (MCL) for the Russian designed neutron power detectors is reached. Minimal Control Level is that power level in which the neutron power level is sufficiently above

background noise to provide a reliable reading. Inclusion of Self-Powered Neutron Detectors (SPND's) will provide a neutron signal over a wide response range from a low level neutron reading up to approximately eight percent (8%) reactor power. The SPND's will also provide useful telemetry for studying TOPAZ-II startup operation.

6. At one to three percent above MCL, approximately 6-9% power, the neutron power regulator switches on, shifting the ARS to closed loop control. Primary feedback control is provided by neutron power rate regulation; the coolant temperature limit system provides a safety backup.
7. The MCL signal also turns on the electromagnetic (EM) pump, establishing sodium-potassium (NaK) coolant flow at 25% of full flow.
8. When coolant temperature reaches 100 C, the thermal cover ejected.
9. After the coolant has heated to 230 C, the control system provides maximum battery power the EM pump, increasing flow to approximately 50%. The EM pump is supplied in parallel by the load current produced by its three dedicated thermionic fuel elements (TFE's). This current is negligible at this point.
10. At a nominal neutron power level of 110 kW, the upper limit, the neutron regulator stabilizes power.
11. Useful thermionic power is generated as cesium (Cs) pressure increases. The Cs system is warmed up with the NaK system by way of a heat exchanger. The power from the TFE's is converted into heat by a series of load resistors.
12. Once a TFE load current of 60 amps is reached, the cesium vent valve opens. The Helium-Cesium (He-Cs) mixture in the TFE interelectrode gap is replaced by Cs as the He vents out.
13. The power supply system (PSS) regulator switches on when output power reaches a current level $\geq$ 100 amps and a voltage level of $\geq$ 27 volts. The PSS establishes the neutron power set-point, within design limits. The PSS directs TFE power to the payload.
14. Once the PSS is operating, the startup battery switches are opened and the battery electrolyte is vented into space. Electromagnetic pump power is supplied solely by its three TFE's.

15. The startup sequence is complete once the reactor system is producing steady, reliable power. The Russian mission profile allowed for 70 minutes for startup. The time required by the Nuclear Electric Propulsion Space Test Program (NEPSTP) mission will be different, since it will be commenced from a different altitude, and only when the spacecraft is in communications with the ground station.

C. SYSTEMS TESTING

In addition to the non-nuclear testing within the Topaz International Program, TIP, the system has been extensively analyzed within the Russian test program. Among the test results that have a direct effect upon startup control are: the Russian Plant 82 Nuclear Ground Test, in which a loss of coolant accident (LOCA) occurred, and the cesium pressure oscillations observed at testing at the New Mexico Engineering Research Institute (NMERI).

1. Loss of Coolant Accident

A loss of coolant accident occurred after approximately one year of nuclear testing at the Plant 82 ground site. A NaK leak developed from a crack in a weld on an EM pump discharge line (Flight Safety Team, 1992). The initial symptoms of this event were an in increase in the temperature rise across the core of approximately 15 C and current and voltage oscillations. The coolant temperature and pressure conditions led to boiling within the coolant channels, causing power oscillations of about 4 kW_{th}. The loss of flow casualty led to a loss of all coolant as the NaK was released into the vacuum test chamber. The resulting increases in core temperatures led to the deformation of structural materials and the development of cracks within the $ZrH_{1.85}$ reflectors. The release of hydrogen following this damage added enough negative reactivity to shutdown the reactor, even though the operators had attempted to maintain criticality by manually rotating all control drums outward.

This LOCA has several implications for the successful implementation of a ACS design. The system demonstrated the robustness of its design. This accident did not develop into a radiological hazard even though operator action in attempting to maintain power was only compounding the casualty. The TOPAZ-II has a demonstrated structural

safety margin with adequate provisions for heat transfer without coolant to prevent serious damage to the TFE's or the reactor vessel (Flight Safety Team, 1992). Both the U.S. designed ACS and the operating procedures must preclude continued operation following a LOCA.

This accident also highlighted limitations of the temperature sensor package planned for the flight system. There are no in core temperature sensors. The ground system temperature sensors are located on the inlet and outlet coolant pipes. The flight system has sensors on the outlet pipes only. Due to the leak location, these sensors did not detect the coolant temperature increase following the LOCA. Therefore, the temperature limit regulation cannot be relied upon as the sole indication of this type of casualty. Without further supervisory safety monitoring, the ARS would react to the loss of current produced by a LOCA by attempting to increase reactor power. The lessons learned from this incident must be analyzed and incorporated into control system design.

2. Cesium Oscillations

The first TOPAZ-II unit tested as part of the TSET program , the V-71 prototype, experienced periodic oscillations in its output current. The second unit tested, Ya-21U, also exhibited wide swings in power during startup These oscillations were enigmatic since the Russian tests did not reveal this behavior (Morris, et al., 1994). The test facility at NMERI includes a Russian supplied "Baikal" vacuum test stand with U.S. control and monitoring modifications (Wold, 1994). The root cause for these oscillations has been traced to instabilities in cesium pressure (Morris, et al., 1994). The cesium system relies upon a careful balance between pressures and temperatures to supply a constant Cs flow. The presence of cold spots in the Cs system, particularly during startup, disrupts this equilibrium. This effect is significant from a controls system standpoint since the tracking and stabilizing these oscillations is problematic.

The first TOPAZ-II unit tested as part of the TSET program , the V-71 prototype, experienced periodic oscillations in its output current. The second unit tested, Ya-21U, also exhibited wide swings in power during startup These oscillations were enigmatic since the Russian tests did not reveal this behavior (Morris, et al., 1994). The test

facility at NMERI includes a Russian supplied "Baikal" vacuum test stand with U.S. control and monitoring modifications (Wold, 1994). The root cause for these oscillations has been traced to instabilities in cesium pressure (Morris, et al., 1994). The cesium system relies upon a careful balance between pressures and temperatures to supply a constant Cs flow. The presence of cold spots in the Cs system, particularly during startup, disrupts this equilibrium. This effect is significant from a controls system standpoint since the tracking and stabilizing these oscillations is problematic.

VII. STARTUP CONTROL

A. AUTOMATIC REGULATION SYSTEM

Automatic Regulation System (ARS) functions are divided between three separate controllers, as shown in Figure 17. The following parameters apply to the Russian ARS design The Supply Current Regulator establishes the reactor power setpoint based upon TFE supply current, with a ±3.5 amp deadband. The Reactor Power Regulator compares reactor power as measured by the neutron detectors to the this setpoint and sends commands to the Drum Drive Controller. The Reactor Power Regulator deadband is ±250 watt. The Drum Drive Controller directs operation of the control drum motor. The purpose of the coolant temperature limiter is supervisory. If reactor coolant outlet temperature exceeds 585 C, the neutron power setpoint cannot be increased. If the coolant temperature reaches 600 C, the temperature limiter lowers the setpoint, resulting in inward motion of the control drums. The Telemetry and Command System (TCS) provides overall system control.

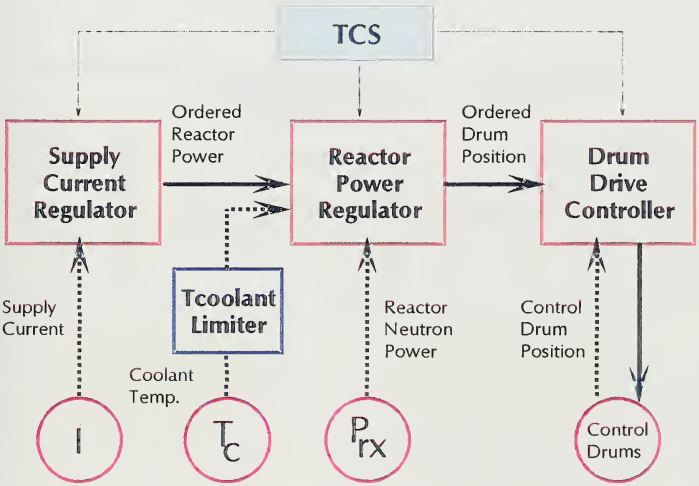

Figure 17. Control System Block Diagram.

This system has two modes of regulation: Startup Mode and Operating Mode. In startup mode, the reactor power follows the preset control band shown in Figure 16 (above). After startup, the regulator shifts to Operating Mode and the Supply Current Regulator establishes the ordered neutron power level. The coolant temperature limiter provides safety override.

B. SYSTEM MODELING

1. Current Models

There are many models available for simulating the TOPAZ-II system. Three models that are of particular interest for startup control design are the Thermionic Transient Analysis Model (TITAM), the Reactor System Dynamic Simulator, and the Sliding Mode Control Model. Figure 18 shows the common elements within these simulations. The neutronic model includes the reactor kinetics equations. The thermal model accounts for the temperature changes throughout the system and provides reactivity feedback to the neutronic model. The electrical model includes the thermionic conversion processes, which affect system temperature through electrical energy transfer. The control system model includes the control law and the control drum drive response.

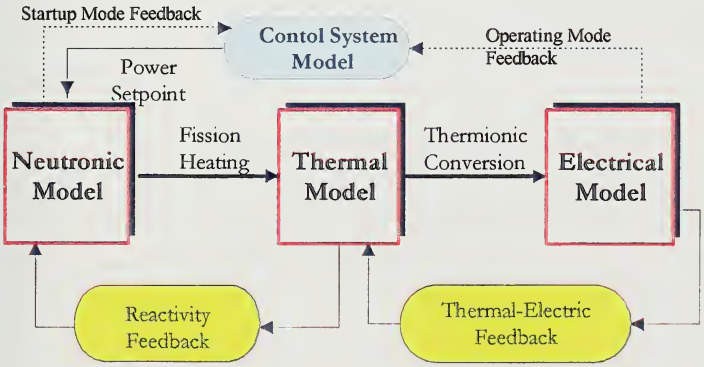

Figure 18. TOPAZ-II Modeling.

a. Comparison of Simulations

Analysis of these three mathematical models is based upon comparison of their component models and an examination of the differences among their results. This permits development of a hybrid control model that incorporates desired features from each simulation.

b. TITAM

The Thermionic Transient Analysis Model is programmed with modular components that simulate the neutronic, thermionic, thermohydraulic, and electrical behavior of the TOPAZ-II system. This model was developed as part of the Topaz International Project research. The program simulates transient and steady-state operation with either fission or electric heating. The equations within this model are based upon a complete, rigorous application of the physics principles behind the TOPAZ-II technology. The TITAM results show excellent agreement with both the Russian simulations and measurements taken at the TSET facility. (Paramonov and El-Genk, 1994). Since a benchmark of this simulator has been successfully performed, the hybrid control model will use its equations unless there is sufficient justification for another choice. The authors also generously provided a modified version of the TITAM simulation that would allow analysis of step power transients and the determination of equilibrium conditions at different power levels.

c. Reactor System Real-time Dynamic Simulator

The TOPAZ-II Reactor System Real-time Dynamic Simulator is an IBM PC based system that was designed as a test system for TOPAZ-II Reactor Control Unit (RCU) development and qualification. The simulator model has certain limitations. The neutronic calculations are derived from the same analysis as the TITAM; however, the thermohydraulic and electrical models are based upon empirical correlation using first order linear differential equations. The purpose behind this simplification was to allow for real-time computation, a requirement of RCU testing. The Real-time Dynamic Simulator does not model the behavior of several subsystems, including the Electromagnetic (EM) pump, the batteries, and many of the gas systems. Another of its limitations is that the effect of

gear backlash is not included. Within these constraints, the Dynamic Simulator provides a reasonable approximation of TOPAZ-II behavior. Its response outside the a linear range of these approximations must be analyzed.

d. Sliding Mode Control Model

Sliding mode control is a variable structure control technique that uses an robust control structure. The use of high speed switching enables high accuracy, robust control of system response within a specially designed regime (called a sliding manifold). Yuri B. Shtessel developed a sliding mode control design for the TOPAZ-II system as part of research funded by the United States Air Force Office of Scientific Research (Shtessel, 1994). The mathematical modeling in the derivation of the control law includes a physics-based reactor kinetics model, a sophisticated model of the control drum drive, and a limited thermal and electrical model. The reactivity feedback model only includes the effect of moderator temperature changes and therefore does not account for the expected initially negative feedback from increasing system temperatures. The thermal model only tracks moderator and fuel temperatures. The electrical model assumes a constant cesium pressure, which does not fully account for thermionic startup conditions.

2. Reactor Kinetics

All three models use reactor kinetics formulae based upon the theory presented in Chapter III. (For convenience, Equations **(6)** and **(7)** are repeated below). The only difference is in the treatment of $Q(t)$, the fission equivalent source term. This is the value of initial neutron power for a reactor that has never been operated at high power. In the TITAM model, $Q(t)$ is set to zero. Power initialization is accounted for elsewhere within TITAM programming. In both the Reactor Simulator and the Sliding Mode equations, $Q(t) = 1.46 \times 10^{-5}\ {}^{W}/_{s}$.

$$\frac{dP(t)}{dt} = \frac{\rho(t) - \bar{\beta}(t)}{\ell^*} P(t) - \sum_{i=1}^{N} \lambda_i C_i(t) + Q(t)$$

$$\frac{dC_i(t)}{dt} = \frac{\beta_i}{\ell^*} P(t) - \lambda_i C_i(t) \quad (i = 1, N)$$

where: P = reactor power (W)

$\overline{\beta}$ = effective delayed neutron fraction

ρ(t) = reactivity

λ_i = delayed neutron fraction of ith group

β_i = decay constant of the delayed neutron precursor

ℓ^* = prompt neutron lifetime

C_i = equivalent delayed neutron precursor concentration

$Q(t)$ = fission equivalent source power

N = number of delayed neutron precursor groups

3. Reactivities[1]

There are differences within the reactivity modeling in each simulation. All of the simulations include control drum reactivity. The Sliding Mode Control Model only accounts for the temperature feedback reactivity of the moderator, the dominant term. The impact of this simplification requires analysis. A comparison of the differences among each model follows.

a. Control drums

The power regulation system sets control drum reactivity for reactor control. The value of the drum reactivity is initially negative since the drums contain reactor poison plates. Outward rotation of the drums reduces the magnitude of this negative reactivity, thus adding positive reactivity to the core. The control drum reactivity reported in TITAM is derived from personal communications with Russian researchers in 1992 and is given below as Equation (10) (Paramonov and El-Genk, 1994). The source of the Equation (11), which is used within the Reactor Simulation Model and the Sliding Mode Control Model, is from personal communications in 1993 (Kwok, 1994). The value of ϕ, the initial drum reactivity, has a range of possible values due to uncertainties in the description of the feedback reactivity of the reactor (Shtessel, 1994). The existence of these

[1] All reactivities in this section are reported in units of 10^{-2} ($'s).

uncertainties makes an adaptive control scheme an appropriate choice for this type of system.

$$\rho_{\substack{Drums \\ (TITAM)}}(\theta) = 9.41\times10^{-11}\theta^5 - 3.57\times10^{-8}\theta^4 + 2.21\times10^{-6}\theta^3 + \ldots + 3.72\times10^{-4}\theta^2 - 2.5\times10^{-3}\theta + \phi \quad (10)$$

$$\rho_{\substack{Drums \\ (Sliding)}}(\theta) = 6.89\times10^{-11}\theta^5 - 2.33\times10^{-8}\theta^4 + 3.28\times10^{-7}\theta^3 + \ldots + 4.57\times10^{-4}\theta^2 - 5.88\times10^{-3}\theta + \phi \quad (11)$$

where: ρ_{Drums} = control drum reactivity ($)
θ = drum angle (°)
ϕ = initial reactivity ($)

The resulting reactivity values for these equations are graphed in Figure 19 below. The data reveal the maximum difference to be about ten percent of the peak value with similar curve shapes for each equation. The formula shown in Equation (11) will be used in the hybrid control model since it is the most current curve-fit in the literature. This is a conservative choice from a controls standpoint since the Reactor Simulator and Sliding Mode Control models have a lower absolute range of reactivity, which limits control authority.

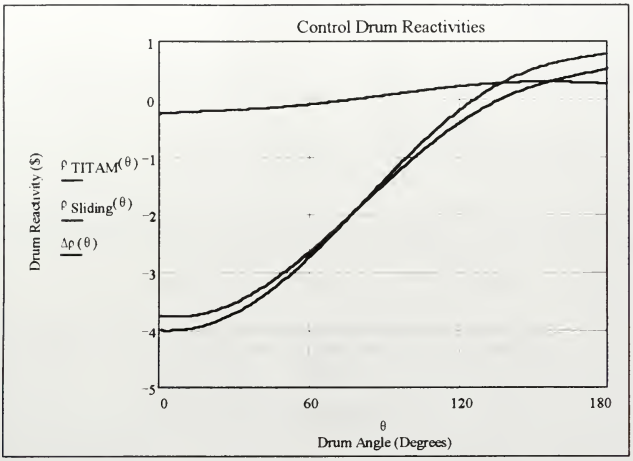

Figure 19. Control Drum Reactivities.

b. Moderator

Moderator reactivity is an important parameter and is the largest contributor to the overall temperature reactivity. As shown in Figure 20, moderator reactivity is positive; therefore, an increase in moderator temperature adds positive feedback. The TITAM model uses a two piece fit, as given in Equation (12). Both the Reactor Simulator and the Sliding Mode models use the same polynomial approximation shown in Equation (13). The TITAM equation had a typographical error in the source document, report No. UNM-ISNPS-3-1994. Equation (12) below is derived from personal communications with the authors (Paramonov and El-Genk). Since the TITAM model has a slight discontinuity (see Figure 20), Equation (13) is preferred for startup control modeling. The Sliding Mode model has higher reactivity values, resulting in more positive feedback. This worst-case feedback effect justifies the choice as a cautious decision.

$$\rho_{\substack{Moderator \\ (TITAM)}} = 60 \cdot f(x) - 1.04 \times 10^{-3}(T_m - T_0) \qquad (12)$$

$$\text{where } f(x) = 0.007413\left(\frac{T_m}{T_0}\right)^2 + 0.006795\left(\frac{T_m}{T_0}\right) - 0.014208, \quad \text{for } 1 \le \frac{T_m}{T_0} \le \frac{T_0 + 175}{T_0}$$

$$= 0.03027\sqrt{\left(\frac{T_m}{T_0}\right) - \frac{T_0 + 100}{T_0}}, \quad \text{for } \left(\frac{T_m}{T_0}\right) \ge \frac{T_0 + 175}{T_0}$$

$$\rho_{\substack{Moderator \\ (Sliding)}} = -8.22 \times 10^{-14}(T_m - T_0)^5 + 1.60 \times 10^{-10}(T_m - T_0)^4 - 1.11 \times 10^{-7}(T_m - T_0)^3 + \ldots$$
$$+ 2.92 \times 10^{-5}(T_m - T_0)^2 + 1.76 \times 10^{-3}(T_m - T_0) \qquad (13)$$

where: $\rho_{Moderator}$ = moderator reactivity ($)
T_m = moderator temperature (K)
T_0 = reference temperature (K)

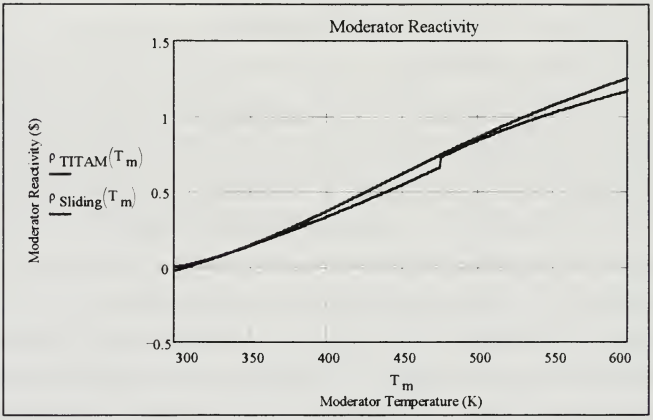

Figure 20. Moderator Reactivity.

c. *UO_2 Fuel*

The TITAM modeling uses a single function in its fuel reactivity formula, Equation (14), derived from 1993 research (Paramonov and El-Genk, 1994). The Reactor Simulator uses a two piece model, Equation (15). The Reactor Simulator model is derived from an initial report (Gunther, 1992) and uses a linear extrapolation for values above 800 K. The choice of constants for this linear fit portion produced the discontinuity

shown in Figure 21. Additionally, there is a large divergence between the two models in the calculated fuel reactivity at higher temperatures, a region of particular interest for reactor casualty analysis. The poor fit between the two parts of Equation (15) lead to the choice of the TITAM fuel reactivity formula for the hybrid control model. The TITAM model also has lower absolute values, making it a conservative choice for startup control since fuel temperature reactivity adds prompt negative feedback, aiding stability. Using a lower magnitude of fuel reactivity lowers the simulated feedback effect.

$$\rho_{\substack{Fuel \\ (TITAM)}} = 0.432 \times 10^{-3}(T_f - T_0) - 0.64\left(\sqrt{\frac{T_f}{T_0}} - 1\right) \qquad (14)$$

$$\rho_{\substack{Fuel \\ (Simulator)}} = 1.2 \times 10^{-3}(T_f - T_0) - 1.38\left(\sqrt{\frac{T_f}{T_0}} - 1\right), \; T_f < 800\ K \qquad (15)$$

$$= -1.0 \times 10^{-1} - 2.2 \times 10^{-4}(T_f - T_0), \text{ for } T_f \geq 800\ K$$

where: ρ_{Fuel} = fuel reactivity ($)

T_f = fuel temperature (K)

T_0 = reference temperature (K)

Note: The TOPAZ II Reactor System Real-time Dynamic Simulator report (Kwok, 1993) gives a value of -2.2×10^{-2} $/K for the slope of the fuel reactivity with respect to fuel temperature. The value of -2.2×10^{-4} $/K is taken from the simulator program code directly.

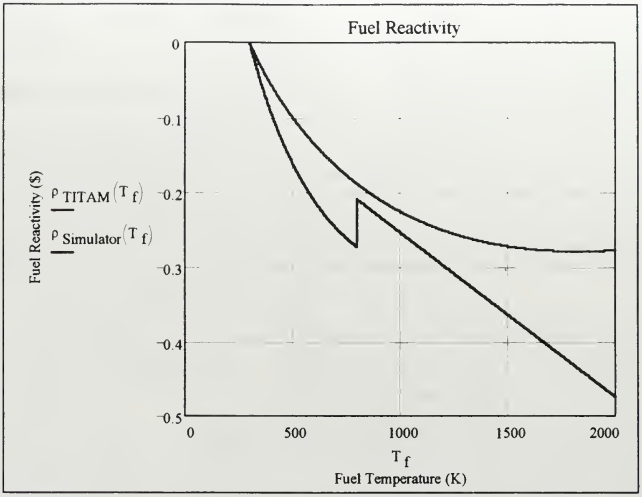

Figure 21. Fuel Reactivity.

d. Core Plates

Both the TITAM and Reactor Simulator models use a linear approximation for the core support plate reactivity (see Equation (16) and Equation (17), below). The core plate reactivity is nearly equal to the fuel reactivity over the same range of temperatures. Since the time heating profile is different for each core component, the overall reactivity effect of core plate heating is reduced. This phenomenon will be analyzed after presentation of the other reactivity models.

$$\underset{(TITAM)}{\rho_{cp}} = -1.44 \times 10^{-4}(T_{cp} - T_0) \qquad (16)$$

$$\underset{(Simulator)}{\rho_{cp}} = -2.22 \times 10^{-4}(T_{cp} - T_0) \qquad (17)$$

where: ρ_{cp} = core plate reactivity ($)

T_{cp} = core plate temperature (K)

T_0 = reference temperature (K)

e. Reflector

The beryllium reflector has a positive temperature coefficient of reactivity, as shown in Equation (18) and Equation (19). The value of this reactivity is significant to control system design since reflector ejection results in the loss of this positive reactivity, establishing the net negative reactivity required for shutdown.

$$\underset{(TITAM)}{\rho_{ref}} = 0.36\left(1 - \sqrt{\frac{T_0}{T_{ref}}}\right) \qquad (18)$$

$$\underset{(Simulator)}{\rho_{ref}} = 0.38\left(1 - \sqrt{\frac{T_0}{T_{ref}}}\right) \qquad (19)$$

where: ρ_{ref} = reflector reactivity ($)
T_{ref} = reflector temperature (K)
T_0 = reference temperature (K)

f. Electrodes

Calculation of the reactivity of the electrode is slightly more complex since the TITAM and Reactor Simulator models, Equations (20) and (21) respectively, depend upon both the emitter and collector temperatures. Figure 22 shows the calculated electrode reactivity profile for the first 1000 seconds of a startup.

$$\underset{(TITAM)}{\rho_e} = -0.12\left(\sqrt{\frac{T_e}{T_0}} - 1\right) - 7.44 \times 10^{-2}\left(\sqrt{\frac{T_c}{T_0}} - 1\right) \qquad (20)$$

$$\underset{Simulator}{\rho_e} = 8.52 \times 10^{-2} - 4.26 \times 10^{-2}\left(\sqrt{\frac{T_e}{T_0}} + \sqrt{\frac{T_c}{T_0}}\right) \qquad (21)$$

where: ρ_e = electrode reactivity ($)
T_e = emitter temperature (K)
T_c = collector temperature (K)
T_0 = reference temperature (K)

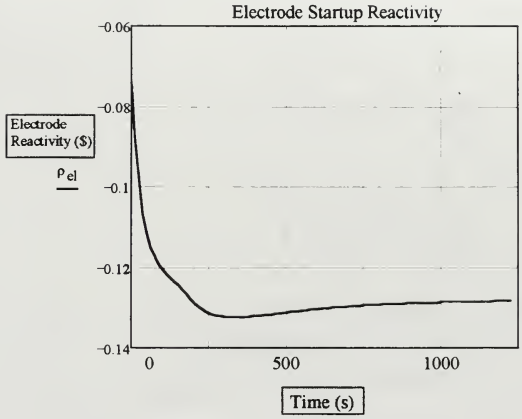

Figure 22. Electrode Reactivity During Startup.

g. Reactivity Analysis

Temperature reactivity forms the major feedback mechanism during startup. Consideration this reactivity is crucial to control system development. The validity of assumptions used within each model requires investigation. Each component heats up during startup, contributing its own reactivity value to the net core reactivity. Figure 23 shows the net temperature reactivity feedback values calculated using the hybrid control model. The net reactivity line shown demonstrates the dominance of the moderator's temperature effect upon the system. This line is for comparison purposes only, since it give the net value for an isothermal core. Since the temperature differences among components during operation is substantial, the temperature reactivity must be examined during transient conditions.

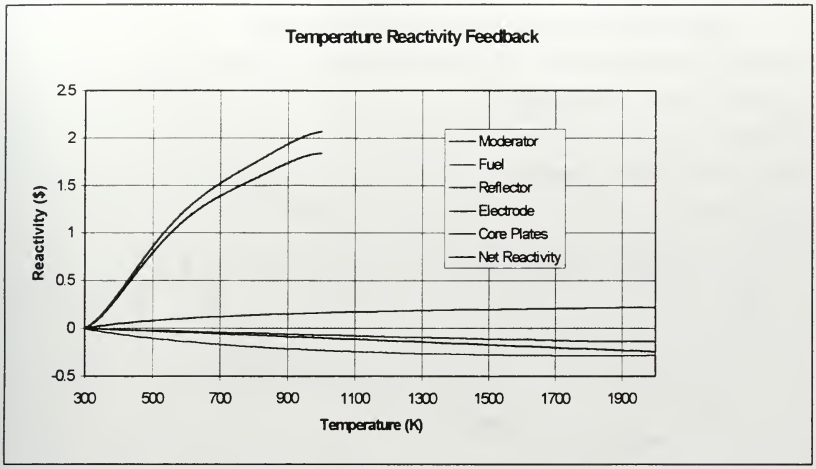

Figure 23. Temperature Reactivity Feedback.

The temperature changes following a step power increase from 5% to 95% full fission power were calculated using the TITAM simulation. The hybrid model reactivity equations simulates the reactivity behavior for this transient shown in Figure 24. This computation shows that the positive feedback effect of the moderator reactivity has a substantial time delay. The net reactivity is still negative until approximately six minutes after the step power increase. Analysis performed for the *Preliminary Nuclear Safety Assessment* obtained similar results (Flight Safety Team, 1992). This provides a gauge for the fidelity of the hybrid reactivity equations. The Reactor Simulator model yields a comparable reactivity profile as long as its thermal modeling is adequate. Since the Sliding Mode Control Model only includes the moderator reactivity, its simulation would not account for the initial negative feedback. The impact of this deficiency requires additional analysis.

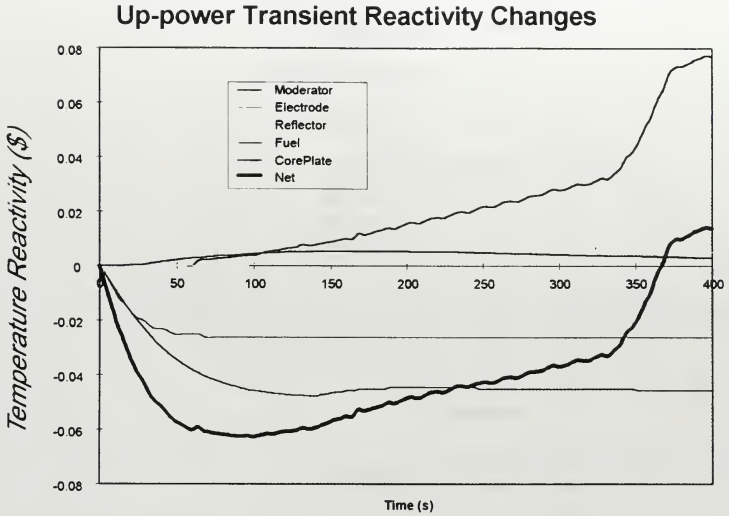

Figure 24. Reactivity Changes Following Up-power Transient.

4. Thermal Model

Among the available models, TITAM has the most complete thermal-hydraulic equations. The TITAM simulator results correlate well with measured data (Paramonov and El-Genk, 1994). The Reactor Simulator uses simple first-order exponential build-up equations, based upon empirical estimates of the system step-power response. *The Reactor Simulator User's Guide and Reference Manual* does not indicate any final comparison of its simulation results to established data (Kwok, 1993). The Sliding Mode Control Model also has first order approximations for thermal modeling; however, its results were compared favorably with the TITAM data (Shtessel, 1994). The hybrid control model uses somewhat simplified versions of the TITAM thermal equations. Also, the hybrid control model does not contain the additional refinements in the TITAM model that account for axial effects. The system temperature equations are provided roughly in order from the core (heat source) to the radiator (heat sink). Each symbol will be defined upon its initial use.

a. Fuel Temperature

The heat transfer relationship shown in Equation (22) is modified from the TITAM modeling in that it does not account for the fuel gap void. This space is between the UO_2 fuel pellets and the inner surface of the emitter. The fuel gap disappears as the fuel expands and fuses in the available space (Flight Safety Team, 1992). After the gap is filled, the heat transfer mode through the gap shifts from radiative to conductive. The TITAM model includes this transition stage. This effect is not included in the hybrid control model.

$$M_f Cp_f \frac{dT_f}{dt} = P - h_f A_f (T_f - T_e) \qquad (22)$$

Where M_f = fuel mass (kg)

Cp_f = fuel heat capacity $\left(\frac{\mathrm{W}}{\mathrm{kg \cdot K}}\right)$

P = thermal power (W)

T_f = fuel temperature (K)

h_f = fuel heat transfer coefficient $\left(\frac{\mathrm{W}}{\mathrm{m^2 \cdot K}}\right)$

A_f = fuel area $\left(\mathrm{m^2}\right)$

T_e = emitter temperature (K)

b. Emitter Temperature

The emitter temperature equation is derived from an energy balance dividing heat from the fuel between the transfer to the collector and the energy losses due to electron cooling and electrical lead losses. The electric power variables in Equation (23) are calculated with the equations described in the Thermionic Emission Model section of this chapter.

$$M_e Cp_e \frac{dT_e}{dt} = h_f A_f (T_f - T_e) - h_e A_e (T_e - T_c) - P_{ec} + \tfrac{1}{2} P_{jle} \qquad (23)$$

Where M_e = emitter mass (kg)

Cp_e = emitter heat capacity $\left(\frac{\mathrm{W}}{\mathrm{kg}\cdot\mathrm{K}}\right)$

T_e = emitter temperature (K)

h_e = emitter heat transfer coefficient $\left(\frac{\mathrm{W}}{\mathrm{m}^2\cdot\mathrm{K}}\right)$

A_e = emitter area $\left(\mathrm{m}^2\right)$

T_e = emitter temperature (K)

T_c = collector temperature (K)

P_{ec} = electron cooling power (W)

P_{jle} = joule heating loss (W)

c. Electrode Gap Temperature

$$M_g Cp_g \frac{dT_g}{dt} = h_e A_e (T_e - T_g) - h_g A_g (T_g - T_c) \qquad (24)$$

Where M_g = gap mass (kg)

Cp_g = gap heat capacity $\left(\frac{\mathrm{W}}{\mathrm{kg}\cdot\mathrm{K}}\right)$

T_g = gap temperature (K)

h_g = gap heat transfer coefficient $\left(\frac{\mathrm{W}}{\mathrm{m}^2\cdot\mathrm{K}}\right)$

A_g = gap area $\left(\mathrm{m}^2\right)$

d. Adjusted Gap Conductance $\left(h_g\right)$

The calculation of the gap heat transfer coefficient is somewhat complex it involves radiative heat transfer through cesium plasma when the system reaches operating temperatures. The gap contains helium gas at startup that is eventually replaced by cesium. TITAM simulates this effect with a linear exchange rate that is adjustable by the user.

$$h_g = \frac{k_g}{d_g} + 3\sigma\varepsilon^{eff} T_g^3 \qquad (25)$$

Where h_g = gap heat transfer coefficient $\left(\frac{\mathrm{W}}{\mathrm{m}^2 \cdot \mathrm{K}}\right)$

k_g = gap conductivity $\left(\frac{\mathrm{W} \cdot \mathrm{m}}{\mathrm{kg} \cdot \mathrm{K}}\right)$

σ = Stephan - Boltzman's constant

$\left(6 \times 10^{-12} \frac{\mathrm{W}}{\mathrm{m}^2 \cdot \mathrm{K}^4}\right)$

ε^{eff} = effective gap emissivity

T_g = gap temperature (K)

e. Cs Vapor Conductivity $\left(k_g\right)$

$$k_g = \frac{1.10 \times 10^{-6}\left(\frac{T_e^{1.5} - T_c^{1.5}}{T_e - T_c}\right)}{d_g + 1.14 \times 10^{-5}\left(\frac{T_e + T_c}{P_{cs}}\right)} \qquad (26)$$

Where k_g = gap conductivity $\left(\frac{\mathrm{W} \cdot \mathrm{m}}{\mathrm{kg} \cdot \mathrm{K}}\right)$

d_g = gap size (m)

T_e = emitter temperature (K)

T_c = collector temperature (K)

P_{Cs} = cesium pressure (Torr)

f. Cs Gap Effective Emissivity

$$\varepsilon^{eff} = 0.142 + {}^{1.26 \times 10^{-5}}\!/_{\mathrm{K}} \cdot T_e \qquad (27)$$

Where ε^{eff} = effective gap emissivity

T_g = gap temperature (K)

g. Collector Temperature

The collector temperature is calculated with Equation (28). This is simplified from the TITAM model by not determining the insulator and clad temperatures directly. The temperature differences between these elements is minimal due to the high heat transfer coefficients of the TFE materials. The collector mass and heat capacities values in the hybrid model are modified to account for the insulator and clad. This change maintains accuracy with a desirable reduction of the number of points in the heat transfer model.

$$M_c Cp_c \frac{dT_c}{dt} = h_g A_g (T_g - T_c) - h_c A_c (T_c - T_{NaK}) + P_{ec} + \tfrac{1}{2} P_{jle} - P_e \qquad (28)$$

Where M_c = collector mass (kg)

Cp_c = collector heat capacity $\left(\frac{\mathrm{W}}{\mathrm{kg}\cdot\mathrm{K}}\right)$

T_g = electrode gap temperature (K)

h_c = collector heat transfer coefficient $\left(\frac{\mathrm{W}}{\mathrm{m}^2\cdot\mathrm{K}}\right)$

A_c = collector area $\left(\mathrm{m}^2\right)$

T_{NaK} = coolant temperature (K)

T_c = collector temperature (K)

P_{ec} = electron cooling power (W)

P_{jle} = joule heating loss (W)

P_e = electric power (W)

h. Coolant Bulk Temperature

$$M_{NaK} Cp_{NaK} \frac{dT_{NaK}}{dt} = h_c A_c (T_c - T_{NaK}) - 2\dot{m} Cp_{NaK} (T_{NaK} - T_{inlet}) \qquad (29)$$

Where M_{NaK} = coolant mass (kg)

Cp_{NaK} = coolant heat capacity $\left(\frac{\mathrm{W}}{\mathrm{kg}\cdot\mathrm{K}}\right)$

T_{NaK} = coolant bulk temperature (K)

h_c = collector heat transfer coefficient $\left(\frac{\mathrm{W}}{\mathrm{m}^2\cdot\mathrm{K}}\right)$

A_c = collector area $\left(\mathrm{m}^2\right)$

T_c = coolant temperature (K)

$\dot{m}$ = collector flow rate $\left(\mathrm{kg}/\mathrm{s}\right)$

T_{in} = coolant inlet temperature (K)

5. Thermionic Emission Model

The TITAM model includes much detailed analysis of the thermionic process. However, since the system startup does not include steady state control of electric power, certain simplifications are in order. Both the Reactor Simulator and the Sliding Mode Control Model use linear first order approximations. The hybrid control model includes simplified thermionic equations with the other power calculations required in its thermal model.

a. Electron Cooling

This term accounts for the heat transfer in form of electron flow across the interelectrode gap. As much as 20% of the thermal power is transferred by this mechanism (Flight Safety, 1992). The equation for the emitter work function, ϕ_e, is found within the Chapter III, Basic Theory.

$$P_{ec} = JA_e\left(\frac{\phi_e}{e} + \frac{2k_B T_e}{e}\right) \qquad (30)$$

Where J = current density $\left(\mathrm{A}/\mathrm{m}^2\right)$

A_e = emitter area $\left(\mathrm{m}^2\right)$

φ_c = emitter work function (eV)

k_B = Boltzmann's Constant

$\left(1.38 \times 10^{-23}\ \mathrm{J}/\mathrm{K}\right)$

e = fundamental unit of charge (C)

$\dot{m}$ = collector flow rate $\left(\mathrm{kg}/\mathrm{s}\right)$

T_{in} = coolant inlet temperature (K)

T_e = emitter temperature (K)

b. Lead Joule Heating

$$P_{jle} = \left(JA_{le}\right)^2 R_{le} \tag{31}$$

Where J = current density $\left(\mathrm{A}/\mathrm{m}^2\right)$

A_e = emitter area $\left(\mathrm{m}^2\right)$

φ_c = emitter work function (eV)

k_B = Boltzmann's Constant

$\left(1.38 \times 10^{-23}\ \mathrm{J}/\mathrm{K}\right)$

e = fundamental unit of charge (C)

$\dot{m}$ = collector flow rate $\left(\mathrm{kg}/\mathrm{s}\right)$

T_{in} = coolant inlet temperature (K)

T_e = emitter temperature (K)

c. Thermionic Current

$$\frac{dI}{dt} = -0.11\left(I - 0.37k_c P\right) \tag{32}$$

Where I = thermionic current (A)
k_c = conversion efficiency
P = reactor power (W)

d. Thermionic Power

$$\frac{dP_e}{dt} = -0.11\left(P_e - 0.37k_cP\right) \quad (33)$$

Where P_e = thermionic power (W)
k_c = conversion efficiency
P = reactor power (W)

6. Control Drum Model

The control drum is essential for control system design. The TITAM model does not include the control drum and stepper motor characteristics. The Reactor Simulator does not account for the hysteresis and backlash within this component. Only the Sliding Mode Control Model has complete equations for simulation.

7. Hybrid Control Model

The hybrid control model uses the equations discussed within the previous sections. The TITAM analysis report provided the values for most material and system parameters (Paramonov and El-Genk, 1994). The material properties are found within the Appendix of the same report. An additional approximation within the hybrid model is the use of linear values for many of the temperature dependent parameters such as thermal conductivity. The major exception to this simplification was for the thermal conductivity of the UO_2 fuel, which exhibits a large non-linear range of values over the temperatures of interest. For this material, the exponential approximation given in the Appendix of the TITAM report is incorporated with the hybrid system model. For most materials, temperature effects are easily accommodated by incorporating temperature dependent terms within the heat transfer equations.

a. Hybrid Model Implementation

The model is developed using Simulink®. The overall system diagram is shown in Figure 25. For comparison, note the correlation of this block diagram with the Automatic Regulating System described in Figure 17. Each system block contains the appropriate section of the simulation. The Matlab® function block within each group contain the differential equations that form the system control model. The regulating block calculates the appropriate control drum commands for each mode of operation. The control drum calculates control drum angle after receiving the stepper motor commands from the regulating system block. The reactivity block calculates the net reactivity based upon temperature feedback and control drum position. The reactor model block determines reactor fission power and delayed neutron precursor concentrations. The thermal model calculates the resulting system temperatures based upon the fission power signal. The thermionics block determines the resulting electrical power parameters.

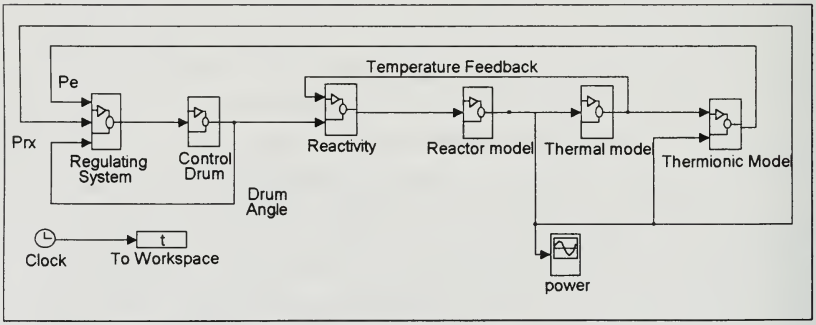

Figure 25. Simulink® Implementation of Hybrid Control Model.

The regulating system block presented in Figure 26 develops a control drum stepper motor signal. This block simulates the two basic modes of operation, startup and operating, and controls the stepper motor during the initial drum positioning during the startup sequence.

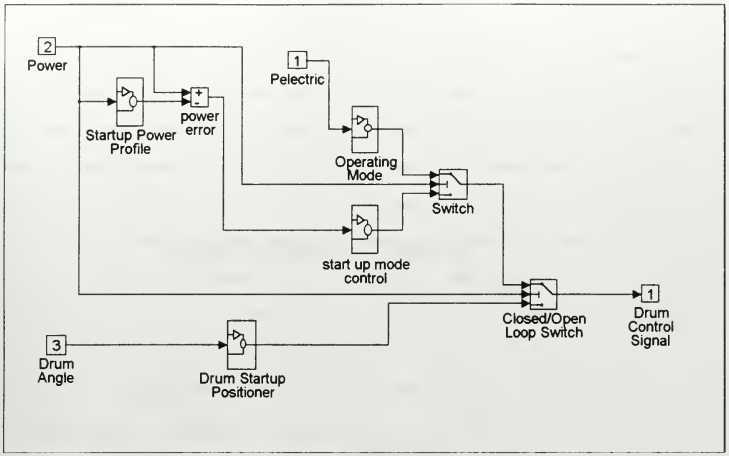

Figure 26. Regulating System Block.

The regulating system block has different modes of behavior based for each stage within the startup. Each model includes an adjustable deadband to preclude system hunting. As noted earlier, limitations of the TOPAZ-II nuclear instruments result unreliable power level readings at low fission rates. Therefore, the initial drum positioning is in accordance with a programmed sequence. The drums are rotated out to 154° and then back in to 145°. This open loop behavior is accomplished with the block given in Figure 27.

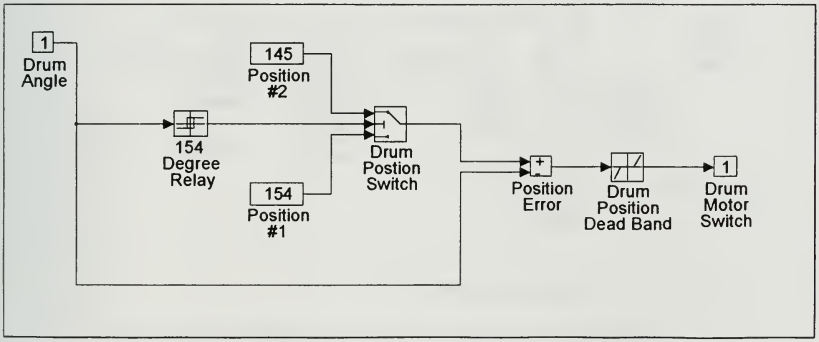

Figure 27. Startup Drum Positioning.

During startup mode, the reactor power must be controlled within the power rate limitations of 600 W/s, when power is less than 35 kW, and 80 W/s when power is above that setpoint (See **Figure 16**, above). This operating envelope is achieved using the Startup Power Profile block shown below, Figure 28. This block implements of the power rate limit by shifting to the lower power rate if power should exceed the setpoint. Thus, the lower limit may be set sooner than predicted if power overshoots the ordered level. Also, the higher power rate limit will be used if the power should undershoot during startup. Note that the overall goal of this design was to approximate the envelope. There is no provision to limit power for instantaneous levels that exceed the limits. Since the Russian designed controller produces short periods of power rate overshoot, strict adherence is not essential (Shtessel, 1994). The limits themselves are based upon material concerns which are dependent upon the duration of heat-up rate excursions. Should further analysis indicate that the heat-up rates are excessive, it would be easy to incorporate such an instantaneous heat-up rate limiting feature within this existing design.

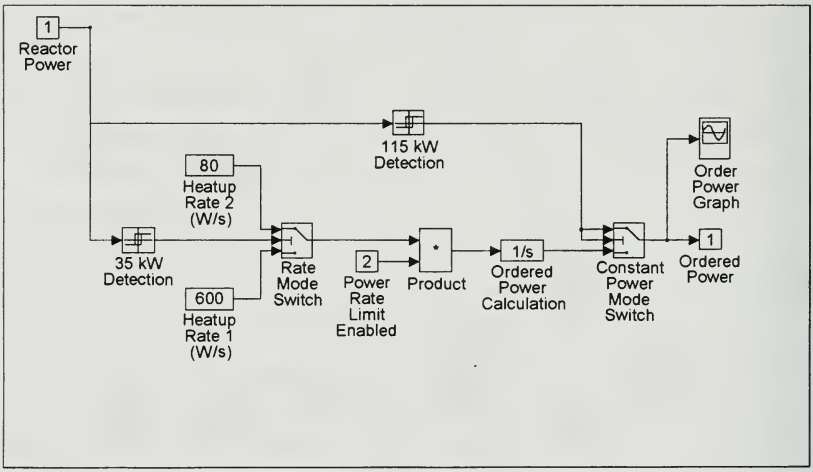

Figure 28. Startup Mode Power Profile Block.

Figure 29 shows the construction of the Reactor Model block. The Reactor Simulator and Sliding Mode Models are easily investigated by replacing the Matlab® file for the function block with one developed for the respective model. Figure 30

shows simplification that may be used when the reactor is sub-prompt critical; that is, core reactivity is less than the value of the effective delayed neutron fraction and power is changing relatively slowly. This simplification was validated by the TITAM simulation report (Paramonov and El-Genk, 1994). Non fission heating in a nuclear reactor is primarily due to radioactive decay of fission products after full power operation.

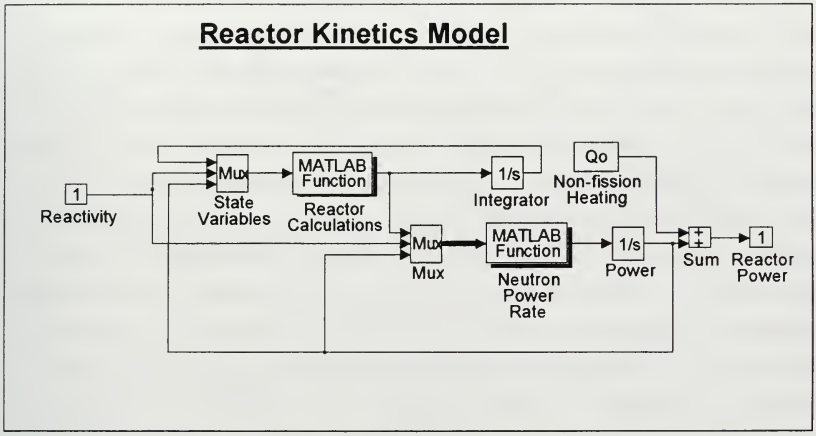

Figure 29. Reactor Model Details.

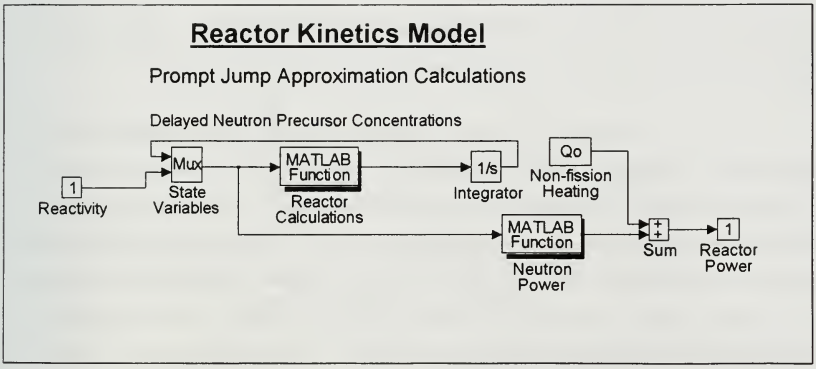

Figure 30. Reactor Model - Prompt Jump Approximation Implementation.

b. Model Evaluation

The following section assesses the overall effectiveness of the resulting model. The thermal model is validated by comparing simulated temperature behavior to a predetermined power history without temperature feedback. Another benchmark was provided by examining the data obtained from power changes performed upon the single TFE experiment rig. The hybrid model was compared to the TITAM results for a step up-power maneuver from 5% to 95% power following a system startup. A step power maneuver was chosen in order to isolate such non-linear effects as cesium filling and the ejection of the radiator. The differences between the reactivity equations for these models are minor; therefore, both of these simulations were examined in an open loop mode. This was accomplished in the TITAM simulation by simulating heating from TFE resistors, rather than the fission source. For the hybrid control model, the reactivity temperature feedback was set to zero, leaving only the control drum reactivity. As shown in Figure 31, there is a good match between the results of both simulations. However, the temperature rise following TFE loading in the hybrid model results does not agree with experimental data. Examination of the underlying equations reveals that this discrepancy is caused by a 1.6% difference in the steady state values to temperature at the 100% power level. Since this error is relatively small and does not significantly impact the start-up parameters, the simulation was not altered. As shown by the model response to the step power changes, the model tracks expected behavior in other respects. The fuel temperature response is shown; the results for the other parameters of concern are similar.

For further analysis, the hybrid control model was replaced by the Reactor Simulator Model and then the Sliding Mode control model for comparison to the TITAM data. The Reactor Simulator Model has some discrepancies. It appears that the time constants chosen for this model require refinement. Figure 32 shows the equilibrium fuel temperatures obtained from TITAM simulations. The non-linear behavior can be expected since the NaK coolant flow also has electrical power dependence. The Sliding Mode Control Model has better correspondence with TITAM for the two temperatures it tracks. However, the since the Sliding Mode Control Model does not include any negative temperature feedback, a different analysis would be required to benchmark this simulation.

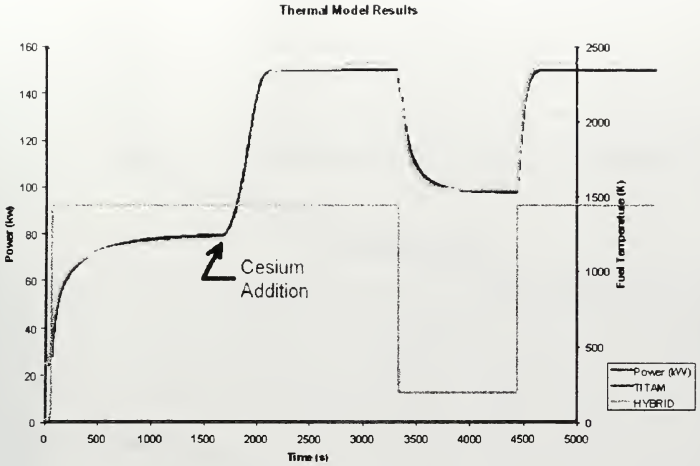

Figure 31. Thermal Model Comparison.

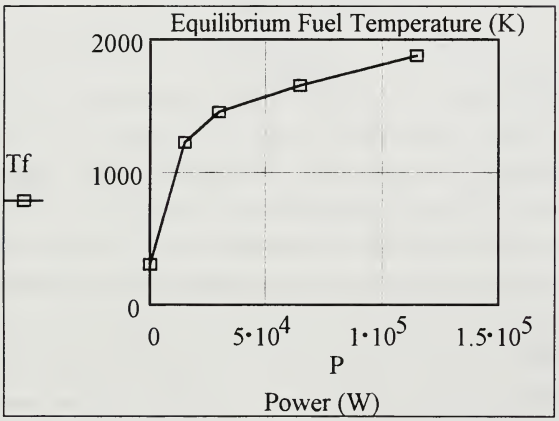

Figure 32. Equilibrium Fuel Temperatures.

The validity of the reactor model section and its compatibility with the thermal model was verified by using the net reactivity from TITAM data as input. The resulting system response compared favorably, as shown in Figure 33. The power response

shows a noise component. These oscillations are primarily artifacts induced by the time intervals chosen for the integration of the differential equations. The magnitude of this deviation can be greatly reduced by reducing length of these time steps. However, the times required for calculations are greatly increased. This phenomenon is important for the analysis of the Sliding Mode controller, and will be considered next.

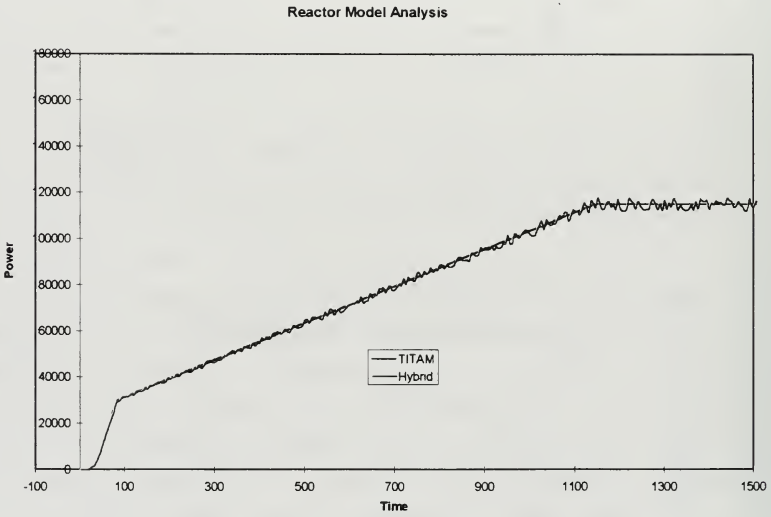

Figure 33. Reactor Model Evaluation.

By restoring the temperature feedback effect, analysis of the lack of negative feedback within the Sliding Mode Control Model is possible. The control drum reactivities were used for comparison in order to track the differences between the control system response in both cases. Figure 34 presents the resulting control drum reactivities for the Hybrid model, which incorporates the negative feedback, and the Sliding Mode model, which does not. As can be easily seen, the magnitude of the error produced by disregarding negative is not significant.

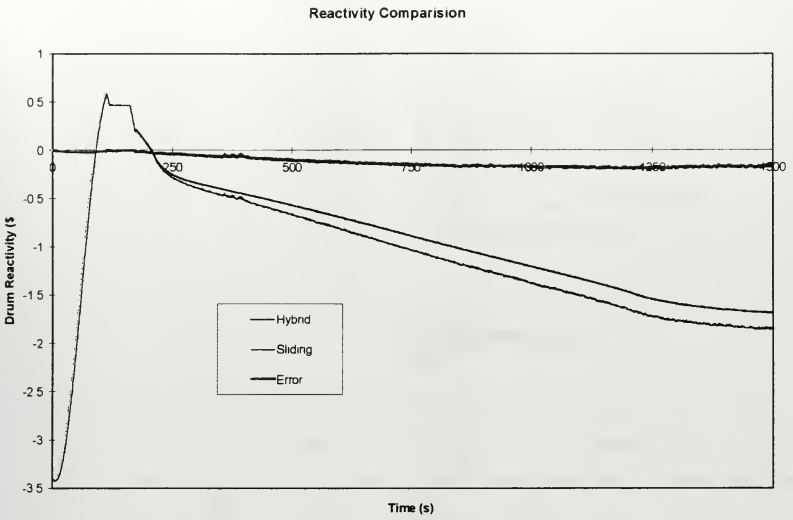

Figure 34. Negative Feedback Comparison.

C. CONTROL SYSTEM DESIGN

Since the system incorporates both neutron power and current control regimes, two distinct control laws are required for regulating system design. There are two different regulation schemes available for analysis. The original Russian design proposed a proportional feedback law for neutron power regulation and a fixed power rate change for payload current regulation. This programming is included in the Reactor Simulator code (Kwok). The Sliding Mode Control research includes control laws for adaptive control.

Sliding control is a useful approach to systems with imprecise models or measuring. Such a control scheme is appropriate for the TOPAZ-II system since the feedback parameter, reactor power as measured by neutron current, can have a large degree of uncertainty (on the order of 50%). Since these detectors cannot be calibrated after launch, their accuracy over time is uncertain. Sliding control is a robust control scheme that applies an optimization process upon the error function. This error function is modeled as a series of nth order differential equations. The optimization process is obtained by minimizing the integral of time multiplied by the absolute error. For neutron and current regulation, the

sliding surfaces given in Equation (34) were derived from the hybrid equations developed above.

$$\sigma_1 = \eta'' + 0.759\eta' + 0.327 = 0$$
$$\sigma_2 = \varepsilon''' + 2.68\varepsilon'' + 1.944\varepsilon' + 0.639\varepsilon = 0 \qquad (34)$$

where: $\eta = P - P_{ordered}$
= power tracking error

$\varepsilon = I - I_{ref}$
= current tracking error

Both switching control laws are synthesized from $U = V_{drum} * \text{sign}(\sigma)$, where U is the motor control signal which is a step signal with values between +27 to -27 V. Since these control laws involve higher order derivatives and the sign operator, a non-linear function, the system control must be carefully designed so as to prevent chattering. This behavior is kept in check by smoothing the control law, which improves system robustness. Within Matlab®, this is readily implemented with a saturate block. Other options include increasing the system sampling frequency, which increases the resulting control response calculations. However, this additional computational overhead is not desirable in view of the requirement to test the control system with a simple microprocessor. Figure 35 gives the system used within the Hybrid model, where hunting has been reduced with the use of a saturation block. The sliding mode control report did not include the characteristics of the method used in his analysis (Shtessel, 1994). The trade-off in adjusting the control law is that some tracking precision and bandwidth is lost. (Slotine and Li, 1991)

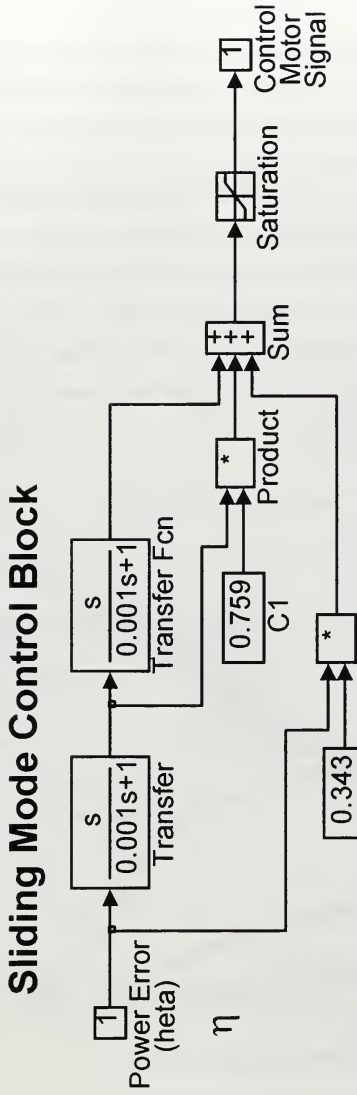

Figure 35. Sliding Mode Control Implementation.

D. DESIGN EVALUATION

For both control schemes, a standard startup was evaluated with the closed system temperature feedback enabled. The results for the proportional control and sliding mode control schemes are shown in Figure 36. Examination of both curves show that the sliding mode control scheme has a faster response to such an input. The proportional control exhibits more noticeable lag, but does not show significant overshoot or undershoot. The instantaneous power rate exceeds the startup limit for a few short periods. Both control laws track the ordered reactor power with good precision. The sliding control proved to be very sensitive to the range selected for the saturation. Without proper values, the random noise like signal produced by the quantization of the simulator was enough to produce chattering. Further evaluation revealed that a random noise signal of ~5% of power signal was enough to induce severe oscillations.

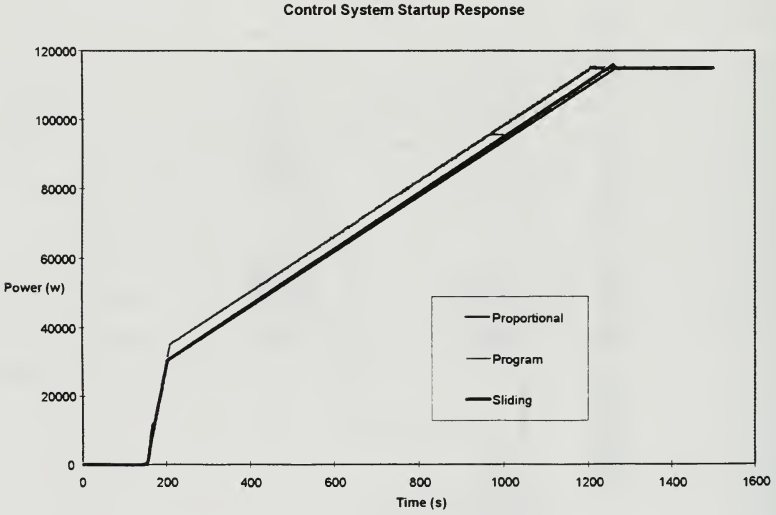

Figure 36. Control System Evaluation.

E. SCENARIO ANALYSIS

In this section, performance of the hybrid control system design is considered in the case of different casualties and startup conditions. This step is critical in design acceptance in order to meet the goal of reducing risk to as low as reasonably achievable.

1. Reactivity Addition Casualty

Addition of large amounts of positive reactivity will cause a power excursions. The worst case casualty considered was a failure of the control system, leading to control drum withdrawal to the limit. Figure 37 shows the result of such a power excursion upon the hybrid simulation model. This casualty was the first analyzed since it was also considered in the Preliminary Nuclear Safety Assessment, which provided for easy comparison between the two models.

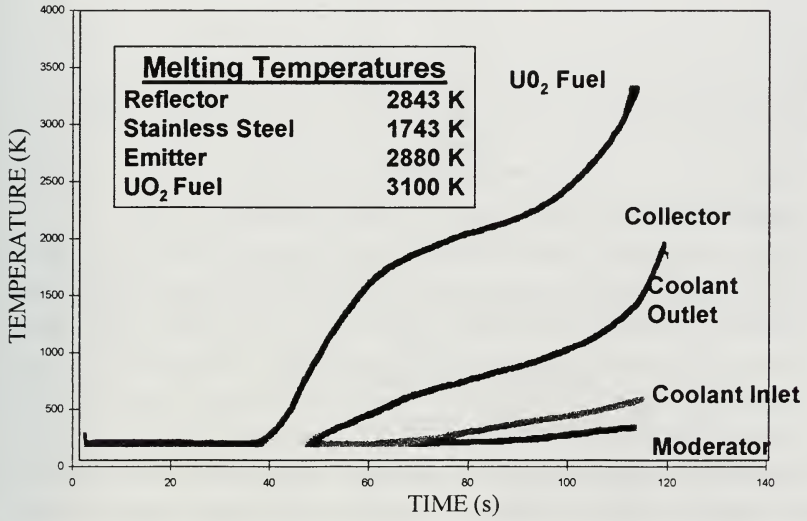

Figure 37. Control System Failure.

The dramatic effects revealed by the data shown in Figure 37 reveal that fuel temperatures most quickly rise to meet the limits. Therefore, the behavior of fuel temperature provides a good indication of the adequacy of control system safety response. With temperature limiting safety feature in effect, thermal limits are not reached for this type of casualty, as shown in Figure 38. Since the complete simultaneous failure of both the control system and the associated safety temperature limiting is unlikely, no further protection of the system is required. Sufficient protection for such a casualty would be easily accommodated through the use of redundant safety circuits, a standard practice within reactor control system design.

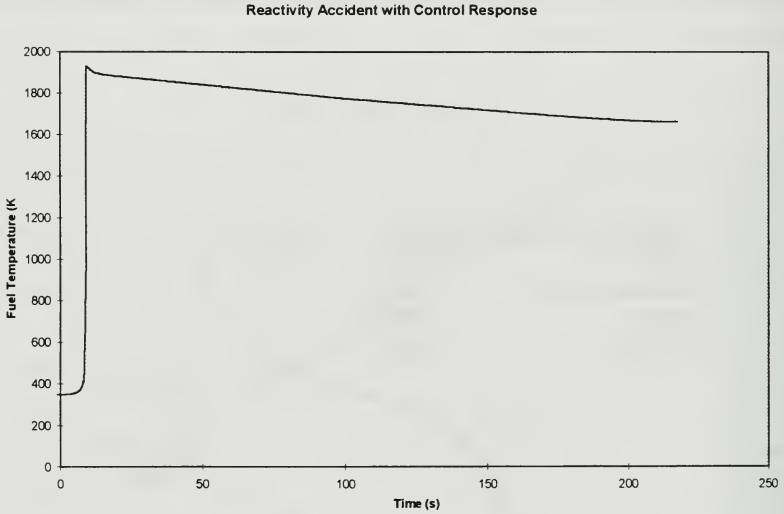

Figure 38. Temperature Limiting Response.

2. Loss of Coolant Accident

In this casualty, the reactor response is considered after a coolant system leak. For ease of analysis, an exponential loss of coolant flow was assumed followed by a complete loss of coolant flow. An actual loss of coolant would be more severe, since the remaining NaK would provide some thermal heat capacity to absorb heat. For this case, in accordance with

the actual loss of coolant casualty experience during the Russian experiments, it is assumed that the coolant limiter would not be effective in initiating safety system response. As shown in Figure 39, limiting core temperatures are reached, making this casualty of particular concern for overall system evaluation.

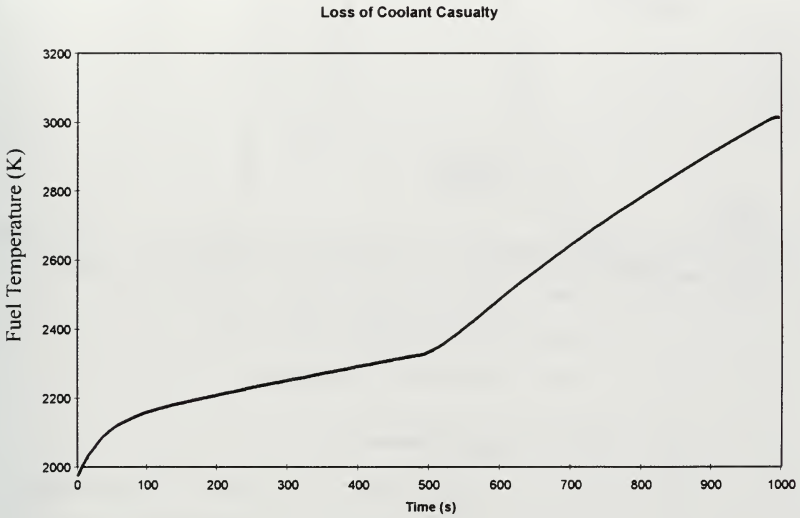

Figure 39. Loss of Coolant Casualty Analysis.

Since the temperature limiter is the only operational safety feature originally planned for the TOPAZ-II system, system modification would be required. For a loss of coolant casualty, there are several options to initiate reflector ejection. The NaK coolant pressure bellows could provide an input upon loss of pressure. However, mechanical bellows are not as reliable as purely electronic means. Another option would be to track differential coolant temperature. An anomaly with coolant flow would be detectable through this means with some time delay. The fastest acting option would be to use means that could directly detect the presence of the coolant. Since the coolant is a liquid metal, resistance detection seems a reasonable solution. As shown in Figure 40 below, fuel temperatures can be kept below limits if the reflector ejection is initiated in time.

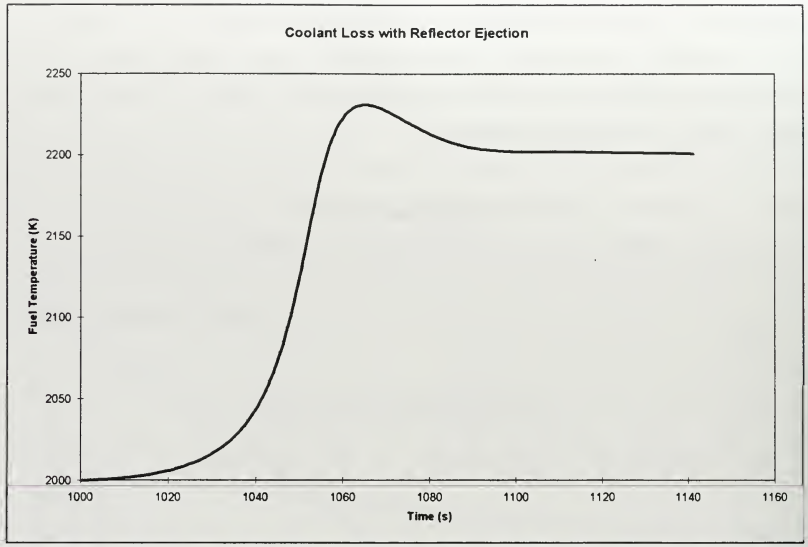

Figure 40. Coolant Loss with Protective Action

3. Cesium Pressure Oscillations

The presence of cold spots within the Cs system will cause undesired oscillations in the output current. The main consequence with for the control system is that the system should not attempt to maintain fission power during such a swing in current output. Such a response would cause additional thermal power changes, which would be likely to cause further oscillations. The option examined within the hybrid simulation was to also track differential coolant temperatures in order to provide a backup means of maintaining the constant power output. As shown in Figure 41, such a strategy does prevent the control system from following the output current instability. Additional options would include delaying current following mode until current oscillations had ceased. Experience with the TOPAZ test facility showed that the system would stabilize without operator action. However, since the presence of such current swings was a newly observed phenomenon, it can not be reliably predicted. Therefore, delaying onset of current tracking mode would require careful control by the ground station.

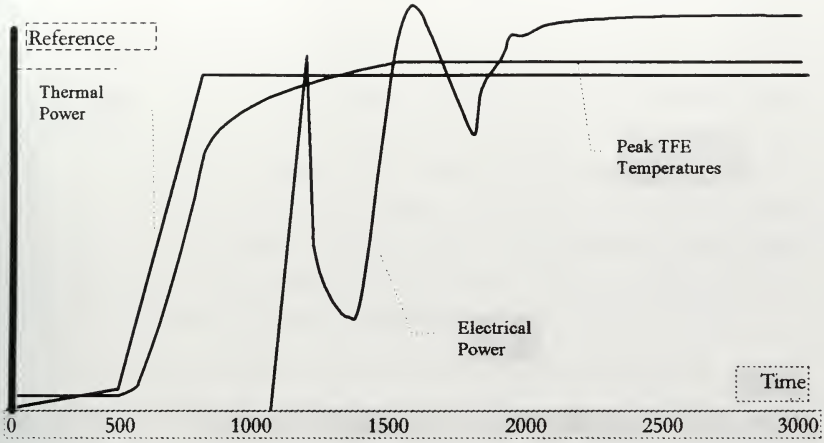

Figure 41. Cesium Pressure Induced Oscillations.

VIII. CONCLUSIONS

Analysis of the startup the TOPAZ-II nuclear space reactor indicates that design of a control system to meet required performance standards is realizable. In particular, sliding mode control is well suited for use within such a system. Regardless of the control method chosen, careful attention must be give to the simplifications and approximations used. The startup system behavior includes many non-linear elements. The effectiveness of a hybrid simulation that can incorporate these elements is shown. The assumptions contained within the dynamic simulator model require further refinement to become a more reliable test mechanism for evaluating startup control programming.

The sliding mode control method of power regulation is shown to be an efficient means of establishing the desired reactor power profiles. The sensitivity of the controller to non-linear measurement is a key concern. The noise sensitivity is an important consideration especially in view of the high radiation environment present both in space and around an operating nuclear core.

The physical robustness of the system was demonstrated following the loss of coolant casualty. The preliminary analysis presented here provides groundwork for evaluating control system changes with respect to reducing risks to as low as reasonably achievable.

IX. RECOMMENDATIONS

The Reactor Simulator model could be improved by incorporating some of the elements effectively demonstrated within the Hybrid Model presented here. The Matlab® implementation of the hybrid simulation provided real-time results when compiled. This indicates that the requirement for real-time evaluation can be maintained.

The noise characteristics of the system require further evaluation to ensure the proper selection of controller method. This is particularly true in the low power regimes, where the detectors will be providing a noisier signal. The installation of low range neutron detectors would provide a means of reducing this concern substantially.

The initiation of reactor shut down following a loss of coolant casualty requires system modification. The use of a resistance based coolant detection system is proposed. Additionally, the monitoring of coolant differential temperatures would provide a secondary means of monitoring system thermal power output.

APPENDIX. SIMULINK® PROGRAM CODE

The Simulink® code files used in the closed loop hybrid simulation is presented here for reference.

```
function [ret,x0,str,ts,xts]=closed(t,x,u,flag);
%CLOSED is the M-file description of the SIMULINK system
named CLOSED.
% The block-diagram can be displayed by typing: CLOSED.
%
% SYS=CLOSED(T,X,U,FLAG) returns depending on FLAG certain
% system values given time point, T, current state vector,
X,
% and input vector, U.
% FLAG is used to indicate the type of output to be returned
in SYS.
%
% Setting FLAG=1 causes CLOSED to return state derivatives,
FLAG=2
% discrete states, FLAG=3 system outputs and FLAG=4 next
sample
% time. For more information and other options see SFUNC.
%
% Calling CLOSED with a FLAG of zero:
% [SIZES]=CLOSED([],[],[],0), returns a vector, SIZES, which
%  contains the sizes of the state vector and other
parameters.
% SIZES(1) number of states
% SIZES(2) number of discrete states
% SIZES(3) number of outputs
% SIZES(4) number of inputs
% SIZES(5) number of roots (currently unsupported)
% SIZES(6) direct feedthrough flag
% SIZES(7) number of sample times
%
% For the definition of other parameters in SIZES, see
SFUNC.
% See also, TRIM, LINMOD, LINSIM, EULER, RK23, RK45, ADAMS,
GEAR.

% Note: This M-file is only used for saving graphical
information;
% after the model is loaded into memory an internal model
```

```
% representation is used.

% the system will take on the name of this mfile:
sys = mfilename;
new_system(sys)
simver(1.3)
if (0 == (nargin + nargout))
 set_param(sys,'Location',[99,158,739,491])
 open_system(sys)
end;
set_param(sys,'algorithm', 'RK-45')
set_param(sys,'Start time', '0.0')
set_param(sys,'Stop time', '3000')
set_param(sys,'Min step size', '0.001')
set_param(sys,'Max step size', '.2')
set_param(sys,'Relative error','1e-3')


set_param(sys,'Return vars', '')
set_param(sys,'AssignWideVectorLines','on');

add_block('built-in/Note',[sys,'/','Reactivity'])
set_param([sys,'/','Reactivity'],...
'position',[265,70,270,75])

add_block('built-in/Note',[sys,'/','Power'])
set_param([sys,'/','Power'],...
'position',[395,70,400,75])


% Subsystem 'Core Reactivity'.

new_system([sys,'/','Core Reactivity'])
set_param([sys,'/','Core
Reactivity'],'Location',[0,59,274,252])

add_block('built-in/Inport',[sys,'/','Core Reactivity/x'])
set_param([sys,'/','Core Reactivity/x'],...
 'position',[65,55,85,75])

add_block('built-in/S-Function',[sys,'/',['Core
Reactivity/S-function',13,'M-file                          which
plots',13,'lines',13,'']])
```

```
set_param([sys,'/',['Core  Reactivity/S-function',13,'M-file
which plots',13,'lines',13,'']],...
  'function name','sfunyst',...
  'parameters','ax, color, npts, dt',...
  'position',[130,55,180,75])
add_line([sys,'/','Core Reactivity'],[90,65;125,65])
set_param([sys,'/','Core Reactivity'],...
  'Mask
Display','plot(0,0,100,100,[83,76,63,52,42,38,28,16,11,84,11
,11,11,90,90,11],[75,58,47,54,72,80,84,74,65,65,65,90,40,40,
90,90])',...
  'Mask Type','Storage scope.')
set_param([sys,'/','Core Reactivity'],...
  'Mask  Dialogue','Storage  scope  using  MATLAB  graph
window.\nEnter plotting ranges and line type.|Initial Time
Range:|Initial y-min:|Initial y-max:|Storage pts.:|Line type
(rgbw-.:xo):')
set_param([sys,'/','Core Reactivity'],...
  'Mask Translate','npts = @4; color = @5; ax = [0, @1, @2,
@3]; dt=-1;')
set_param([sys,'/','Core Reactivity'],...
  'Mask Help','This block uses a MATLAB figure window to
plot the input signal. The graph limits are automatically
scaled to the min and max values of the signal stored in the
scope''s signal buffer. Line type must be in quotes. See the
M-file sfunyst.m.')
set_param([sys,'/','Core Reactivity'],...
  'Mask
Entries','5\/-10\/10\/200\/''y-/g--/c-./w:/m*/ro/b+''\/')


% Finished composite block 'Core Reactivity'.


set_param([sys,'/','Core Reactivity'],...
  'position',[280,165,310,205])


% Subsystem 'Reactor Model'.

new_system([sys,'/','Reactor Model'])
set_param([sys,'/','Reactor
Model'],'Location',[10,79,751,471])
```

```
add_block('built-in/Note',[sys,'/','Reactor    Model/Reactor
Kinetics Model'])
set_param([sys,'/','Reactor      Model/Reactor      Kinetics
Model'],...
  'Font Weight','bold',...
  'Font Underline',1,...
  'Font Size',16,...
  'position',[320,5,325,10])

add_block('built-in/Inport',[sys,'/','Reactor
Model/Reactivity'])
set_param([sys,'/','Reactor Model/Reactivity'],...
  'position',[55,165,75,185])

add_block('built-in/Mux',[sys,'/',['Reactor
Model/State',13,'Variables']])
set_param([sys,'/',['Reactor
Model/State',13,'Variables']],...
  'inputs','2',...
  'position',[160,136,190,169])

add_block('built-in/Integrator',[sys,'/','Reactor
Model/Integrator'])
set_param([sys,'/','Reactor Model/Integrator'],...
  'Initial','[Co ]',...
  'position',[450,140,480,170])

add_block('built-in/MATLAB           Fcn',[sys,'/',['Reactor
Model/Reactor',13,'Calculations']])
set_param([sys,'/',['Reactor
Model/Reactor',13,'Calculations']],...
  'Drop Shadow',4,...
  'MATLAB Fcn','rx_pja',...
  'Output Width','6',...
  'position',[265,136,340,174])

add_block('built-in/Note',[sys,'/','Reactor    Model/Delayed
Neutron Precursor Concentrations'])
set_param([sys,'/','Reactor Model/Delayed Neutron Precursor
Concentrations'],...
  'position',[285,95,290,100])

add_block('built-in/Note',[sys,'/','Reactor     Model/Prompt
Jump Approximation Calculations'])
```

```
set_param([sys,'/','Reactor Model/Prompt Jump Approximation
Calculations'],...
  'Font Size',12,...


'position',[315,50,320,55])

add_block('built-in/MATLAB           Fcn',[sys,'/',['Reactor
Model/Neutron',13,'Power']])
set_param([sys,'/',['Reactor Model/Neutron',13,'Power']],...
  'Drop Shadow',4,...
  'MATLAB Fcn','P_pja',...
  'Output Width','1',...
  'position',[480,201,555,239])

add_block('built-in/Outport',[sys,'/',['Reactor
Model/Reactor',13,'Power']])
set_param([sys,'/',['Reactor Model/Reactor',13,'Power']],...
  'position',[685,205,705,225])

add_block('built-in/Sum',[sys,'/','Reactor Model/Sum'])
set_param([sys,'/','Reactor Model/Sum'],...
  'position',[620,205,640,225])

add_block('built-in/Constant',[sys,'/',['Reactor
Model/Non-fission',13,'Heating']])
set_param([sys,'/',['Reactor
Model/Non-fission',13,'Heating']],...
  'Value','Qo',...
  'position',[525,127,565,153])
add_line([sys,'/','Reactor
Model'],[80,175;135,175;135,160;155,160])
add_line([sys,'/','Reactor
Model'],[485,155;495,155;495,130;140,130;140,145;155,145])
add_line([sys,'/','Reactor Model'],[195,155;260,155])
add_line([sys,'/','Reactor Model'],[345,155;445,155])
add_line([sys,'/','Reactor Model'],[645,215;680,215])
add_line([sys,'/','Reactor Model'],[560,220;615,220])
add_line([sys,'/','Reactor
Model'],[570,140;600,140;600,210;615,210])
add_line([sys,'/','Reactor
Model'],[225,155;225,220;475,220])
```

```
% Finished composite block 'Reactor Model'.

set_param([sys,'/','Reactor Model'],...
  'position',[325,69,355,121])


% Subsystem ['Control',13,'Drum',13,'Position'].

new_system([sys,'/',['Control',13,'Drum',13,'Position']])
set_param([sys,'/',['Control',13,'Drum',13,'Position']],'Loc
ation',[27,43,780,497])

add_block('built-in/Note',[sys,'/',['Control',13,'Drum',13,'
Position/Drum Model']])
set_param([sys,'/',['Control',13,'Drum',13,'Position/Drum
Model']],...
  'position',[150,5,155,10])


add_block('built-in/Inport',[sys,'/',['Control',13,'Drum',13
,'Position/Reactor',13,'Power']])
set_param([sys,'/',['Control',13,'Drum',13,'Position/Reactor
',13,'Power']],...
  'position',[30,40,50,60])

add_block('built-in/Relay',[sys,'/',['Control',13,'Drum',13,
'Position/5 kW',13,'Detection']])
set_param([sys,'/',['Control',13,'Drum',13,'Position/5
kW',13,'Detection']],...
  'On_switch_value','5000',...
  'Off_switch_value','-5000',...
  'position',[115,188,145,212])


%    Subsystem    ['Control',13,'Drum',13,'Position/In    //
Out',13,'Switch'].

new_system([sys,'/',['Control',13,'Drum',13,'Position/In  //
Out',13,'Switch']])
set_param([sys,'/',['Control',13,'Drum',13,'Position/In   //
Out',13,'Switch']],'Location',[159,417,467,586])

add_block('built-in/Outport',[sys,'/',['Control',13,'Drum',1
3,'Position/In // Out',13,'Switch/out_1']])
```

```
set_param([sys,'/',['Control',13,'Drum',13,'Position/In   //
Out',13,'Switch/out_1']],...
  'position',[265,70,285,90])

add_block('built-in/Inport',[sys,'/',['Control',13,'Drum',13
,'Position/In // Out',13,'Switch/in_1']])
set_param([sys,'/',['Control',13,'Drum',13,'Position/In   //
Out',13,'Switch/in_1']],...
  'position',[35,30,55,50])

add_block('built-in/Relational
Operator',[sys,'/',['Control',13,'Drum',13,'Position/In   //
Out',13,'Switch/Relational',13,'Operator']])
set_param([sys,'/',['Control',13,'Drum',13,'Position/In   //
Out',13,'Switch/Relational',13,'Operator']],...
  'Operator','>',...
  'position',[140,32,170,63])

add_block('built-in/Sum',[sys,'/',['Control',13,'Drum',13,'P
osition/In // Out',13,'Switch/Sum']])
set_param([sys,'/',['Control',13,'Drum',13,'Position/In   //
Out',13,'Switch/Sum']],...
  'inputs','+-',...
  'position',[215,64,235,91])


add_block('built-in/Relational
Operator',[sys,'/',['Control',13,'Drum',13,'Position/In   //
Out',13,'Switch/Relational',13,'Operator1']])
set_param([sys,'/',['Control',13,'Drum',13,'Position/In   //
Out',13,'Switch/Relational',13,'Operator1']],...
  'Operator','<',...
  'position',[140,92,170,123])

add_block('built-in/Constant',[sys,'/',['Control',13,'Drum',
13,'Position/In // Out',13,'Switch/Constant']])
set_param([sys,'/',['Control',13,'Drum',13,'Position/In   //
Out',13,'Switch/Constant']],...
  'Value','0',...
  'position',[65,105,85,125])
add_line([sys,'/',['Control',13,'Drum',13,'Position/In    //
Out',13,'Switch']],[60,40;135,40])
add_line([sys,'/',['Control',13,'Drum',13,'Position/In    //
Out',13,'Switch']],[95,40;95,100;135,100])
```

```
add_line([sys,'/',['Control',13,'Drum',13,'Position/In    //
Out',13,'Switch']],[90,115;135,115])
add_line([sys,'/',['Control',13,'Drum',13,'Position/In    //
Out',13,'Switch']],[110,115;110,55;135,55])
add_line([sys,'/',['Control',13,'Drum',13,'Position/In    //
Out',13,'Switch']],[175,110;185,110;185,85;210,85])
add_line([sys,'/',['Control',13,'Drum',13,'Position/In    //
Out',13,'Switch']],[175,50;185,50;185,70;210,70])
add_line([sys,'/',['Control',13,'Drum',13,'Position/In    //
Out',13,'Switch']],[240,80;260,80])
set_param([sys,'/',['Control',13,'Drum',13,'Position/In   //
Out',13,'Switch']],...
  'Mask
Display','plot(-50,-50,50,50,[-50,50],[0,0],[0,0],[-50,50],[
-40,0],[-30,-30],[0,40],[30,30])',...
  'Mask Type','Sign',...
  'Mask Dialogue','y = sign(x)')
set_param([sys,'/',['Control',13,'Drum',13,'Position/In   //
Out',13,'Switch']],...
  'Mask Help','Sign Function:\n\t\t\ty = 1 if x > 0\n\t\t\ty
= 0 if x = 0\n\t\t\ty = -1 if x < 0')


%            Finished            composite            block
['Control',13,'Drum',13,'Position/In // Out',13,'Switch'].

set_param([sys,'/',['Control',13,'Drum',13,'Position/In   //
Out',13,'Switch']],...
  'position',[475,187,505,213])


%                                                    Subsystem
['Control',13,'Drum',13,'Position/Drum',13,'Response',13,'Mo
del'].


new_system([sys,'/',['Control',13,'Drum',13,'Position/Drum',
13,'Response',13,'Model']])
set_param([sys,'/',['Control',13,'Drum',13,'Position/Drum',1
3,'Response',13,'Model']],'Location',[94,85,665,353])
```

```
add_block('built-in/Product',[sys,'/',['Control',13,'Drum',1
3,'Position/Drum',13,'Response',13,'Model/Product']])
set_param([sys,'/',['Control',13,'Drum',13,'Position/Drum',1
3,'Response',13,'Model/Product']],...
  'position',[230,143,260,167])

add_block('built-in/Integrator',[sys,'/',['Control',13,'Drum
',13,'Position/Drum',13,'Response',13,'Model/Integrator']])
set_param([sys,'/',['Control',13,'Drum',13,'Position/Drum',1
3,'Response',13,'Model/Integrator']],...
  'position',[315,142,345,168])

add_block('built-in/Outport',[sys,'/',['Control',13,'Drum',1
3,'Position/Drum',13,'Response',13,'Model/Drum',13,'Position
']])
set_param([sys,'/',['Control',13,'Drum',13,'Position/Drum',1
3,'Response',13,'Model/Drum',13,'Position']],...
  'position',[440,145,460,165])

add_block('built-in/Constant',[sys,'/',['Control',13,'Drum',
13,'Position/Drum',13,'Response',13,'Model/Drum Speed']])
set_param([sys,'/',['Control',13,'Drum',13,'Position/Drum',1
3,'Response',13,'Model/Drum Speed']],...
  'orientation',2,...
  'Value','1.4',...
  'position',[240,77,275,103])

add_block('built-in/Inport',[sys,'/',['Control',13,'Drum',13
,'Position/Drum',13,'Response',13,'Model/In                //
Out',13,'Switch']])
set_param([sys,'/',['Control',13,'Drum',13,'Position/Drum',1
3,'Response',13,'Model/In // Out',13,'Switch']],...
  'position',[80,150,100,170])
add_line([sys,'/',['Control',13,'Drum',13,'Position/Drum',13
,'Response',13,'Model']],[235,90;120,90;120,150;225,150])
add_line([sys,'/',['Control',13,'Drum',13,'Position/Drum',13
,'Response',13,'Model']],[265,155;310,155])
add_line([sys,'/',['Control',13,'Drum',13,'Position/Drum',13
,'Response',13,'Model']],[350,155;435,155])
add_line([sys,'/',['Control',13,'Drum',13,'Position/Drum',13
,'Response',13,'Model']],[105,160;225,160])
```

```
%            Finished            composite            block
['Control',13,'Drum',13,'Position/Drum',13,'Response',13,'Mo
del'].

set_param([sys,'/',['Control',13,'Drum',13,'Position/Drum',1
3,'Response',13,'Model']],...
  'position',[535,175,565,225])




add_block('built-in/Saturation',[sys,'/',['Control',13,'Drum
',13,'Position/Drum',13,'Limits']])
set_param([sys,'/',['Control',13,'Drum',13,'Position/Drum',1
3,'Limits']],...
  'Lower Limit','0',...
  'Upper Limit','18000',...
  'position',[610,188,640,212])

add_block('built-in/Outport',[sys,'/',['Control',13,'Drum',1
3,'Position/Drum Angle']])
set_param([sys,'/',['Control',13,'Drum',13,'Position/Drum
Angle']],...
  'position',[700,190,720,210])


%                                                    Subsystem
['Control',13,'Drum',13,'Position/Drum',13,'Angle'].

new_system([sys,'/',['Control',13,'Drum',13,'Position/Drum',
13,'Angle']])
set_param([sys,'/',['Control',13,'Drum',13,'Position/Drum',1
3,'Angle']],'Location',[0,59,274,252])

add_block('built-in/Inport',[sys,'/',['Control',13,'Drum',13
,'Position/Drum',13,'Angle/x']])
set_param([sys,'/',['Control',13,'Drum',13,'Position/Drum',1
3,'Angle/x']],...
  'position',[65,55,85,75])

add_block('built-in/S-Function',[sys,'/',['Control',13,'Drum
',13,'Position/Drum',13,'Angle/S-function',13,'M-file  which
plots',13,'lines',13,'']])
```

```
set_param([sys,'/',['Control',13,'Drum',13,'Position/Drum',1
3,'Angle/S-function',13,'M-file                          which
plots',13,'lines',13,'']],...
  'function name','sfunyst',...
  'parameters','ax, color, npts, dt',...
  'position',[130,55,180,75])
add_line([sys,'/',['Control',13,'Drum',13,'Position/Drum',13
,'Angle']],[90,65;125,65])
set_param([sys,'/',['Control',13,'Drum',13,'Position/Drum',1
3,'Angle']],...
  'Mask
Display','plot(0,0,100,100,[83,76,63,52,42,38,28,16,11,84,11
,11,11,90,90,11],[75,58,47,54,72,80,84,74,65,65,65,90,40,40,
90,90])',...
  'Mask Type','Storage scope.')


set_param([sys,'/',['Control',13,'Drum',13,'Position/Drum',1
3,'Angle']],...
  'Mask  Dialogue','Storage  scope  using  MATLAB  graph
window.\nEnter plotting ranges and line type.|Initial Time
Range:|Initial y-min:|Initial y-max:|Storage pts.:|Line type
(rgbw-.:xo):')



set_param([sys,'/',['Control',13,'Drum',13,'Position/Drum',1
3,'Angle']],...
  'Mask Translate','npts = @4; color = @5; ax = [0, @1, @2,
@3]; dt=-1;')
set_param([sys,'/',['Control',13,'Drum',13,'Position/Drum',1
3,'Angle']],...
  'Mask Help','This block uses a MATLAB figure window to
plot the input signal. The graph limits are automatically
scaled to the min and max values of the signal stored in the
scope''s signal buffer. Line type must be in quotes. See the
M-file sfunyst.m.')
set_param([sys,'/',['Control',13,'Drum',13,'Position/Drum',1
3,'Angle']],...
  'Mask
Entries','5\/-10\/10\/200\/''y-/g--/c-./w:/m*/ro/b+''\/')
```

```
%            Finished            composite            block
['Control',13,'Drum',13,'Position/Drum',13,'Angle'].

set_param([sys,'/',['Control',13,'Drum',13,'Position/Drum',1
3,'Angle']],...
  'position',[690,65,720,105])


%                                                    Subsystem
['Control',13,'Drum',13,'Position/Startup',13,'Drum',13,'Pos
itioning'].

new_system([sys,'/',['Control',13,'Drum',13,'Position/Startu
p',13,'Drum',13,'Positioning']])
set_param([sys,'/',['Control',13,'Drum',13,'Position/Startup
',13,'Drum',13,'Positioning']],'Location',[24,152,771,460])

add_block('built-in/Outport',[sys,'/',['Control',13,'Drum',1
3,'Position/Startup',13,'Drum',13,'Positioning/Drum',13,'Mot
or',13,'Switch']])
set_param([sys,'/',['Control',13,'Drum',13,'Position/Startup
',13,'Drum',13,'Positioning/Drum',13,'Motor',13,'Switch']],.
..
  'position',[655,140,675,160])

add_block('built-in/Dead
Zone',[sys,'/',['Control',13,'Drum',13,'Position/Startup',13
,'Drum',13,'Positioning/Drum',13,'Position',13,'Dead
Band']])
set_param([sys,'/',['Control',13,'Drum',13,'Position/Startup
',13,'Drum',13,'Positioning/Drum',13,'Position',13,'Dead
Band']],...
  'Lower_value','-0.01',...
  'Upper_value','0.01',...
  'position',[560,137,590,163])


add_block('built-in/Sum',[sys,'/',['Control',13,'Drum',13,'P
osition/Startup',13,'Drum',13,'Positioning/Position',13,'Err
or']])
```

```
set_param([sys,'/',['Control',13,'Drum',13,'Position/Startup
',13,'Drum',13,'Positioning/Position',13,'Error']],...
  'inputs','+-',...
  'position',[485,140,505,160])

add_block('built-in/Switch',[sys,'/',['Control',13,'Drum',13
,'Position/Startup',13,'Drum',13,'Positioning/Drum',13,'Post
ion',13,'Switch']])
set_param([sys,'/',['Control',13,'Drum',13,'Position/Startup
',13,'Drum',13,'Positioning/Drum',13,'Postion',13,'Switch']]
,...
  'Threshold','1',...
  'position',[340,94,370,126])

add_block('built-in/Inport',[sys,'/',['Control',13,'Drum',13
,'Position/Startup',13,'Drum',13,'Positioning/Drum',13,'Angl
e']])
set_param([sys,'/',['Control',13,'Drum',13,'Position/Startup
',13,'Drum',13,'Positioning/Drum',13,'Angle']],...
  'position',[25,25,45,45])

add_block('built-in/Constant',[sys,'/',['Control',13,'Drum',
13,'Position/Startup',13,'Drum',13,'Positioning/Position',13
,'#1']])
set_param([sys,'/',['Control',13,'Drum',13,'Position/Startup
',13,'Drum',13,'Positioning/Position',13,'#1']],...
  'Value','154',...
  'position',[225,165,275,185])

add_block('built-in/Constant',[sys,'/',['Control',13,'Drum',
13,'Position/Startup',13,'Drum',13,'Positioning/Position',13
,'#2']])
set_param([sys,'/',['Control',13,'Drum',13,'Position/Startup
',13,'Drum',13,'Positioning/Position',13,'#2']],...
  'Value','145',...
  'position',[225,35,275,55])

add_block('built-in/Relay',[sys,'/',['Control',13,'Drum',13,
'Position/Startup',13,'Drum',13,'Positioning/154
',13,'Degree',13,'Relay']])
set_param([sys,'/',['Control',13,'Drum',13,'Position/Startup
',13,'Drum',13,'Positioning/154
',13,'Degree',13,'Relay']],...
  'On_switch_value','154',...
```

```
  'Off_switch_value','0',...
  'On_output_value','10',...
  'position',[155,98,185,122])
add_line([sys,'/',['Control',13,'Drum',13,'Position/Startup'
,13,'Drum',13,'Positioning']],[280,45;300,45;300,100;335,100
])


add_line([sys,'/',['Control',13,'Drum',13,'Position/Startup'
,13,'Drum',13,'Positioning']],[280,175;300,175;300,120;335,1
20])
add_line([sys,'/',['Control',13,'Drum',13,'Position/Startup'
,13,'Drum',13,'Positioning']],[190,110;335,110])
add_line([sys,'/',['Control',13,'Drum',13,'Position/Startup'
,13,'Drum',13,'Positioning']],[375,110;420,110;420,145;480,1
45])




add_line([sys,'/',['Control',13,'Drum',13,'Position/Startup'
,13,'Drum',13,'Positioning']],[50,35;65,35;65,110;150,110])
add_line([sys,'/',['Control',13,'Drum',13,'Position/Startup'
,13,'Drum',13,'Positioning']],[595,150;650,150])
add_line([sys,'/',['Control',13,'Drum',13,'Position/Startup'
,13,'Drum',13,'Positioning']],[510,150;555,150])
add_line([sys,'/',['Control',13,'Drum',13,'Position/Startup'
,13,'Drum',13,'Positioning']],[65,110;65,260;420,260;420,155
;480,155])


%            Finished            composite            block
['Control',13,'Drum',13,'Position/Startup',13,'Drum',13,'Pos
itioning'].

set_param([sys,'/',['Control',13,'Drum',13,'Position/Startup
',13,'Drum',13,'Positioning']],...
  'position',[185,250,215,300])

add_block('built-in/Switch',[sys,'/',['Control',13,'Drum',13
,'Position/Startup',13,'Mode',13,'Switch']])
set_param([sys,'/',['Control',13,'Drum',13,'Position/Startup
',13,'Mode',13,'Switch']],...
  'Threshold','1',...
```

```
  'position',[385,184,415,216])


%                                                    Subsystem
['Control',13,'Drum',13,'Position/Power',13,'Rate',13,'Posit
ioning'].

new_system([sys,'/',['Control',13,'Drum',13,'Position/Power'
,13,'Rate',13,'Positioning']])
set_param([sys,'/',['Control',13,'Drum',13,'Position/Power',
13,'Rate',13,'Positioning']],'Location',[40,48,705,323])


%                                                    Subsystem
['Control',13,'Drum',13,'Position/Power',13,'Rate',13,'Posit
ioning/Startup',13,'Power',13,'Profile'].

new_system([sys,'/',['Control',13,'Drum',13,'Position/Power'
,13,'Rate',13,'Positioning/Startup',13,'Power',13,'Profile']
])
set_param([sys,'/',['Control',13,'Drum',13,'Position/Power',
13,'Rate',13,'Positioning/Startup',13,'Power',13,'Profile']]
,'Location',[27,43,780,476])




add_block('built-in/Inport',[sys,'/',['Control',13,'Drum',13
,'Position/Power',13,'Rate',13,'Positioning/Startup',13,'Pow
er',13,'Profile/Reactor',13,'Power']])
set_param([sys,'/',['Control',13,'Drum',13,'Position/Power',
13,'Rate',13,'Positioning/Startup',13,'Power',13,'Profile/Re
actor',13,'Power']],...

  'position',[30,10,50,30])

add_block('built-in/Product',[sys,'/',['Control',13,'Drum',1
3,'Position/Power',13,'Rate',13,'Positioning/Startup',13,'Po
wer',13,'Profile/Product']])
set_param([sys,'/',['Control',13,'Drum',13,'Position/Power',
13,'Rate',13,'Positioning/Startup',13,'Power',13,'Profile/Pr
oduct']],...
  'position',[390,209,420,251])
```

```
add_block('built-in/Inport',[sys,'/',['Control',13,'Drum',13
,'Position/Power',13,'Rate',13,'Positioning/Startup',13,'Pow
er',13,'Profile/Power',13,'Rate',13,'Limit',13,'Enabled']])
set_param([sys,'/',['Control',13,'Drum',13,'Position/Power',
13,'Rate',13,'Positioning/Startup',13,'Power',13,'Profile/Po
wer',13,'Rate',13,'Limit',13,'Enabled']],...
  'Port','2',...
  'position',[330,230,350,250])

add_block('built-in/Integrator',[sys,'/',['Control',13,'Drum
',13,'Position/Power',13,'Rate',13,'Positioning/Startup',13,
'Power',13,'Profile/Ordered',13,'Power',13,'Calculation']])
set_param([sys,'/',['Control',13,'Drum',13,'Position/Power',
13,'Rate',13,'Positioning/Startup',13,'Power',13,'Profile/Or
dered',13,'Power',13,'Calculation']],...
  'Initial','5000',...
  'position',[465,220,505,240])

add_block('built-in/Constant',[sys,'/',['Control',13,'Drum',
13,'Position/Power',13,'Rate',13,'Positioning/Startup',13,'P
ower',13,'Profile/Heatup',13,'Rate 2',13,'(W//s)']])
set_param([sys,'/',['Control',13,'Drum',13,'Position/Power',
13,'Rate',13,'Positioning/Startup',13,'Power',13,'Profile/He
atup',13,'Rate 2',13,'(W//s)']],...
  'Value','80',...
  'position',[170,140,215,160])

add_block('built-in/Constant',[sys,'/',['Control',13,'Drum',
13,'Position/Power',13,'Rate',13,'Positioning/Startup',13,'P
ower',13,'Profile/Heatup',13,'Rate 1',13,'(W//s)']])




set_param([sys,'/',['Control',13,'Drum',13,'Position/Power',
13,'Rate',13,'Positioning/Startup',13,'Power',13,'Profile/He
atup',13,'Rate 1',13,'(W//s)']],...
  'Value','600',...
  'position',[170,265,215,285])
```

```
add_block('built-in/Switch',[sys,'/',['Control',13,'Drum',13
,'Position/Power',13,'Rate',13,'Positioning/Startup',13,'Pow
er',13,'Profile/Rate',13,'Mode',13,'Switch']])
set_param([sys,'/',['Control',13,'Drum',13,'Position/Power',
13,'Rate',13,'Positioning/Startup',13,'Power',13,'Profile/Ra
te',13,'Mode',13,'Switch']],...
  'Threshold','1',...
  'position',[260,204,290,236])

add_block('built-in/Relay',[sys,'/',['Control',13,'Drum',13,
'Position/Power',13,'Rate',13,'Positioning/Startup',13,'Powe
r',13,'Profile/35 kW',13,'Detection']])
set_param([sys,'/',['Control',13,'Drum',13,'Position/Power',
13,'Rate',13,'Positioning/Startup',13,'Power',13,'Profile/35
kW',13,'Detection']],...
  'On_switch_value','35000',...
  'Off_switch_value','-35000',...
  'position',[110,208,140,232])

add_block('built-in/Relay',[sys,'/',['Control',13,'Drum',13,
'Position/Power',13,'Rate',13,'Positioning/Startup',13,'Powe
r',13,'Profile/115 kW',13,'Detection']])
set_param([sys,'/',['Control',13,'Drum',13,'Position/Power',
13,'Rate',13,'Positioning/Startup',13,'Power',13,'Profile/11
5 kW',13,'Detection']],...
  'On_switch_value','115000',...
  'Off_switch_value','-35000',...
  'On_output_value','115000')
set_param([sys,'/',['Control',13,'Drum',13,'Position/Power',
13,'Rate',13,'Positioning/Startup',13,'Power',13,'Profile/11
5 kW',13,'Detection']],...
  'position',[365,98,395,122])

add_block('built-in/Switch',[sys,'/',['Control',13,'Drum',13
,'Position/Power',13,'Rate',13,'Positioning/Startup',13,'Pow
er',13,'Profile/Constant',13,'Power',13,'Mode',13,'Switch']]
)
set_param([sys,'/',['Control',13,'Drum',13,'Position/Power',
13,'Rate',13,'Positioning/Startup',13,'Power',13,'Profile/Co
nstant',13,'Power',13,'Mode',13,'Switch']],...
  'Threshold','1',...
  'position',[570,204,600,236])
```

```
add_block('built-in/Outport',[sys,'/',['Control',13,'Drum',1
3,'Position/Power',13,'Rate',13,'Positioning/Startup',13,'Po
wer',13,'Profile/Ordered',13,'Power']])
set_param([sys,'/',['Control',13,'Drum',13,'Position/Power',
13,'Rate',13,'Positioning/Startup',13,'Power',13,'Profile/Or
dered',13,'Power']],...
  'position',[650,210,670,230])



%                                                    Subsystem
['Control',13,'Drum',13,'Position/Power',13,'Rate',13,'Posit
ioning/Startup',13,'Power',13,'Profile/Order',13,'Power',13,
'Graph'].

new_system([sys,'/',['Control',13,'Drum',13,'Position/Power'
,13,'Rate',13,'Positioning/Startup',13,'Power',13,'Profile/O
rder',13,'Power',13,'Graph']])
set_param([sys,'/',['Control',13,'Drum',13,'Position/Power',
13,'Rate',13,'Positioning/Startup',13,'Power',13,'Profile/Or
der',13,'Power',13,'Graph']],'Location',[0,59,274,252])

add_block('built-in/Inport',[sys,'/',['Control',13,'Drum',13
,'Position/Power',13,'Rate',13,'Positioning/Startup',13,'Pow
er',13,'Profile/Order',13,'Power',13,'Graph/x']])
set_param([sys,'/',['Control',13,'Drum',13,'Position/Power',
13,'Rate',13,'Positioning/Startup',13,'Power',13,'Profile/Or
der',13,'Power',13,'Graph/x']],...
  'position',[65,55,85,75])

add_block('built-in/S-Function',[sys,'/',['Control',13,'Drum
',13,'Position/Power',13,'Rate',13,'Positioning/Startup',13,
'Power',13,'Profile/Order',13,'Power',13,'Graph/S-function',
13,'M-file which plots',13,'lines',13,'']])
set_param([sys,'/',['Control',13,'Drum',13,'Position/Power',
13,'Rate',13,'Positioning/Startup',13,'Power',13,'Profile/Or
der',13,'Power',13,'Graph/S-function',13,'M-file       which
plots',13,'lines',13,'']],...
  'function name','sfunyst')
set_param([sys,'/',['Control',13,'Drum',13,'Position/Power',
13,'Rate',13,'Positioning/Startup',13,'Power',13,'Profile/Or
der',13,'Power',13,'Graph/S-function',13,'M-file       which
plots',13,'lines',13,'']],...
  'parameters','ax, color, npts, dt')
```

```
set_param([sys,'/',['Control',13,'Drum',13,'Position/Power',
13,'Rate',13,'Positioning/Startup',13,'Power',13,'Profile/Or
der',13,'Power',13,'Graph/S-function',13,'M-file       which
plots',13,'lines',13,'']],...
  'position',[130,55,180,75])
add_line([sys,'/',['Control',13,'Drum',13,'Position/Power',1
3,'Rate',13,'Positioning/Startup',13,'Power',13,'Profile/Ord
er',13,'Power',13,'Graph']],[90,65;125,65])
set_param([sys,'/',['Control',13,'Drum',13,'Position/Power',
13,'Rate',13,'Positioning/Startup',13,'Power',13,'Profile/Or
der',13,'Power',13,'Graph']],...
  'Mask



Display','plot(0,0,100,100,[83,76,63,52,42,38,28,16,11,84,11
,11,11,90,90,11],[75,58,47,54,72,80,84,74,65,65,65,90,40,40,
90,90])')
set_param([sys,'/',['Control',13,'Drum',13,'Position/Power',
13,'Rate',13,'Positioning/Startup',13,'Power',13,'Profile/Or
der',13,'Power',13,'Graph']],...




 'Mask Type','Storage scope.')
set_param([sys,'/',['Control',13,'Drum',13,'Position/Power',
13,'Rate',13,'Positioning/Startup',13,'Power',13,'Profile/Or
der',13,'Power',13,'Graph']],...
  'Mask Dialogue','Storage scope using MATLAB graph
window.\nEnter plotting ranges and line type.|Initial Time
Range:|Initial y-min:|Initial y-max:|Storage pts.:|Line type
(rgbw-.:xo):')
set_param([sys,'/',['Control',13,'Drum',13,'Position/Power',
13,'Rate',13,'Positioning/Startup',13,'Power',13,'Profile/Or
der',13,'Power',13,'Graph']],...
  'Mask Translate','npts = @4; color = @5; ax = [0, @1, @2,
@3]; dt=-1;')
set_param([sys,'/',['Control',13,'Drum',13,'Position/Power',
13,'Rate',13,'Positioning/Startup',13,'Power',13,'Profile/Or
der',13,'Power',13,'Graph']],...
  'Mask Help','This block uses a MATLAB figure window to
plot the input signal. The graph limits are automatically
scaled to the min and max values of the signal stored in the
```

```
scope''s signal buffer. Line type must be in quotes. See the
M-file sfunyst.m.')
set_param([sys,'/',['Control',13,'Drum',13,'Position/Power',
13,'Rate',13,'Positioning/Startup',13,'Power',13,'Profile/Or
der',13,'Power',13,'Graph']],...
  'Mask
Entries','5\/-10\/10\/200\/''y-/g--/c-./w:/m*/ro/b+''\/')


%            Finished            composite            block
['Control',13,'Drum',13,'Position/Power',13,'Rate',13,'Posit
ioning/Startup',13,'Power',13,'Profile/Order',13,'Power',13,
'Graph'].

set_param([sys,'/',['Control',13,'Drum',13,'Position/Power',
13,'Rate',13,'Positioning/Startup',13,'Power',13,'Profile/Or
der',13,'Power',13,'Graph']],...
  'position',[665,95,695,135])
add_line([sys,'/',['Control',13,'Drum',13,'Position/Power',1
3,'Rate',13,'Positioning/Startup',13,'Power',13,'Profile']],
[145,220;255,220])
add_line([sys,'/',['Control',13,'Drum',13,'Position/Power',1
3,'Rate',13,'Positioning/Startup',13,'Power',13,'Profile']],
[220,275;240,275;240,230;255,230])
add_line([sys,'/',['Control',13,'Drum',13,'Position/Power',1
3,'Rate',13,'Positioning/Startup',13,'Power',13,'Profile']],
[220,150;240,150;240,210;255,210])
add_line([sys,'/',['Control',13,'Drum',13,'Position/Power',1
3,'Rate',13,'Positioning/Startup',13,'Power',13,'Profile']],
[355,240;385,240])
add_line([sys,'/',['Control',13,'Drum',13,'Position/Power',1
3,'Rate',13,'Positioning/Startup',13,'Power',13,'Profile']],
[425,230;460,230])
add_line([sys,'/',['Control',13,'Drum',13,'Position/Power',1
3,'Rate',13,

'Positioning/Startup',13,'Power',13,'Profile']],[295,220;385
,220])
add_line([sys,'/',['Control',13,'Drum',13,'Position/Power',1
3,'Rate',13,'Positioning/Startup',13,'Power',13,'Profile']],
[55,20;80,20;80,220;105,220])
```

```
add_line([sys,'/',['Control',13,'Drum',13,'Position/Power',1
3,'Rate',13,'Positioning/Startup',13,'Power',13,'Profile']],
[605,220;645,220])
add_line([sys,'/',['Control',13,'Drum',13,'Position/Power',1
3,'Rate',13,'Positioning/Startup',13,'Power',13,'Profile']],
[510,230;565,230])
add_line([sys,'/',['Control',13,'Drum',13,'Position/Power',1
3,'Rate',13,'Positioning/Startup',13,'Power',13,'Profile']],
[400,110;540,110;540,220;565,220])
add_line([sys,'/',['Control',13,'Drum',13,'Position/Power',1
3,'Rate',13,'Positioning/Startup',13,'Power',13,'Profile']],
[80,20;80,110;360,110])
add_line([sys,'/',['Control',13,'Drum',13,'Position/Power',1
3,'Rate',13,'Positioning/Startup',13,'Power',13,'Profile']],
[540,210;565,210])
add_line([sys,'/',['Control',13,'Drum',13,'Position/Power',1
3,'Rate',13,'Positioning/Startup',13,'Power',13,'Profile']],
[618,220;640,115;660,115])


%            Finished            composite            block
['Control',13,'Drum',13,'Position/Power',13,'Rate',13,'Posit
ioning/Startup',13,'Power',13,'Profile'].

set_param([sys,'/',['Control',13,'Drum',13,'Position/Power',
13,'Rate',13,'Positioning/Startup',13,'Power',13,'Profile']]
,...
  'position',[150,91,180,144])

add_block('built-in/Dead
Zone',[sys,'/',['Control',13,'Drum',13,'Position/Power',13,'
Rate',13,'Positioning/Power Level',13,'Dead Band']])
set_param([sys,'/',['Control',13,'Drum',13,'Position/Power',
13,'Rate',13,'Positioning/Power Level',13,'Dead Band']],...
  'Lower_value','-100',...
  'Upper_value','100',...
  'position',[375,47,405,73])

add_block('built-in/Outport',[sys,'/',['Control',13,'Drum',1
3,'Position/Power',13,'Rate',13,'Positioning/Drum',13,'Motor
',13,'Switch']])
set_param([sys,'/',['Control',13,'Drum',13,'Position/Power',
13,'Rate',13,'Positioning/Drum',13,'Motor',13,'Switch']],...
  'position',[505,50,525,70])
```

```
add_block('built-in/Sum',[sys,'/',['Control',13,'Drum',13,'P
osition/Power',13,'Rate',13,'Positioning/Power',13,'Error']]
)
set_param([sys,'/',['Control',13,'Drum',13,'Position/Power',
13,'Rate',13,'Positioning/Power',13,'Error']],...
  'inputs','-+',...
  'position',[260,42,280,73])


add_block('built-in/Inport',[sys,'/',['Control',13,'Drum',13
,'Position/Power',13,'Rate',13,'Positioning/Rate',13,'Mode',
13,'Selected']])




set_param([sys,'/',['Control',13,'Drum',13,'Position/Power',
13,'Rate',13,'Positioning/Rate',13,'Mode',13,'Selected']],..
.
  'Port','2',...
  'position',[40,120,60,140])

add_block('built-in/Inport',[sys,'/',['Control',13,'Drum',13
,'Position/Power',13,'Rate',13,'Positioning/Rx Power']])
set_param([sys,'/',['Control',13,'Drum',13,'Position/Power',
13,'Rate',13,'Positioning/Rx Power']],...
  'position',[35,40,55,60])
add_line([sys,'/',['Control',13,'Drum',13,'Position/Power',1
3,'Rate',13,'Positioning']],[185,120;195,120;195,65;255,65])
add_line([sys,'/',['Control',13,'Drum',13,'Position/Power',1
3,'Rate',13,'Positioning']],[60,50;255,50])
add_line([sys,'/',['Control',13,'Drum',13,'Position/Power',1
3,'Rate',13,'Positioning']],[65,130;145,130])
add_line([sys,'/',['Control',13,'Drum',13,'Position/Power',1
3,'Rate',13,'Positioning']],[410,60;500,60])
add_line([sys,'/',['Control',13,'Drum',13,'Position/Power',1
3,'Rate',13,'Positioning']],[285,60;370,60])
add_line([sys,'/',['Control',13,'Drum',13,'Position/Power',1
3,'Rate',13,'Positioning']],[60,50;85,50;85,105;145,105])
```

```
%            Finished             composite             block
['Control',13,'Drum',13,'Position/Power',13,'Rate',13,'Posit
ioning'].

set_param([sys,'/',['Control',13,'Drum',13,'Position/Power',
13,'Rate',13,'Positioning']],...
  'position',[200,56,230,109])
add_line([sys,'/',['Control',13,'Drum',13,'Position']],[510,
200;530,200])
add_line([sys,'/',['Control',13,'Drum',13,'Position']],[220,
275;265,275;265,210;380,210])
add_line([sys,'/',['Control',13,'Drum',13,'Position']],[55,5
0;95,50;95,200;110,200])
add_line([sys,'/',['Control',13,'Drum',13,'Position']],[235,
85;300,85;300,190;380,190])
add_line([sys,'/',['Control',13,'Drum',13,'Position']],[150,
200;380,200])
add_line([sys,'/',['Control',13,'Drum',13,'Position']],[570,
200;605,200])
add_line([sys,'/',['Control',13,'Drum',13,'Position']],[645,
200;695,200])
add_line([sys,'/',['Control',13,'Drum',13,'Position']],[645,
200;650,360;100,360;100,275;180,275])



add_line([sys,'/',['Control',13,'Drum',13,'Position']],[655,
200;655,85;685,85])


add_line([sys,'/',['Control',13,'Drum',13,'Position']],[420,
200;470,200])
add_line([sys,'/',['Control',13,'Drum',13,'Position']],[95,5
0;185,50;195,70])
add_line([sys,'/',['Control',13,'Drum',13,'Position']],[150,
200;165,200;165,95;195,95])


%            Finished             composite             block
['Control',13,'Drum',13,'Position'].

set_param([sys,'/',['Control',13,'Drum',13,'Position']],...
  'position',[100,120,130,170])
```

```
add_block('built-in/To
Workspace',[sys,'/',['Reactor',13,'Power']])
set_param([sys,'/',['Reactor',13,'Power']],...
  'mat-name','P',...
  'buffer','40000',...
  'position',[440,147,490,163])


% Subsystem 'Rx Power'.

new_system([sys,'/','Rx Power'])
set_param([sys,'/','Rx Power'],'Location',[0,59,274,252])

add_block('built-in/Inport',[sys,'/','Rx Power/x'])
set_param([sys,'/','Rx Power/x'],...
  'position',[65,55,85,75])

add_block('built-in/S-Function',[sys,'/',['Rx
Power/S-function',13,'M-file                                    which
plots',13,'lines',13,'']])
set_param([sys,'/',['Rx  Power/S-function',13,'M-file  which
plots',13,'lines',13,'']],...
  'function name','sfunyst',...
  'parameters','ax, color, npts, dt',...
  'position',[130,55,180,75])
add_line([sys,'/','Rx Power'],[90,65;125,65])
set_param([sys,'/','Rx Power'],...
  'Mask
Display','plot(0,0,100,100,[83,76,63,52,42,38,28,16,11,84,11
,11,11,90,90,11],[75,58,47,54,72,80,84,74,65,65,65,90,40,40,
90,90])',...
  'Mask Type','Storage scope.')
set_param([sys,'/','Rx Power'],...
  'Mask  Dialogue','Storage  scope  using  MATLAB  graph
window.\nEnter plotting ranges and line type.|Initial Time
Range:|Initial y-min:|Initial y-max:|Storage pts.:|Line type
(rgbw-.:xo):')
set_param([sys,'/','Rx Power'],...
  'Mask Translate','npts = @4; color = @5; ax = [0, @1, @2,
@3]; dt=-1;')
set_param([sys,'/','Rx Power'],...
```

```
 'Mask Help','This block uses a MATLAB figure window to plot
the input signal. The graph limits are automatically scaled
to the min and max values of the signal stored in the
scope''s signal buffer. Line type must be in quotes. See the
M-file sfunyst.m.')
set_param([sys,'/','Rx Power'],...
  'Mask
Entries','5\/-10\/10\/200\/''y-/g--/c-./w:/m*/ro/b+''\/')



% Finished composite block 'Rx Power'.

set_param([sys,'/','Rx Power'],...
  'position',[445,235,475,275])


% Subsystem ['Temperature',13,'Response'].

new_system([sys,'/',['Temperature',13,'Response']])
set_param([sys,'/',['Temperature',13,'Response']],'Location'
,[4,42,787,498])
open_system([sys,'/',['Temperature',13,'Response']])


% Subsystem ['Temperature',13,'Response/Tm Graph'].

new_system([sys,'/',['Temperature',13,'Response/Tm Graph']])
set_param([sys,'/',['Temperature',13,'Response/Tm
Graph']],'Location',[0,59,274,252])

add_block('built-in/Inport',[sys,'/',['Temperature',13,'Resp
onse/Tm Graph/x']])
set_param([sys,'/',['Temperature',13,'Response/Tm
Graph/x']],...
  'position',[65,55,85,75])

add_block('built-in/S-Function',[sys,'/',['Temperature',13,'
Response/Tm        Graph/S-function',13,'M-file        which
plots',13,'lines',13,'']])
set_param([sys,'/',['Temperature',13,'Response/Tm
Graph/S-function',13,'M-file                              which
plots',13,'lines',13,'']],...
  'function name','sfunyst',...
```

```
  'parameters','ax, color, npts, dt',...
  'position',[130,55,180,75])
add_line([sys,'/',['Temperature',13,'Response/Tm
Graph']],[90,65;125,65])
set_param([sys,'/',['Temperature',13,'Response/Tm
Graph']],...
  'Mask
Display','plot(0,0,100,100,[83,76,63,52,42,38,28,16,11,84,11
,11,11,90,90,11],[75,58,47,54,72,80,84,74,65,65,65,90,40,40,
90,90])',...
  'Mask Type','Storage scope.')
set_param([sys,'/',['Temperature',13,'Response/Tm
Graph']],...



'Mask Dialogue','Storage scope using MATLAB graph
window.\nEnter plotting ranges and line type.|Initial Time
Range:|Initial y-min:|Initial y-max:|Storage pts.:|Line type
(rgbw-.:xo):')
set_param([sys,'/',['Temperature',13,'Response/Tm
Graph']],...
  'Mask Translate','npts = @4; color = @5; ax = [0, @1, @2,
@3]; dt=-1;')
set_param([sys,'/',['Temperature',13,'Response/Tm
Graph']],...
  'Mask Help','This block uses a MATLAB figure window to
plot the input signal. The graph limits are automatically
scaled to the min and max values of the signal stored in the
scope''s signal buffer. Line type must be in quotes. See the
M-file sfunyst.m.')
set_param([sys,'/',['Temperature',13,'Response/Tm
Graph']],...
  'Mask
Entries','5\/-10\/10\/200\/''y-/g--/c-./w:/m*/ro/b+''\/')


% Finished composite block ['Temperature',13,'Response/Tm
Graph'].

set_param([sys,'/',['Temperature',13,'Response/Tm
Graph']],...
  'position',[625,315,655,355])
```

```
add_block('built-in/Note',[sys,'/',['Temperature',13,'Respon
se/Tm']])
set_param([sys,'/',['Temperature',13,'Response/Tm']],...
  'position',[300,255,305,260])


% Subsystem ['Temperature',13,'Response/Tm Dynamics'].

new_system([sys,'/',['Temperature',13,'Response/Tm
Dynamics']])
set_param([sys,'/',['Temperature',13,'Response/Tm
Dynamics']],'Location',[18,61,780,513])

add_block('built-in/Mux',[sys,'/',['Temperature',13,'Respons
e/Tm Dynamics/Tm Op']])
set_param([sys,'/',['Temperature',13,'Response/Tm
Dynamics/Tm Op']],...
  'inputs','2',...
  'position',[300,231,330,264])

add_block('built-in/Switch',[sys,'/',['Temperature',13,'Resp
onse/Tm Dynamics/TFE',13,'Loading']])
set_param([sys,'/',['Temperature',13,'Response/Tm
Dynamics/TFE',13,'Loading']],...
  'Threshold','30000',...
  'position',[220,239,250,271])

add_block('built-in/Outport',[sys,'/',['Temperature',13,'Res
ponse/Tm Dynamics/Tm Rate']])
set_param([sys,'/',['Temperature',13,'Response/Tm
Dynamics/Tm Rate']],...
  'position',[695,287,715,313])




add_block('built-in/Switch',[sys,'/',['Temperature',13,'Resp
onse/Tm Dynamics/Cs add',13,'TFE Load']])
set_param([sys,'/',['Temperature',13,'Response/Tm
Dynamics/Cs add',13,'TFE Load']],...
  'Threshold','Tcs',...
  'position',[605,284,635,316])
```

```
add_block('built-in/Inport',[sys,'/',['Temperature',13,'Resp
onse/Tm Dynamics/Time']])
set_param([sys,'/',['Temperature',13,'Response/Tm
Dynamics/Time']],...
  'Port','2',...
  'position',[505,290,525,310])

add_block('built-in/MATLAB
Fcn',[sys,'/',['Temperature',13,'Response/Tm     Dynamics/Tm
Equilibrium',13,'(Low Power)']])
set_param([sys,'/',['Temperature',13,'Response/Tm
Dynamics/Tm Equilibrium',13,'(Low Power)']],...
  'MATLAB Fcn','298.09755+0.012550343*u',...
  'Output Width','1',...
  'position',[110,314,185,356])

add_block('built-in/MATLAB
Fcn',[sys,'/',['Temperature',13,'Response/Tm     Dynamics/Tm
Equilibrium',13,'(High Power)']])
set_param([sys,'/',['Temperature',13,'Response/Tm
Dynamics/Tm Equilibrium',13,'(High Power)']],...
  'MATLAB Fcn','664.13298+1.238966e-8*u*u',...
  'Output Width','1',...
  'position',[100,119,175,161])

add_block('built-in/MATLAB
Fcn',[sys,'/',['Temperature',13,'Response/Tm
Dynamics/Startup Dynamics']])
set_param([sys,'/',['Temperature',13,'Response/Tm
Dynamics/Startup Dynamics']],...
  'MATLAB    Fcn','(6.3617662    -0.0056230422*u(1)/u(2)*825
-1379.8541*u(2)/u(1)/825)*u(2)/825',...
  'Output Width','1',...
  'position',[390,334,465,376])

add_block('built-in/MATLAB
Fcn',[sys,'/',['Temperature',13,'Response/Tm
Dynamics/Operating',13,'Dynamics']])
set_param([sys,'/',['Temperature',13,'Response/Tm
Dynamics/Operating',13,'Dynamics']],...
  'MATLAB Fcn','-0.002*( u(1) - u(2) ) ',...
  'Output Width','1',...
  'position',[390,229,465,271])
```

```
add_block('built-in/Inport',[sys,'/',['Temperature',13,'Resp
onse/Tm Dynamics/Power']])
set_param([sys,'/',['Temperature',13,'Response/Tm
Dynamics/Power']],...
  'Port','3',...
  'position',[20,130,40,150])


add_block('built-in/Inport',[sys,'/',['Temperature',13,'Resp
onse/Tm Dynamics/Tm']])
set_param([sys,'/',['Temperature',13,'Response/Tm
Dynamics/Tm']],...
  'orientation',2,...
  'position',[590,205,610,225])
add_line([sys,'/',['Temperature',13,'Response/Tm
Dynamics']],[335,250;385,250])
add_line([sys,'/',['Temperature',13,'Response/Tm
Dynamics']],[585,215;275,215;275,240;295,240])
add_line([sys,'/',['Temperature',13,'Response/Tm
Dynamics']],[255,255;295,255])
add_line([sys,'/',['Temperature',13,'Response/Tm
Dynamics']],[180,140;205,140;215,245])
add_line([sys,'/',['Temperature',13,'Response/Tm
Dynamics']],[530,300;600,300])
add_line([sys,'/',['Temperature',13,'Response/Tm
Dynamics']],[640,300;690,300])
add_line([sys,'/',['Temperature',13,'Response/Tm
Dynamics']],[470,355;565,355;565,310;600,310])
add_line([sys,'/',['Temperature',13,'Response/Tm
Dynamics']],[45,140;60,140;60,255;215,255])
add_line([sys,'/',['Temperature',13,'Response/Tm
Dynamics']],[190,335;190,265;215,265])
add_line([sys,'/',['Temperature',13,'Response/Tm
Dynamics']],[60,145;60,140;95,140])
add_line([sys,'/',['Temperature',13,'Response/Tm
Dynamics']],[60,255;60,335;105,335])
add_line([sys,'/',['Temperature',13,'Response/Tm
Dynamics']],[470,250;565,250;565,290;600,290])
add_line([sys,'/',['Temperature',13,'Response/Tm
Dynamics']],[335,250;355,250;355,355;385,355])
```

```
% Finished composite block ['Temperature',13,'Response/Tm
Dynamics'].

set_param([sys,'/',['Temperature',13,'Response/Tm
Dynamics']],...
  'position',[300,307,330,363])

add_block('built-in/Integrator',[sys,'/',['Temperature',13,'
Response/Tm Integrator']])
set_param([sys,'/',['Temperature',13,'Response/Tm
Integrator']],...
  'Initial','To',...
  'position',[410,322,440,348])

add_block('built-in/Note',[sys,'/',['Temperature',13,'Respon
se/Tf']])
set_param([sys,'/',['Temperature',13,'Response/Tf']],...
  'position',[290,105,295,110])

add_block('built-in/To
Workspace',[sys,'/',['Temperature',13,'Response/time']])



set_param([sys,'/',['Temperature',13,'Response/time']],...
  'mat-name','t',...
  'buffer','40000',...
  'position',[210,227,260,243])

add_block('built-in/Integrator',[sys,'/',['Temperature',13,'
Response/Tf Integrator']])
set_param([sys,'/',['Temperature',13,'Response/Tf
Integrator']],...
  'Initial','To',...
  'position',[400,162,430,188])


% Subsystem ['Temperature',13,'Response/Tf Dynamics'].

new_system([sys,'/',['Temperature',13,'Response/Tf
Dynamics']])
set_param([sys,'/',['Temperature',13,'Response/Tf
Dynamics']],'Location',[118,104,709,472])
```

```
add_block('built-in/Outport',[sys,'/',['Temperature',13,'Res
ponse/Tf Dynamics/Tf Rate']])
set_param([sys,'/',['Temperature',13,'Response/Tf
Dynamics/Tf Rate']],...
  'position',[545,150,565,170])

add_block('built-in/Sum',[sys,'/',['Temperature',13,'Respons
e/Tf Dynamics/Sum']])
set_param([sys,'/',['Temperature',13,'Response/Tf
Dynamics/Sum']],...
  'position',[410,285,430,305])

add_block('built-in/Switch',[sys,'/',['Temperature',13,'Resp
onse/Tf Dynamics/TFE',13,'Load',13,'Switch']])
set_param([sys,'/',['Temperature',13,'Response/Tf
Dynamics/TFE',13,'Load',13,'Switch']],...
  'Threshold','Tload',...
  'position',[485,144,515,176])


% Subsystem ['Temperature',13,'Response/Tf Dynamics/Cs
Addition',13,'Dynamics'].

new_system([sys,'/',['Temperature',13,'Response/Tf
Dynamics/Cs Addition',13,'Dynamics']])
set_param([sys,'/',['Temperature',13,'Response/Tf
Dynamics/Cs
Addition',13,'Dynamics']],'Location',[36,179,729,468])

add_block('built-in/Switch',[sys,'/',['Temperature',13,'Resp
onse/Tf Dynamics/Cs Addition',13,'Dynamics/Switch']])
set_param([sys,'/',['Temperature',13,'Response/Tf
Dynamics/Cs Addition',13,'Dynamics/Switch']],...
  'Threshold','Tcs',...
  'position',[160,29,190,61])


add_block('built-in/Inport',[sys,'/',['Temperature',13,'Resp
onse/Tf Dynamics/Cs Addition',13,'Dynamics/Time']])
set_param([sys,'/',['Temperature',13,'Response/Tf
Dynamics/Cs Addition',13,'Dynamics/Time']],...
  'Port','2',...
  'position',[15,5,35,25])
```

```
add_block('built-in/Switch',[sys,'/',['Temperature',13,'Resp
onse/Tf        Dynamics/Cs        Addition',13,'Dynamics/Cs
Addition',13,'Switch']])
set_param([sys,'/',['Temperature',13,'Response/Tf
Dynamics/Cs                       Addition',13,'Dynamics/Cs
Addition',13,'Switch']],...
  'Threshold','Tcs',...
  'position',[585,94,620,136])

add_block('built-in/Outport',[sys,'/',['Temperature',13,'Res
ponse/Tf        Dynamics/Cs        Addition',13,'Dynamics/Cs
Heatup',13,'Rate']])
set_param([sys,'/',['Temperature',13,'Response/Tf
Dynamics/Cs                       Addition',13,'Dynamics/Cs
Heatup',13,'Rate']],...
  'orientation',2,...
  'position',[580,15,600,35])

add_block('built-in/Constant',[sys,'/',['Temperature',13,'Re
sponse/Tf Dynamics/Cs Addition',13,'Dynamics/Constant']])
set_param([sys,'/',['Temperature',13,'Response/Tf
Dynamics/Cs Addition',13,'Dynamics/Constant']],...
  'orientation',2,...
  'Value','0',...
  'position',[600,185,620,205])

add_block('built-in/MATLAB
Fcn',[sys,'/',['Temperature',13,'Response/Tf     Dynamics/Cs
Addition',13,'Dynamics/Tf Dynamics',13,'Cs Addition']])
set_param([sys,'/',['Temperature',13,'Response/Tf
Dynamics/Cs    Addition',13,'Dynamics/Tf    Dynamics',13,'Cs
Addition']],...
  'MATLAB    Fcn','sqrt(polyval([-7.6606914e-6    0.032593747
0.0179884],u(1)))*u(2)/115e3',...
  'Output Width','1')
set_param([sys,'/',['Temperature',13,'Response/Tf
Dynamics/Cs    Addition',13,'Dynamics/Tf    Dynamics',13,'Cs
Addition']],...
  'position',[445,79,520,121])

add_block('built-in/Memory',[sys,'/',['Temperature',13,'Resp
onse/Tf Dynamics/Cs Addition',13,'Dynamics/Memory']])
set_param([sys,'/',['Temperature',13,'Response/Tf
Dynamics/Cs Addition',13,'Dynamics/Memory']],...
```

```
  'position',[220,30,260,60])

add_block('built-in/Mux',[sys,'/',['Temperature',13,'Respons
e/Tf Dynamics/Cs Addition',13,'Dynamics/Mux']])
set_param([sys,'/',['Temperature',13,'Response/Tf
Dynamics/Cs Addition',13,'Dynamics/Mux']],...
  'inputs','2',...

 'position',[395,61,430,139])

add_block('built-in/Abs',[sys,'/',['Temperature',13,'Respons
e/Tf Dynamics/Cs Addition',13,'Dynamics/Abs']])
set_param([sys,'/',['Temperature',13,'Response/Tf
Dynamics/Cs Addition',13,'Dynamics/Abs']],...
  'position',[350,68,380,92])

add_block('built-in/Sum',[sys,'/',['Temperature',13,'Respons
e/Tf Dynamics/Cs Addition',13,'Dynamics/Sum']])
set_param([sys,'/',['Temperature',13,'Response/Tf
Dynamics/Cs Addition',13,'Dynamics/Sum']],...
  'inputs','-+',...
  'position',[290,64,320,91])

add_block('built-in/Demux',[sys,'/',['Temperature',13,'Respo
nse/Tf Dynamics/Cs Addition',13,'Dynamics/Demux']])
set_param([sys,'/',['Temperature',13,'Response/Tf
Dynamics/Cs Addition',13,'Dynamics/Demux']],...
  'outputs','2',...
  'position',[50,75,105,110])

add_block('built-in/Note',[sys,'/',['Temperature',13,'Respon
se/Tf Dynamics/Cs Addition',13,'Dynamics/Tf']])
set_param([sys,'/',['Temperature',13,'Response/Tf
Dynamics/Cs Addition',13,'Dynamics/Tf']],...
  'position',[75,45,80,50])

add_block('built-in/Note',[sys,'/',['Temperature',13,'Respon
se/Tf Dynamics/Cs Addition',13,'Dynamics/P']])
set_param([sys,'/',['Temperature',13,'Response/Tf
Dynamics/Cs Addition',13,'Dynamics/P']],...
  'position',[130,105,135,110])

add_block('built-in/Inport',[sys,'/',['Temperature',13,'Resp
onse/Tf Dynamics/Cs Addition',13,'Dynamics/State']])
```

```
set_param([sys,'/',['Temperature',13,'Response/Tf
Dynamics/Cs Addition',13,'Dynamics/State']],...
  'position',[10,85,30,105])

add_block('built-in/Note',[sys,'/',['Temperature',13,'Respon
se/Tf Dynamics/Cs Addition',13,'Dynamics/Tf initial']])
set_param([sys,'/',['Temperature',13,'Response/Tf
Dynamics/Cs Addition',13,'Dynamics/Tf initial']],...
  'position',[310,30,315,35])
add_line([sys,'/',['Temperature',13,'Response/Tf Dynamics/Cs
Addition',13,'Dynamics']],[525,100;580,100])
add_line([sys,'/',['Temperature',13,'Response/Tf Dynamics/Cs
Addition',13,'Dynamics']],[595,195;560,195;560,130;580,130])




add_line([sys,'/',['Temperature',13,'Response/Tf Dynamics/Cs
Addition',13,'Dynamics']],[625,115;635,115;635,25;605,25])
add_line([sys,'/',['Temperature',13,'Response/Tf Dynamics/Cs
Addition',13,'Dynamics']],[40,15;550,15;550,115;580,115])
add_line([sys,'/',['Temperature',13,'Response/Tf Dynamics/Cs
Addition',13,'Dynamics']],[195,45;215,45])
add_line([sys,'/',['Temperature',13,'Response/Tf Dynamics/Cs
Addition',13,'Dynamics']],[265,45;265,25;140,25;140,35;155,3
5])
add_line([sys,'/',['Temperature',13,'Response/Tf Dynamics/Cs
Addition',13,'Dynamics']],[35,95;45,95])
add_line([sys,'/',['Temperature',13,'Response/Tf Dynamics/Cs
Addition',13,'Dynamics']],[435,100;440,100])
add_line([sys,'/',['Temperature',13,'Response/Tf Dynamics/Cs
Addition',13,'Dynamics']],[110,85;130,85;130,55;155,55])
add_line([sys,'/',['Temperature',13,'Response/Tf Dynamics/Cs
Addition',13,'Dynamics']],[95,15;95,45;155,45])
add_line([sys,'/',['Temperature',13,'Response/Tf Dynamics/Cs
Addition',13,'Dynamics']],[110,100;245,100;245,120;390,120])
add_line([sys,'/',['Temperature',13,'Response/Tf Dynamics/Cs
Addition',13,'Dynamics']],[265,45;275,45;285,70])
add_line([sys,'/',['Temperature',13,'Response/Tf Dynamics/Cs
Addition',13,'Dynamics']],[110,85;285,85])
add_line([sys,'/',['Temperature',13,'Response/Tf Dynamics/Cs
Addition',13,'Dynamics']],[385,80;390,80])
```

```
add_line([sys,'/',['Temperature',13,'Response/Tf Dynamics/Cs
Addition',13,'Dynamics']],[325,80;345,80])


% Finished composite block ['Temperature',13,'Response/Tf
Dynamics/Cs Addition',13,'Dynamics'].

set_param([sys,'/',['Temperature',13,'Response/Tf
Dynamics/Cs Addition',13,'Dynamics']],...
  'position',[255,187,285,238])

add_block('built-in/MATLAB
Fcn',[sys,'/',['Temperature',13,'Response/Tf     Dynamics/Tf
Dynamics',13,'(No Loading)']])
set_param([sys,'/',['Temperature',13,'Response/Tf
Dynamics/Tf Dynamics',13,'(No Loading)']],...
  'MATLAB   Fcn','1.201131601e-4*u(2)+polyval([-2.0220458e-8
7.3516563e-5 -0.087210261 20.092539996],u(1))',...
  'Output Width','1')
set_param([sys,'/',['Temperature',13,'Response/Tf
Dynamics/Tf Dynamics',13,'(No Loading)']],...
  'position',[195,279,270,321])

add_block('built-in/Inport',[sys,'/',['Temperature',13,'Resp
onse/Tf Dynamics/Time']])
set_param([sys,'/',['Temperature',13,'Response/Tf
Dynamics/Time']],...
  'Port','3',...
  'position',[15,150,35,170])


%   Subsystem   ['Temperature',13,'Response/Tf   Dynamics/Tf
Dynamics',13,'(Operating)'].

new_system([sys,'/',['Temperature',13,'Response/Tf
Dynamics/Tf Dynamics',13,'(Operating)']])
set_param([sys,'/',['Temperature',13,'Response/Tf
Dynamics/Tf
Dynamics',13,'(Operating)']],'Location',[62,71,721,547])

add_block('built-in/Inport',[sys,'/',['Temperature',13,'Resp
onse/Tf Dynamics/Tf Dynamics',13,'(Operating)/Power']])
set_param([sys,'/',['Temperature',13,'Response/Tf
Dynamics/Tf Dynamics',13,'(Operating)/Power']],...
```

```
  'Port','2',...
  'position',[35,175,55,195])

add_block('built-in/MATLAB
Fcn',[sys,'/',['Temperature',13,'Response/Tf     Dynamics/Tf
Dynamics',13,'(Operating)/Tf Equilibrium']])
set_param([sys,'/',['Temperature',13,'Response/Tf
Dynamics/Tf Dynamics',13,'(Operating)/Tf Equilibrium']],...
  'MATLAB  Fcn','polyval(  [  2.7674712e-13  0  -0.019137039
299.54525] , u ) + 9.9191989*sqrt(u)',...
  'Output Width','1')
set_param([sys,'/',['Temperature',13,'Response/Tf
Dynamics/Tf Dynamics',13,'(Operating)/Tf Equilibrium']],...
  'position',[105,164,180,206])

add_block('built-in/Sum',[sys,'/',['Temperature',13,'Respons
e/Tf                                                Dynamics/Tf
Dynamics',13,'(Operating)/Tf',13,'Deviance']])
set_param([sys,'/',['Temperature',13,'Response/Tf
Dynamics/Tf
Dynamics',13,'(Operating)/Tf',13,'Deviance']],...
  'inputs','+-',...
  'position',[225,114,250,141])

add_block('built-in/Constant',[sys,'/',['Temperature',13,'Re
sponse/Tf    Dynamics/Tf    Dynamics',13,'(Operating)/Heatup
Rate']])
set_param([sys,'/',['Temperature',13,'Response/Tf
Dynamics/Tf Dynamics',13,'(Operating)/Heatup Rate']],...
  'Value','-0.022569155',...
  'position',[215,302,365,328])

add_block('built-in/Constant',[sys,'/',['Temperature',13,'Re
sponse/Tf   Dynamics/Tf   Dynamics',13,'(Operating)/Cooldown
Rate']])
set_param([sys,'/',['Temperature',13,'Response/Tf
Dynamics/Tf Dynamics',13,'(Operating)/Cooldown Rate']],...
  'Value','-0.01',...
  'position',[295,191,435,219])

add_block('built-in/Switch',[sys,'/',['Temperature',13,'Resp
onse/Tf Dynamics/Tf Dynamics',13,'(Operating)/Switch']])
```

```
set_param([sys,'/',['Temperature',13,'Response/Tf
Dynamics/Tf Dynamics',13,'(Operating)/Switch']],...
  'position',[460,234,490,266])

add_block('built-in/Product',[sys,'/',['Temperature',13,'Res
ponse/Tf      Dynamics/Tf      Dynamics',13,'(Operating)/Tf
rate',13,'Calculation']])
set_param([sys,'/',['Temperature',13,'Response/Tf
Dynamics/Tf                    Dynamics',13,'(Operating)/Tf
rate',13,'Calculation']],...
  'position',[525,123,555,147])

add_block('built-in/Outport',[sys,'/',['Temperature',13,'Res
ponse/Tf Dynamics/Tf Dynamics',13,'(Operating)/Tf Rate']])
set_param([sys,'/',['Temperature',13,'Response/Tf
Dynamics/Tf Dynamics',13,'(Operating)/Tf Rate']],...
  'position',[615,125,635,145])

add_block('built-in/Inport',[sys,'/',['Temperature',13,'Resp
onse/Tf Dynamics/Tf Dynamics',13,'(Operating)/Tf']])
set_param([sys,'/',['Temperature',13,'Response/Tf
Dynamics/Tf Dynamics',13,'(Operating)/Tf']],...
  'position',[30,110,50,130])
add_line([sys,'/',['Temperature',13,'Response/Tf Dynamics/Tf
Dynamics',13,'(Operating)']],[60,185;100,185])
add_line([sys,'/',['Temperature',13,'Response/Tf Dynamics/Tf
Dynamics',13,'(Operating)']],[185,185;195,185;195,135;220,13
5])
add_line([sys,'/',['Temperature',13,'Response/Tf Dynamics/Tf
Dynamics',13,'(Operating)']],[55,120;220,120])
add_line([sys,'/',['Temperature',13,'Response/Tf Dynamics/Tf
Dynamics',13,'(Operating)']],[495,250;500,250;500,140;520,14
0])
add_line([sys,'/',['Temperature',13,'Response/Tf Dynamics/Tf
Dynamics',13,'(Operating)']],[560,135;610,135])
add_line([sys,'/',['Temperature',13,'Response/Tf Dynamics/Tf
Dynamics',13,'(Operating)']],[255,130;275,130;275,250;455,25
0])
add_line([sys,'/',['Temperature',13,'Response/Tf Dynamics/Tf
Dynamics',13,'(Operating)']],[440,205;445,205;455,240])
```

```
add_line([sys,'/',['Temperature',13,'Response/Tf Dynamics/Tf
Dynamics',13,'(Operating)']],[370,315;390,315;390,260;455,26
0])
add_line([sys,'/',['Temperature',13,'Response/Tf Dynamics/Tf
Dynamics',13,'(Operating)']],[275,130;520,130])


% Finished composite block ['Temperature',13,'Response/Tf
Dynamics/Tf Dynamics',13,'(Operating)'].

set_param([sys,'/',['Temperature',13,'Response/Tf
Dynamics/Tf Dynamics',13,'(Operating)']],...
  'position',[295,52,325,103])

add_block('built-in/Inport',[sys,'/',['Temperature',13,'Resp
onse/Tf Dynamics/Tf']])



set_param([sys,'/',['Temperature',13,'Response/Tf
Dynamics/Tf']],...
  'position',[20,20,40,40])

add_block('built-in/Mux',[sys,'/',['Temperature',13,'Respons
e/Tf Dynamics/Mux']])
set_param([sys,'/',['Temperature',13,'Response/Tf
Dynamics/Mux']],...
  'inputs','2',...
  'position',[105,101,135,134])

add_block('built-in/Inport',[sys,'/',['Temperature',13,'Resp
onse/Tf Dynamics/Power']])
set_param([sys,'/',['Temperature',13,'Response/Tf
Dynamics/Power']],...
  'Port','2',...
  'position',[15,80,35,100])
add_line([sys,'/',['Temperature',13,'Response/Tf
Dynamics']],[140,120;160,120;160,300;190,300])
add_line([sys,'/',['Temperature',13,'Response/Tf
Dynamics']],[160,200;250,200])
add_line([sys,'/',['Temperature',13,'Response/Tf
Dynamics']],[435,295;450,295;450,170;480,170])
add_line([sys,'/',['Temperature',13,'Response/Tf
Dynamics']],[290,215;375,215;375,290;405,290])
```

```
add_line([sys,'/',['Temperature',13,'Response/Tf
Dynamics']],[275,300;405,300])
add_line([sys,'/',['Temperature',13,'Response/Tf
Dynamics']],[330,80;370,80;370,150;480,150])
add_line([sys,'/',['Temperature',13,'Response/Tf
Dynamics']],[45,30;65,30;65,110;100,110])
add_line([sys,'/',['Temperature',13,'Response/Tf
Dynamics']],[40,160;480,160])
add_line([sys,'/',['Temperature',13,'Response/Tf
Dynamics']],[520,160;540,160])
add_line([sys,'/',['Temperature',13,'Response/Tf
Dynamics']],[75,160;75,225;250,225])
add_line([sys,'/',['Temperature',13,'Response/Tf
Dynamics']],[65,65;290,65])
add_line([sys,'/',['Temperature',13,'Response/Tf
Dynamics']],[40,90;290,90])
add_line([sys,'/',['Temperature',13,'Response/Tf
Dynamics']],[50,90;50,125;100,125])


% Finished composite block ['Temperature',13,'Response/Tf
Dynamics'].

set_param([sys,'/',['Temperature',13,'Response/Tf
Dynamics']],...
  'position',[300,148,330,202])

add_block('built-in/To
Workspace',[sys,'/',['Temperature',13,'Response/Tm out']])




set_param([sys,'/',['Temperature',13,'Response/Tm out']],...
  'mat-name','Tm',...
  'buffer','40000',...
  'position',[680,392,730,408])

add_block('built-in/Mux',[sys,'/',['Temperature',13,'Respons
e/Mux']])
set_param([sys,'/',['Temperature',13,'Response/Mux']],...
  'inputs','3',...
  'position',[685,244,715,276])
```

```
add_block('built-in/MATLAB
Fcn',[sys,'/',['Temperature',13,'Response/Te Calculation']])
set_param([sys,'/',['Temperature',13,'Response/Te
Calculation']],...
  'MATLAB Fcn','-6.8425844+0.99243093*u',...
  'position',[555,181,630,219])


% Subsystem ['Temperature',13,'Response/ Tf Graph'].

new_system([sys,'/',['Temperature',13,'Response/          Tf
Graph']])
set_param([sys,'/',['Temperature',13,'Response/          Tf
Graph']],'Location',[0,59,274,252])

add_block('built-in/Inport',[sys,'/',['Temperature',13,'Resp
onse/ Tf Graph/x']])
set_param([sys,'/',['Temperature',13,'Response/          Tf
Graph/x']],...
  'position',[65,55,85,75])

add_block('built-in/S-Function',[sys,'/',['Temperature',13,'
Response/     Tf     Graph/S-function',13,'M-file     which
plots',13,'lines',13,'']])
set_param([sys,'/',['Temperature',13,'Response/          Tf
Graph/S-function',13,'M-file                            which
plots',13,'lines',13,'']],...
  'function name','sfunyst',...
  'parameters','ax, color, npts, dt',...
  'position',[130,55,180,75])
add_line([sys,'/',['Temperature',13,'Response/          Tf
Graph']],[90,65;125,65])
set_param([sys,'/',['Temperature',13,'Response/          Tf
Graph']],...
  'Mask
Display','plot(0,0,100,100,[83,76,63,52,42,38,28,16,11,84,11
,11,11,90,90,11],[75,58,47,54,72,80,84,74,65,65,65,90,40,40,
90,90])',...
  'Mask Type','Storage scope.')
set_param([sys,'/',['Temperature',13,'Response/          Tf
Graph']],...
  'Mask  Dialogue','Storage  scope  using  MATLAB  graph
window.\nEnter plotting ranges and line type.|Initial Time
```

```
Range:|Initial y-min:|Initial y-max:|Storage pts.:|Line type
(rgbw-.:xo):')
set_param([sys,'/',['Temperature',13,'Response/          Tf
Graph']],...
  'Mask Translate','npts = @4; color = @5; ax = [0, @1, @2,
@3]; dt=-1;')




set_param([sys,'/',['Temperature',13,'Response/          Tf
Graph']],...
  'Mask Help','This block uses a MATLAB figure window to
plot the input signal. The graph limits are automatically
scaled to the min and max values of the signal stored in the
scope''s signal buffer. Line type must be in quotes. See the
M-file sfunyst.m.')
set_param([sys,'/',['Temperature',13,'Response/          Tf
Graph']],...
  'Mask
Entries','5\/-10\/10\/200\/''y-/g--/c-./w:/m*/ro/b+''\/')


% Finished composite block ['Temperature',13,'Response/ Tf
Graph'].

set_param([sys,'/',['Temperature',13,'Response/          Tf
Graph']],...
  'position',[475,210,505,250])

add_block('built-in/To
Workspace',[sys,'/',['Temperature',13,'Response/Tf Out']])
set_param([sys,'/',['Temperature',13,'Response/Tf Out']],...
  'mat-name','Tf',...
  'buffer','40000',...
  'position',[680,167,730,183])

add_block('built-in/Clock',[sys,'/',['Temperature',13,'Respo
nse/Clock']])
set_param([sys,'/',['Temperature',13,'Response/Clock']],...
  'position',[140,185,160,205])

add_block('built-in/Inport',[sys,'/',['Temperature',13,'Resp
onse/Power']])
```

```
set_param([sys,'/',['Temperature',13,'Response/Power']],...
  'position',[35,165,55,185])

add_block('built-in/Outport',[sys,'/',['Temperature',13,'Res
ponse/Trx']])
set_param([sys,'/',['Temperature',13,'Response/Trx']],...
  'position',[750,250,770,270])
add_line([sys,'/',['Temperature',13,'Response']],[165,195;29
5,195])
add_line([sys,'/',['Temperature',13,'Response']],[175,195;17
5,335;295,335])
add_line([sys,'/',['Temperature',13,'Response']],[175,235;20
5,235])
add_line([sys,'/',['Temperature',13,'Response']],[435,175;44
5,175;445,135;280,135;280,155;295,155])
add_line([sys,'/',['Temperature',13,'Response']],[435,175;44
0,175;440,230;470,230])
add_line([sys,'/',['Temperature',13,'Response']],[445,335;44
5,285;280,285;280,315;295,315])
add_line([sys,'/',['Temperature',13,'Response']],[445,335;62
0,335])
add_line([sys,'/',['Temperature',13,'Response']],[590,335;59
0,400;675,400])
add_line([sys,'/',['Temperature',13,'Response']],[335,335;40
5,335])
add_line([sys,'/',['Temperature',13,'Response']],[335,175;39
5,175])
add_line([sys,'/',['Temperature',13,'Response']],[60,175;295
,175])


add_line([sys,'/',['Temperature',13,'Response']],[720,260;74
5,260])
add_line([sys,'/',['Temperature',13,'Response']],[545,335;54
5,270;680,270])
add_line([sys,'/',['Temperature',13,'Response']],[635,200;65
0,200;650,260;680,260])
add_line([sys,'/',['Temperature',13,'Response']],[435,175;66
5,175;665,250;680,250])
add_line([sys,'/',['Temperature',13,'Response']],[525,175;52
5,200;550,200])
add_line([sys,'/',['Temperature',13,'Response']],[660,175;67
5,175])
```

```
add_line([sys,'/',['Temperature',13,'Response']],[90,175;90,
355;295,355])


% Finished composite block ['Temperature',13,'Response'].

set_param([sys,'/',['Temperature',13,'Response']],...
  'position',[540,70,570,120])

add_block('built-in/Note',[sys,'/',['Temperature',13,'Feedba
ck']])
set_param([sys,'/',['Temperature',13,'Feedback']],...
  'position',[150,5,155,10])


% Subsystem ['Reactivity',13,'Model'].

new_system([sys,'/',['Reactivity',13,'Model']])
set_param([sys,'/',['Reactivity',13,'Model']],'Location',[20
,117,687,518])

add_block('built-in/Inport',[sys,'/',['Reactivity',13,'Model
/T Rx']])
set_param([sys,'/',['Reactivity',13,'Model/T Rx']],...
  'position',[45,85,65,105])

add_block('built-in/Inport',[sys,'/',['Reactivity',13,'Model
/Drum',13,'Position']])
set_param([sys,'/',['Reactivity',13,'Model/Drum',13,'Positio
n']],...
  'Port','2',...
  'position',[40,175,60,195])

add_block('built-in/MATLAB
Fcn',[sys,'/',['Reactivity',13,'Model/Drum Reactivity']])
set_param([sys,'/',['Reactivity',13,'Model/Drum
Reactivity']],...
  'MATLAB Fcn','polyval([6.89e-13 -2.33e-10 3.28e-9 4.57e-6
-5.88e-5 -0.034009],u)',...
  'Output Width','1',...
  'position',[205,166,290,204])
```

```
%                                                    Subsystem
['Reactivity',13,'Model/Temperature',13,'Reactivity'].

new_system([sys,'/',['Reactivity',13,'Model/Temperature',13,
'Reactivity']])
set_param([sys,'/',['Reactivity',13,'Model/Temperature',13,'
Reactivity']],'Location',[45,158,708,527])

add_block('built-in/Demux',[sys,'/',['Reactivity',13,'Model/
Temperature',13,'Reactivity/Demux']])
set_param([sys,'/',['Reactivity',13,'Model/Temperature',13,'
Reactivity/Demux']],...
  'outputs','3',...
  'position',[110,154,165,186])

add_block('built-in/Inport',[sys,'/',['Reactivity',13,'Model
/Temperature',13,'Reactivity/Reactor',13,'Temperatures']])
set_param([sys,'/',['Reactivity',13,'Model/Temperature',13,'
Reactivity/Reactor',13,'Temperatures']],...
  'position',[50,160,70,180])

add_block('built-in/MATLAB
Fcn',[sys,'/',['Reactivity',13,'Model/Temperature',13,'React
ivity/Fuel',13,'Reactivity (Tf)']])
set_param([sys,'/',['Reactivity',13,'Model/Temperature',13,'
Reactivity/Fuel',13,'Reactivity (Tf)']],...
  'MATLAB Fcn','(0.432e-5*(u-To)-6.4e-3*(sqrt(u/To)-1))',...
  'position',[230,246,305,284])

add_block('built-in/MATLAB
Fcn',[sys,'/',['Reactivity',13,'Model/Temperature',13,'React
ivity/Emitter',13,'Reactivity (Te)']])
set_param([sys,'/',['Reactivity',13,'Model/Temperature',13,'
Reactivity/Emitter',13,'Reactivity (Te)']],...
  'MATLAB                          Fcn','(8.52e-2-4.26e-2*(
4.0257624+0.026717601*sqrt(u)-44.297412/sqrt(u)
))*.01-4.93411008E-05')
set_param([sys,'/',['Reactivity',13,'Model/Temperature',13,'
Reactivity/Emitter',13,'Reactivity (Te)']],...
  'position',[225,151,300,189])
```

```
add_block('built-in/MATLAB
Fcn',[sys,'/',['Reactivity',13,'Model/Temperature',13,'React
ivity/Moderator',13,'Reactivity (Tm)']])
set_param([sys,'/',['Reactivity',13,'Model/Temperature',13,'
Reactivity/Moderator',13,'Reactivity (Tm)']],...
  'MATLAB Fcn','polyval([-8.22e-14 1.6e-10 -1.11e-7 2.92e-5
1.76e-3 0],u-To)*.01',...
  'position',[225,56,300,94])

add_block('built-in/Sum',[sys,'/',['Reactivity',13,'Model/Te
mperature',13,'Reactivity/Sum']])



set_param([sys,'/',['Reactivity',13,'Model/Temperature',13,'
Reactivity/Sum']],...
  'inputs','+++',...
  'position',[415,152,435,188])

add_block('built-in/Outport',[sys,'/',['Reactivity',13,'Mode
l/Temperature',13,'Reactivity/Temperature',13,'Reactivity']]
)
set_param([sys,'/',['Reactivity',13,'Model/Temperature',13,'
Reactivity/Temperature',13,'Reactivity']],...
  'position',[535,160,555,180])
add_line([sys,'/',['Reactivity',13,'Model/Temperature',13,'R
eactivity']],[440,170;530,170])
add_line([sys,'/',['Reactivity',13,'Model/Temperature',13,'R
eactivity']],[305,75;355,75;355,160;410,160])
add_line([sys,'/',['Reactivity',13,'Model/Temperature',13,'R
eactivity']],[305,170;410,170])
add_line([sys,'/',['Reactivity',13,'Model/Temperature',13,'R
eactivity']],[75,170;105,170])
add_line([sys,'/',['Reactivity',13,'Model/Temperature',13,'R
eactivity']],[170,170;220,170])
add_line([sys,'/',['Reactivity',13,'Model/Temperature',13,'R
eactivity']],[170,160;180,160;180,75;220,75])
add_line([sys,'/',['Reactivity',13,'Model/Temperature',13,'R
eactivity']],[170,180;180,180;180,265;225,265])
add_line([sys,'/',['Reactivity',13,'Model/Temperature',13,'R
eactivity']],[310,265;355,265;355,180;410,180])
```

```
%            Finished            composite            block
['Reactivity',13,'Model/Temperature',13,'Reactivity'].

set_param([sys,'/',['Reactivity',13,'Model/Temperature',13,'
Reactivity']],...
  'position',[230,69,260,121])

add_block('built-in/Note',[sys,'/',['Reactivity',13,'Model/R
x',13,'Temperatures']])
set_param([sys,'/',['Reactivity',13,'Model/Rx',13,'Temperatu
res']],...
  'position',[165,50,170,55])

add_block('built-in/Sum',[sys,'/',['Reactivity',13,'Model/Su
m']])
set_param([sys,'/',['Reactivity',13,'Model/Sum']],...
  'position',[365,125,385,145])

add_block('built-in/Note',[sys,'/',['Reactivity',13,'Model/D
rum Angle']])
set_param([sys,'/',['Reactivity',13,'Model/Drum Angle']],...
  'position',[140,140,145,145])




add_block('built-in/To
Workspace',[sys,'/',['Reactivity',13,'Model/Temp',13,'Reacti
vity']])
set_param([sys,'/',['Reactivity',13,'Model/Temp',13,'Reactiv
ity']],...
  'mat-name','r_T',...
  'buffer','40000',...
  'position',[315,32,365,48])

add_block('built-in/To
Workspace',[sys,'/',['Reactivity',13,'Model/Drum',13,'Reacti
vity']])
set_param([sys,'/',['Reactivity',13,'Model/Drum',13,'Reactiv
ity']],...
  'mat-name','r_D',...
  'buffer','40000',...
  'position',[380,177,430,193])
```

```
add_block('built-in/To
Workspace',[sys,'/',['Reactivity',13,'Model/Net',13,'Reactiv
ity']])
set_param([sys,'/',['Reactivity',13,'Model/Net',13,'Reactivi
ty']],...
  'mat-name','r_net',...
  'buffer','40000',...
  'position',[540,25,630,55])

add_block('built-in/Note',[sys,'/',['Reactivity',13,'Model/N
et Core Reactivity']])
set_param([sys,'/',['Reactivity',13,'Model/Net          Core
Reactivity']],...
  'position',[550,175,555,180])

add_block('built-in/Outport',[sys,'/',['Reactivity',13,'Mode
l/Net dk']])
set_param([sys,'/',['Reactivity',13,'Model/Net dk']],...
  'position',[605,250,625,270])

add_block('built-in/Saturation',[sys,'/',['Reactivity',13,'M
odel/Saturation']])
set_param([sys,'/',['Reactivity',13,'Model/Saturation']],...
  'Lower Limit','-5',...
  'Upper Limit','Beq*.9',...
  'position',[525,248,555,272])
add_line([sys,'/',['Reactivity',13,'Model']],[265,95;310,95;
310,130;360,130])
add_line([sys,'/',['Reactivity',13,'Model']],[295,185;310,18
5;310,140;360,140])
add_line([sys,'/',['Reactivity',13,'Model']],[70,95;225,95])
add_line([sys,'/',['Reactivity',13,'Model']],[280,95;280,40;
310,40])
add_line([sys,'/',['Reactivity',13,'Model']],[295,185;375,18
5])
add_line([sys,'/',['Reactivity',13,'Model']],[390,135;455,13
5;455,40;535,40])
add_line([sys,'/',['Reactivity',13,'Model']],[65,185;200,185
])
add_line([sys,'/',['Reactivity',13,'Model']],[560,260;600,26
0])
add_line([sys,'/',['Reactivity',13,'Model']],[455,135;465,26
0;520,260])
```

```
% Finished composite block ['Reactivity',13,'Model'].

set_param([sys,'/',['Reactivity',13,'Model']],...
  'position',[190,69,220,116])
add_line(sys,[135,145;140,145;140,105;185,105])
add_line(sys,[360,95;535,95])
add_line(sys,[415,95;415,255;440,255])
add_line(sys,[415,155;435,155])
add_line(sys,[575,95;585,95;585,50;165,50;165,80;185,80])
add_line(sys,[225,95;245,95;245,185;275,185])
add_line(sys,[235,95;320,95])
add_line(sys,[416,255;40,255;40,145;95,145])

drawnow

% Return any arguments.
if (nargin | nargout)
 % Must use feval here to access system in memory
 if (nargin > 3)
  if (flag == 0)
   eval(['[ret,x0,str,ts,xts]=',sys,'(t,x,u,flag);'])
  else
   eval(['ret =', sys,'(t,x,u,flag);'])
  end
 else
  [ret,x0,str,ts,xts] = feval(sys);
 end
else
 drawnow % Flash up the model and execute load callback
end
```

LIST OF REFERENCES

Angrist, Stanley W., (1987), *Direct Energy Conversion*, 4th ed. , Allyn and Bacon, Inc., Boston, MA.

U.S. Topaz II Flight Safety Team, (1992), *NEP Space Test Program Preliminary Nuclear Safety Assessment*, Ballistic Missile Defense Organization, Washington, DC.

Gunther, N.G. (1992), "Characteristics of the Soviet TOPAZ II Space Power System," *Report No SPI-52-1*, Space Power Inc., San Jose CA.

Huang, Francis F., (1988), *Engineering Thermodynamics: Fundamental and Applications*, 2nd ed., McGraw-Hill Book Company, New York, NY.

Kwok, Kwan S., (1993), *Topaz II Reactor System Real-time Dynamic Simulator*, User's Guide and Reference Manual, Sandia National Laboratories, Albuquerque, NM.

Leachman, R. B., (1965) "Nuclear Fission," Scientific American, Inc., New York, NY.

Larson, Wiley J, and Wertz, James R., (1992), *Space Misston Analysis and Design*, 2nd Ed., Microcosm, Inc., Torrance, CA, and Kluwer Academic Publishers, Dordrecht, Germany.

Malloy, W. et al., (1994), *Topaz International Program: Lessons Learned in Technology Cooperation with Russia*, Booz•Allen & Hamilton, Inc., Springfield, VA.

Marshal, A., (1994), Unpublished Slides, Department of Energy for the Ballistic Missile Defense Office, Washington, DC.

Morris, B, Suriano, M, Taylor, J, (1994), "American Testing of the TOPAZ-II: An Investigation of Output Current Oscillation," *Proceedings of 11th Symposium on Space Nuclear Power Systems*, American Institute of Physics, New York, NY.

Paramonov, Dmitry V., El-Genk, Mohamed S., (1994), *Steady-state and Transient Analyses of the TOPAZ-II Space Nuclear Power System*, The Institute for Space Nuclear Power Studies, University of New Mexico, Albuquerque, NM.

Shtessel, Y. (1994), "Sliding Mode Control of the Space Nuclear Reactor System TOPAZ-II," University of Alabama in Huntsville, Huntsville, AL.

Schmidt, G.L., Thomé, F, Ogloblin, B., and Sinkevich, V. (1994) "TOPAZ-II Non-Nuclear Qualification Test Program," *Proceedings of 11th Symposium on Space Nuclear Power and Propulsion*, Conference Proceedings No. 301, American Institute of Physics, New York, NY.

Slotine, J-J, and Li, W., (1991) Applied Nonlinear Control, Prentice Hall, Englewood, NJ.

Synthesis Group, (1991), *America at the Threshold: America's Space Exploration Initiative*, U.S. Government Printing Office, Washington, DC.

Voss, S., (1994), "TOPAZ-II Design Evolution," *Eleventh Symposium on Space Nuclear Power Systems*, American Institute of Physics.

Wold, S., Izhvanov, O., Vibivanets, V., Schmidt, G., (1994), "TOPAZ-II Thermionic Fuel Element Testing," *Eleventh Symposium on Space Nuclear Power Systems*, American Institute of Physics.

INITIAL DISTRIBUTION LIST

1. Defense Technical Information Center 2
   8725 John J. Kingman Road, Ste 0944
   Ft. Belvoir, VA 22060-6218

2. Library 2
   Naval Postgraduate School
   411 Dyer Rd.
   Monterey, California 93943-5101

3. Chairman 1
   Department of Aeronautics and Astronautics, Code AA
   Naval Postgraduate School
   411 Dyer Rd.
   Monterey, California 93943-5101

4. Professor Oscar Biblarz 2
   Department of Aeronautics and Astronautics, Code AA
   Naval Postgraduate School
   411 Dyer Rd.
   Monterey, California 93943-5101

5. Professor Isaac Kaminer 2
   Department of Aeronautics and Astronautics, Code AA
   Naval Postgraduate School
   411 Dyer Rd.
   Monterey, California 93943-5101

6. TOPAZ International Program 2
   Attn: Frank Thomé
   Frank Wyant
   901 University Blvd., S.E.
   Albuquerque, New Mexico 87106

7. Professor Mohamed S. El-Genk 1
   Chemical and Nuclear Engineering Department
   University of New Mexico
   Albuquerque, New Mexico 87131-1341

8. Lieutenant Cal D. Astrin, USN 2
   49 Meadow Avenue
   San Rafael, California 94901